

Copyright is owned by the Author of the thesis. Permission is given for a copy to be downloaded by an individual for the purpose of research and private study only. The thesis may not be reproduced elsewhere without the permission of the Author.



**Behaviour of complex emulsion systems during
in-vitro gastric digestion**

A thesis presented in partial fulfilment of the requirements for
the degree of

Master of Food Technology

at Massey University, Manawatū,
Palmerston North, New Zealand

Natasha Nayak

2023



ABSTRACT

Understanding the relationship between food structures and their digestion is important in understanding the association between diet and health. However, this becomes difficult as food structures keep varying and evolving through different stages of manufacture, storage, oral processing, and digestion. Mixed biopolymer protein-polysaccharide emulsion gels are simplified models for multicomponent structures present in real food systems. The pH and ionic strength of these systems play an important role in determining the interactions between proteins and anionic polysaccharides.

In the present study, heat-set whey protein emulsion gels ($d_{4,3} \sim 0.5 \mu\text{m}$) with and without low methoxyl pectin (LMP) were formed at acidic (pH 4) and neutral pH (pH 7) favouring associative or segregative interactions. Additionally, the impact of low and high ionic strength (achieved by 10 mM and 100 mM NaCl addition) on emulsion gel structure was studied. The resultant gels were called CO and PE gels where CO refer to control gels and PE refer to gels with added low methoxyl pectin (LMP). These systems were characterized in terms of rheology, microstructure, and fracture properties. The breakdown kinetics of these gels were assessed using dynamic *in vitro* gastric digestion model (Human Gastric Simulator, HGS) and the physicochemical characteristics of the gastric digesta were determined.

For gels made at pH 7, LMP addition led to a decrease in the gelation temperature of CO emulsions, and this effect was more pronounced at low ionic strength. For emulsion gels

formed at low ionic strength, addition of LMP caused the gels to become stronger and less elastic whereas addition of LMP under conditions to emulsion gels formed high ionic strength caused the gels to become weaker and less brittle in comparison to CO gels.

Results from *in vitro* gastric digestion of CO and PE gels formed at pH 7 showed that emulsion gels made at low ionic strength broke down at a faster rate as compared to gels made at high ionic strength. The stability of the emulsion droplets within the gel during gastric digestion was also dependent on the stability of the microstructure. For emulsion gels made at low ionic strength, CO gels were least stable to gastric digestion compared to PE gels. For gels made at high ionic strength the extent of this was discernibly less for PE gels as compared to CO gels. This indicates that pectin addition along with ionic strength played a significant role in the stability of oil droplets during gastric digestion. The extent of gel disintegration and oil released was found to be highly positively correlated.

Heat-set whey protein emulsion gels formed at acidic pH (pH 4) with and without low methoxyl pectin (LMP) gels appeared to be particulate in nature irrespective of ionic strength. LMP addition led to an earlier onset of gelation for PE emulsions as compared to CO emulsions. Increase in ionic strength also led to a decrease in gelation temperature for both CO and PE emulsions. Addition of LMP at low ionic strength, caused the gels to become stronger and more elastic whereas under conditions of high ionic strength, the emulsion gels were stronger but also more brittle.

Results from *in vitro* gastric digestion showed significant differences ($P < 0.05$) in the solid emptying rates, pectin release rates and the extent of lipid release. PE gels made at high ionic strength disintegrated to a lesser extent than PE gels made at low ionic strength. Similarly, CO gels formed at high ionic strength disintegrated to a higher extent as compared to gels formed at low ionic strength. Despite these differences, the oil droplets remained stable during heat-induced gelation, physical shear/ionic changes during simulated oral processing and gastric digestion. A linear positive correlation was found between the rate of the solid emptying from the stomach and the rate of lipid release.

Overall, this research provided new insights on the role of ionic strength and pH in structure formation of protein-polysaccharide emulsion gels. The study also demonstrated how the dynamics of these structural transformations affects *in vitro* gastric digestion. The outcome of this study has the potential to fill the vast knowledge gap of understanding how food structure affects the disintegration and digestion kinetics of complex multicomponent food matrices.

ACKNOWLEDGMENTS

I never thought I would be writing this thesis, let alone this acknowledgement page.

Most of the credit for this Master thesis is to my supervisor Distinguished Professor Harjinder Singh. I would like to thank Professor Harjinder for his patience, for dealing with my back-and-forth behaviour, standing beside me, supporting me and validating whatever progress I was making and mostly for not giving up on me. Thank you for never demeaning my struggle, for being empathic and giving me multiple opportunities to make sure that this thesis saw the light of the day. I appreciate him making time for one-on-one discussions and video meetings, to assist and support me even when he had the busiest of days. I dedicate this thesis to him for all his support.

Equally important has been the role of many other people who have helped me along the way. I would like to thank Prof. Aiqian Ye for the excellent discussions and for his support whenever I needed it. I would like to thank my colleagues and friends at the Riddet Institute for their support both formal and informal. I am deeply grateful for their help and support to complete this path.

I want to thank the Riddet Institute for the financial support and wonderful opportunities it has given me. I wish to thank all the staff at the Riddet Institute and Massey University that helped me with my research, training, and wonderful discussions.

I would like to thank my friends and family that have walked beside me, supported me and believed in me and kept me sane. Especially Alice, Geet and Menu for all your support in New Zealand. To my family, especially mum, Nico and Dhruv. I am eternally grateful for all your love, support, and encouragement.

TABLE OF CONTENTS

ABSTRACT.....	ii
ACKNOWLEDGMENTS	v
TABLE OF CONTENTS.....	vii
LIST OF TABLES.....	xi
LIST OF FIGURES	xiii
LIST OF ACRONYMS AND ABBREVIATIONS.....	xix
1 Introduction.....	1
2 Review of literature	6
2.1 Biopolymers and their functionality in food systems	7
2.2 Protein-polysaccharide interactions.....	8
2.2.1 <i>Liquid systems</i>	8
2.2.2 <i>Co-solubility</i>	9
2.2.3 <i>Thermodynamic Incompatibility</i>	10
2.2.4 <i>Depletion Interaction</i>	10
2.2.5 <i>Complex Coacervation/Complexation</i>	11
2.2.6 <i>Semisolid/solid food systems</i>	11
2.3 Factors that influence protein-polysaccharide interactions	12
2.4 Flocculation in protein-polysaccharide emulsion systems.....	12
2.5 Emulsions.....	16
2.5.1 <i>Emulsion formation</i>	17
2.5.2 <i>Emulsion stability</i>	19

2.5.3	<i>Emulsion gels</i>	21
2.5.4	<i>Emulsion gel formation</i>	22
2.5.5	<i>Rheological properties of emulsion gels</i>	23
2.5.6	<i>Effect of protein-polysaccharide matrices on digestion and postprandial responses</i>	24
2.6	Influence of structure of gastric chyme on satiety and gastric emptying	25
2.7	Influence of protein-polysaccharide systems on gastric emptying, intragastric gelation and satiety	26
2.8	Effect of protein-polysaccharide interactions on protein digestion	26
2.9	Effect of protein-polysaccharide interactions on lipid digestion	28
2.9.1	<i>Gastric colloidal behaviour of milk protein in dairy products under gastric conditions</i>	28
2.9.2	<i>Mechanism of gastric colloidal destabilisation</i>	30
2.9.3	<i>Mechanism for complex structured systems</i>	32
2.10	Conclusions	35
3	Materials and Methods	37
3.1	Materials	37
3.1.1	<i>Emulsion preparation</i>	37
3.1.2	<i>Emulsion gel formation</i>	39
3.2	Properties of liquid emulsions and emulsion gels	39
3.2.1	<i>Zeta potential measurements</i>	39
3.2.2	<i>Particle size characterization by laser diffraction</i>	40
3.2.3	<i>Confocal microscopy</i>	40
3.2.4	<i>Oscillatory rheology</i>	41
3.2.5	<i>Large deformation properties</i>	41
3.3	<i>In vitro</i> dynamic digestion	43

3.3.1	<i>Simulated oral processing</i>	43
3.3.2	<i>Particle size simulation during mastication</i>	43
3.3.3	<i>Simulated bolus preparation</i>	43
3.3.4	<i>In vitro gastric digestion using the Human gastric simulator (HGS)</i>	43
3.3.5	<i>pH measurement</i>	45
3.3.6	<i>Apparent pectin content of the emptied gastric digesta</i>	46
3.3.7	<i>Measurement of the solid content of emptied gastric digesta</i>	46
3.3.8	<i>Measurement of the lipid content of emptied gastric digesta</i>	47
3.3.9	<i>Determination of particle size distribution of emptied digesta</i>	47
3.3.10	<i>Determination of Oil Droplet Size Distribution</i>	47
3.3.11	<i>Statistical Analysis</i>	48
4	The effect of gel structure on the <i>in vitro</i> gastric digestion of protein-polysaccharide emulsion gels: effect of segregative interactions.....	49
4.1	Properties of liquid emulsions prior to heat-induced gelation	51
4.1.1	<i>ζ-potential of liquid emulsions</i>	52
4.1.2	<i>Particle size distribution of liquid emulsions</i>	53
4.1.3	<i>Confocal microscopy of liquid emulsions</i>	55
4.2	Properties of heat-induced emulsion gels	57
4.2.1	<i>Confocal micrographs of emulsion gels</i>	57
4.2.2	<i>Rheological properties</i>	58
4.2.3	<i>Large deformation properties</i>	62
4.3	Behaviour of emulsion gels during dynamic gastric digestion.....	64
4.3.1	<i>pH profile of emptied digesta</i>	64
4.3.2	<i>Changes in the solid content of emptied digesta</i>	67
4.3.3	<i>Release of pectin from emulsion gel during digestion</i>	71

4.3.4	<i>Particle size distribution of emptied digesta</i>	72
4.3.5	<i>Microstructure of emptied digesta</i>	76
4.3.6	<i>Stability of oil droplets during gastric digestion</i>	80
4.3.7	<i>Impact of gel disintegration kinetics on lipid released during dynamic gastric digestion.</i>	85
4.4	Conclusions.....	87
5	The effect of gel structure on gastric digestion of protein-polysaccharide emulsion gels: Effect of associative interactions (pH 4).....	89
5.1	Properties of liquid emulsions prior to heat-induced gelation.....	90
5.1.1	<i>Confocal microscopy of liquid emulsions</i>	90
5.1.2	<i>Confocal micrographs of emulsion gels</i>	91
5.1.3	<i>Rheological properties</i>	93
5.1.4	<i>Large deformation properties</i>	97
5.2	Behaviour of emulsion gels during dynamic gastric digestion.....	100
5.2.1	<i>pH profile of emptied digesta</i>	100
5.2.2	<i>Changes in solid content of emptied digesta</i>	101
5.2.3	<i>Release of pectin from emulsion gel during digestion</i>	105
5.2.4	<i>Particle size distribution of emptied digesta</i>	107
5.2.5	<i>Microstructure of emptied digesta</i>	109
5.2.6	<i>Stability of oil droplets during gastric digestion</i>	114
5.2.7	<i>Impact of gel disintegration on kinetics of lipid release during dynamic gastric digestion</i>	115
5.3	Conclusions.....	117
6	Overall conclusions and future recommendations	118
7	Bibliography.....	125

LIST OF TABLES

Table 2-1 Factors that influence protein–polysaccharide interactions.	14
Table 4-1 Gelation properties during heat-induced gelation for CO (whey protein) and PE (pectin and whey protein) emulsion gels formed at low ionic strength (10 mM) and high ionic strength (100 mM). Gelation time (sec) and gelation temperature (°C) correspond to the time and temperature when an increase of 10 Pa in G' during the heating step was observed. Final storage modulus (KPa) corresponds to the final G' after the cooling step measured at 30 °C. Error bars represent standard deviation (n=5).	60
Table 4-2 Mechanical properties of emulsion gels measured by uniaxial compression, CO (whey protein) and PE (pectin containing whey protein) emulsion gels formed at low ionic strength (10 mM) and high ionic strength (100 mM). Results are shown as mean ± standard deviation of N = 10 independent experiments.	62
Table 4-3 The relationship between the lipid released (%) and solid emptied (%) during gastric digestion for the different gels formed at pH 7, CO (whey protein) and PE (pectin and whey protein) emulsion gels formed at low ionic strength (10 mM) and high ionic strength (100 mM).. The Pearson correlation coefficient value (r), the R square are listed (P < 0.05).	86
Table 5-1 Gelation properties during heat-induced gelation for CO (whey protein) and PE (pectin and whey protein) emulsion gels formed at low ionic strength (10 mM) and high ionic strength (100 mM). Gelation time (sec) and gelation temperature (°C) correspond to the time and temperature when an increase of 10 Pa in G' during the heating step was observed. Final storage modulus (KPa) corresponds to the final G' after the cooling step measured at 30 °C. Error bars represent standard deviation (n=5).	93

Table 5-2 Mechanical properties of emulsion gels measured by uniaxial compression, CO (whey protein) and PE (pectin containing whey protein) emulsion gels formed at low ionic strength (10 mM) and high ionic strength (100 mM). Results are shown as mean \pm standard deviation of N = 10 independent experiments.97

Table 5-3 The relationship between the lipid released (%) and solid emptied (%) during gastric digestion for the different gels formed at pH 4, CO (whey protein) and PE (pectin and whey protein) emulsion gels formed at low ionic strength (10 mM) and high ionic strength (100 mM).. The Pearson correlation coefficient value (r), the R square are listed (P < 0.05). 116

LIST OF FIGURES

Figure 1-1 Rationale of the study.....	5
Figure 2-1 Review of literature summary	6
Figure 2-2 Different types of interactions between protein and polysaccharide in aqueous solutions.....	9
Figure 2-3 Flocculation in protein-polysaccharide emulsions.....	13
Figure 2-4 Schematic representations of two proposed emulsion gel models: an emulsion-filled protein gel and an emulsion gel stabilized by protein (Dickinson, 2012).....	21
Figure 2-5 Emulsion gels formed by varying different properties.....	23
Figure 3-1 Emulsion preparation and emulsion gel formation	38
Figure 4-1 Zeta potential measurements of whey protein emulsions (CO) with 10 mM NaCl, Whey protein-LMP emulsions (PE) with 10 mM NaCl, Whey protein emulsions (CO) with 100 mM NaCl and Whey protein-LMP (PE) with 100 mM NaCl as a function of pH. Stock emulsion refers to primary emulsion (12.5 wt% WPI and 25 wt% soybean oil, $d_{4,3} \sim 0.5 \mu\text{m}$) used to formulate the various treatments. The measurements were replicated at least six times. Error bars represent standard deviations. For Figure 4-1, columns with different letters are significantly different ($P < 0.05$) for each pH.....	51
Figure 4-2 Particle size distributions ($d_{4,3}$) of (2-A) Whey protein emulsions (CO) with 10 mM NaCl, (2-B) Whey protein-Low methoxyl pectin emulsions (PE) with 10 mM NaCl, (2-C) Whey protein emulsions (CO) with 100 mM NaCl and (2-D) Whey protein-Low methoxyl pectin emulsions (PE) with 100 mM NaCl as a function of pH. Stock emulsion refers to primary emulsion (12.5 wt% WPI and 25 wt% soybean oil, $d_{4,3} \sim 0.5$	

µm) used to formulate the various treatments. The measurements were replicated at least six times. Error bars represent standard deviations.....54

Figure 4-3 Confocal micrographs of emulsions before (A-D) and after heat gelation (E-H). Micrographs on the left represent liquid emulsions. A) whey protein emulsions (CO) with 10 mM NaCl, B) Whey protein-Low methoxyl pectin emulsions (PE) with 10 mM NaCl, C) Whey protein emulsions (CO) with 100 mM NaCl D), Whey protein-Low methoxyl pectin emulsions (PE) with 100 mM NaCl. The micrographs on the right represent the corresponding emulsions after heat gelation, namely E) Whey protein emulsion gel (CO) with 10 mM NaCl F), Whey protein-Low methoxyl pectin emulsion gel (PE) with 10 mM NaCl, G) Whey protein emulsion gel (CO) with 100 mM NaCl H), Whey protein-Low methoxyl pectin emulsion gel (PE) with 100 mM NaCl. Red represents the oil and green represents the protein. The scale bar corresponds to 25 µm.56

Figure 4-4 Change in storage modulus (G') during heat induced gelation of emulsions (0.5% strain, 1 Hz) at pH 7: (A) CO (whey protein) and PE (pectin and whey protein) emulsion gels formed at low ionic strength (10 mM); (B), CO (whey protein) and PE (pectin and whey protein) emulsion gels formed at high ionic strength (100 mM). The straight black line denotes the time-dependence of heating at temperature (°C).....59

Figure 4-5 Changes in pH of the emulsion gels during dynamic gastric digestion in the HGS: A, CO (whey protein) and PE (pectin containing whey protein) emulsion gels formed at low ionic strength (low ionic strength-10 mM); B, CO (whey protein) and PE (pectin containing whey protein) emulsion gels formed at high ionic strength (low ionic strength- 100 mM). Error bars represent standard deviation (n=5)..... 66

Figure 4-6 Changes in dry matter of the emulsion gels during dynamic gastric digestion in the HGS as a function of digestion time: A, CO (whey protein) and PE (pectin containing whey protein) emulsion gels formed at low ionic strength (low ionic strength-10 mM); B, CO (whey protein) and PE (pectin containing whey protein) emulsion gels formed at high ionic strength (low ionic strength- 100 mM). Error bars represent standard deviation (n=5).68

Figure 4-7 Low methoxyl pectin content of the gastric digesta (mg/ml) as a function of digestion time (A) and cumulative percent of pectin release (B) during gastric vitro digestion for the soft (gels made with 10 mM NaCl) and hard gels (gels made with 100 mM NaCl). Results are expressed as pectin content (mg/g) of the gastric digesta at each time point on dry weight basis. Based on this data, a cumulative percent of pectin released (%) over digestion time (min) was also plotted. This was calculated based on the release of pectin at specific digestion times..... 71

Figure 4-8 Changes in particle size distribution (volume-weighted average diameter $d_{4,3}$) of (A1 and A2) CO gels (whey protein) and PE gels (pectin and whey protein) emulsion gels formed at low ionic strength (10 mM); (B1 and B2), CO gels (whey protein) and PE gels (pectin and whey protein) emulsion gels formed at high ionic strength (100 mM) during gastric digestion in the human gastric simulator. The legends at the top left of each stack indicate the gastric digestion time. 74

Figure 4-9 The schematic diagram represents possible contributors in the emptied gastric digesta that impact the particle size distribution of the emptied digesta at different length scales. 75

Figure 4-10 CLSM images of gastric digesta as a function of digestion time during dynamic gastric digestion in the HGS: Micrographs on the left represent gastric digesta of gels formed at low ionic strength, whey protein emulsions (CO) with 10 mM NaCl, Whey protein-Low methoxyl pectin emulsions (PE) with 10 mM NaCl at different digestion time points (30 min- 240 min), whereas micrographs on the right represent gastric digesta of gels formed at high ionic strength, whey protein emulsions (CO) with 100 mM NaCl, Whey protein-Low methoxyl pectin emulsions (PE) with 100 mM NaCl. Red represents the oil and green represents the protein. The scale bar corresponds to 25 μm 78

Figure 4-11 Changes in volume-weighted average diameter $d_{4,3}$ of CO (whey protein) and PE (pectin and whey protein) emulsion gels formed at low ionic strength (10 mM); (C1 and C2), CO (whey protein) and PE (pectin and whey protein) emulsion gels formed at high ionic strength (100 mM). The measurements were replicated at least six times. Error

bars represent standard deviations. For Figure 4-11, bars without a common superscript letter differ ($P < 0.05$) as analyzed by one-way ANOVA and the Tukey test.....80

Figure 4-12 Changes in oil droplet size distribution of (B1 and B2) CO (whey protein) and PE (pectin and whey protein) emulsion gels formed at low ionic strength (10 mM); (C1 and C2), CO (whey protein) and PE (pectin and whey protein) emulsion gels formed at high ionic strength (100 mM). The measurements were replicated at least six times. Error bars represent standard deviations.83

Figure 4-13 Changes in fat content (%) of the emptied digesta during dynamic gastric digestion in the HGS: A1, CO (whey protein) and PE (pectin containing whey protein) emulsion gels formed at low ionic strength (low ionic strength-10 mM); A2, CO (whey protein) and PE (pectin containing whey protein) emulsion gels formed at high ionic strength (low ionic strength- 100 mM). Error bars represent standard deviation ($n=5$). 86

Figure 5-1 Confocal micrographs of emulsions before (A-D) and after heat gelation (E-H) formed at pH 4. Micrographs on the left represent liquid emulsions. A) whey protein emulsions (CO) with 10 mM NaCl, B) Whey protein-Low methoxyl pectin emulsions (PE) with 10 mM NaCl, C) Whey protein emulsions (CO) with 100 mM NaCl D), Whey protein-Low methoxyl pectin emulsions (PE) with 100 mM NaCl. The micrographs on the right represent the corresponding emulsions after heat gelation, namely E) Whey protein emulsion gel (CO) with 10 mM NaCl F), Whey protein-Low methoxyl pectin emulsion gel (PE) with 10 mM NaCl, G) Whey protein emulsion gel (CO) with 100 mM NaCl H), Whey protein-Low methoxyl pectin emulsion gel (PE) with 100 mM NaCl. Red represents the oil and green represents the protein. The scale bar corresponds to 25 μm92

Figure 5-2 Change in storage modulus (G') during heat induced gelation of emulsions (0.5% strain, 1 Hz) at pH 7: (A) CO (whey protein) and PE (pectin and whey protein) emulsion gels formed at low ionic strength (10 mM); (B), CO (whey protein) and PE (pectin and whey protein) emulsion gels formed at high ionic strength (100 mM). The straight black line denotes the time-dependence of heating at temperature ($^{\circ}\text{C}$).....96

Figure 5-3 Changes in pH of the emulsion gels during dynamic gastric digestion in the HGS: A, CO (whey protein) and PE (pectin containing whey protein) emulsion gels formed at low ionic strength (low ionic strength-10 mM); B, CO (whey protein) and PE (pectin containing whey protein) emulsion gels formed at high ionic strength (low ionic strength- 100 mM) at pH 4. Error bars represent standard deviation (n=5). Error bars are smaller than the symbol size..... 100

Figure 5-4 Changes in dry matter of the emulsion gels during dynamic gastric digestion in the HGS: A, CO (whey protein) and PE (pectin containing whey protein) emulsion gels formed at low ionic strength (low ionic strength-10 mM); B, CO (whey protein) and PE (pectin containing whey protein) emulsion gels formed at high ionic strength (low ionic strength- 100 mM). Error bars represent standard deviation (n=5). 102

Figure 5-5 (A) The low methoxyl pectin content of the gastric digesta (mg/ml) during gastric digestion and (B) cumulative percent of pectin release during gastric vitro digestion for the soft (gels made with 10 mM NaCl) and hard gels (gels made with 100 mM NaCl). Results are expressed as pectin content (mg/g) of the gastric digesta at each time point on dry weight basis. Based on this data, a cumulative percent of pectin released (%) over digestion time (min) was also plotted. This was calculated based on the release of pectin at specific digestion times..... 106

Figure 5-6 Changes in particle size distribution (volume-weighted average diameter $d_{4,3}$) of (A and B) CO gels (whey protein) and PE gels (pectin and whey protein) emulsion gels formed at low ionic strength (10 mM); (C and D), CO gels (whey protein) and PE gels (pectin and whey protein) emulsion gels formed at high ionic strength (100 mM) during gastric digestion in the human gastric simulator. The legends at the top left of each stack indicate the gastric digestion time. 107

Figure 5-7 CLSM images of gastric digesta as a function of digestion time during dynamic gastric digestion in the HGS of gels formed at low ionic strength; CO (whey protein) and PE (pectin containing whey protein) emulsion gels formed at low ionic strength (ionic strength-10 mM); Red represents the oil and green represents the protein. The scale bar corresponds to 25 μm 112

Figure 5-8 CLSM images of gastric digesta as a function of digestion time during dynamic gastric digestion in the HGS of gels formed at high ionic strength: CO (whey protein) and PE (pectin containing whey protein) emulsion gels formed at high ionic strength (ionic strength-100 mM); Red represents the oil and green represents the protein. The scale bar corresponds to 25 μm 113

Figure 5-9 Changes in volume-weighted average diameter $d_{4,3}$ of CO (whey protein) and PE (pectin and whey protein) emulsion gels formed at low ionic strength (10 mM); (C1 and C2), CO (whey protein) and PE (pectin and whey protein) emulsion gels formed at high ionic strength (100 mM). The measurements were replicated at least six times. Error bars represent standard deviations. The values weren't significantly different ($P < 0.05$) as analysed by one-way ANOVA and the Tukey test. 115

LIST OF ACRONYMS AND ABBREVIATIONS

Isoelectric point	IEP
Elastic or storage modulus	G'
Viscous or loss modulus	G''
Glucono delta lactone	GDL
Hydrochloric acid	HCl
Sodium hydroxide	NaOH
Whey protein isolate	WPI
Sodium chloride	NaCl
Low methoxyl pectin	LMP
Sodium dodecyl sulphate	SDS
Simulated gastric fluid	SGF
Gastrointestinal tract	GIT

1 Introduction

For a long time, it was assumed that the nutrient content of a food reflected its nutritional value and health impact. We know now, through extensive research, that it is a combination of the nutritional content, and the way nutrients are assembled in the food matrix that determines their gastro-intestinal fate and eventual nutritional/health outcomes. For instance, food material properties and structures can be manipulated to some extent under physiological conditions to control the uptake of lipids thus influencing satiety and calorific intake (Singh et al., 2009). To deduce the effect of food structure on nutrient accessibility during digestion, several *in vitro* and *in vivo* studies have been undertaken using single or/and mixed biopolymer iso-caloric systems to establish fundamental relationships between food structure, nutritional composition and physiological outcomes in order to understand the underlying mechanisms occurring during gastrointestinal digestion (Dias et al., 2019; Dougkas et al., 2012; Juvonen et al., 2015; Mackie et al., 2013).

Many foods are typically oil-in-water emulsion systems, in which proteins or phospholipids emulsify the oil phase by forming an interfacial film that confer stability against oil droplet flocculation and coalescence. There have been extensive studies on how these interfaces and structures can be engineered in model emulsion systems to control lipolysis during gastro-intestinal digestion (McClements & Li, 2010; Singh & Sarkar, 2011; Acevedo-Fani & Singh, 2022). However, most structured processed foods, such as yoghurt, ice cream, cheese and meat products are multicomponent emulsion gel systems containing protein, polysaccharides along with salt, sugar, flavours and additives.

Polysaccharides confer a texture enhancing/stabilising effect and affects the textural and organoleptic properties of these systems. For systems containing proteins and polysaccharides, there is extensive research on understanding the complex thermodynamic and physico-chemical interactions occurring between the two, whether associative or segregative, and how these interactions impact on the final stability and functionality of the system (Turgeon et al., 2003; Corredig et al., 2011). For emulsion gels, similar thermodynamic interactions occur as liquid systems with the addition of a gelation or aggregation step that provides network-like structure and helps in partially arresting the thermodynamic interactions giving rise to different microstructures with various structural properties and functionalities (Dickinson, 2012). Most of these studies use highly dilute mixtures or use high amounts of polysaccharide not commonly used in commercial preparations (Semenova et al., 2014; Wijaya et al., 2017). In addition, the structural properties of the food matrix also dictate the rate and which these biopolymers are digested - this topic has not been well studied (Fardet et al., 2019; Golding et al., 2011; Lovegrove et al., 2017).

Emulsion gels, containing both protein and polysaccharide, serve as ideal model systems for semi solid foods because they (1) are representative of complex real foods, (2) can be carefully designed by modulating the thermodynamic and physico-chemical interactions to impart the desired functionality, (3) can be modified by varying the properties of the emulsion gel matrix, properties of oil phase and interactions between the matrix and oil droplets, and (4) can be designed to deliver either lipophilic or hydrophilic bioactive compound where the gel matrix regulates its release and stability.

For protein-stabilised emulsions, gastric proteolysis generally precedes intestinal proteolytic and lipolytic digestion under simulated GI conditions. There is evidence to suggest that preceding protein digestion influences the kinetics of subsequent lipid digestion for protein stabilised emulsion systems (Mackie, 2020; Singh et al., 2009; Ye et al., 2020). Also, the use of a dynamic/semi dynamic gastric digestion model has been reported to shed more light on the complexities of gastric digestion compared to a static *in vitro* digestion system.

It is well known that for whey proteins, their native confirmation, heat-induced denaturation, interfacial absorption, gelation and amenability to environmental conditions (pH, ionic strength) affects their digestion kinetics (Guo et al., 2014; Luo et al., 2015; Macierzanka et al., 2009; Wang et al., 2018). Previous research has also shown how the microstructure of whey protein gels determines the extent of proteolysis (Macierzanka et al., 2012), lipolysis (Sarkar et al., 2015) or the release of encapsulated material (Luo et al., 2019; Remondetto et al., 2004). Recent work undertaken in our laboratory has shown that for heat-induced “soft” (fine-stranded) and “hard” (particulate) whey protein-based emulsion gels made by varying the ionic strength, the rate of protein hydrolysis by pepsin was faster for the soft gel which consequently led to a higher rate of oil droplet release compared to the harder gel (Guo et al., 2014)

For multicomponent systems such as for those containing proteins and polysaccharides, the dynamic structural changes occurring during gastro-intestinal digestion are poorly understood. For this work, low methoxy pectin (LMP) was chosen, as it is a feasible anionic polysaccharide for use in food systems at both acidic and neutral pH. Ionic

strength was chosen as a variable parameter as it is known to impact structural properties of the protein-based emulsion gels and also the interactions between proteins and polysaccharides. The rheological, microstructural and textural properties were used to assess the effects of varying ionic strength and LMP addition on the gel structure. The breakdown kinetics of these gels were assessed under dynamic *in vitro* gastric digestion using the human gastric simulator (HGS) and the physicochemical characteristics of the emptied digesta were determined. A dynamic *in vitro* gastric digestion simulation is better representative of the changes that occur during gastric digestion as compared to a static digestion system. Assessing the behaviour of emulsified lipids containing complex biopolymer systems under physiological conditions would provide a better understanding of the colloidal interactions that occur in complex multicomponent systems during their digestion under gastric digestion. Also, this knowledge on how food structure affects the kinetics of nutrients would potentially help to developing and improving dairy-based food products with enhanced nutritional properties.

Research hypothesis and objectives

Addition of polysaccharide (such as pectin) to protein-based emulsions will influence the microstructure and rheological properties of the resultant emulsion gels. Assessing the behaviour of emulsified lipids containing complex biopolymer systems under physiological conditions would provide a better understanding of the colloidal interactions that occur in complex multicomponent systems during their disintegration. There is enough evidence to suggest that preceding gastric protein digestion and breakdown behaviour influences the kinetics of subsequent lipid release and digestion for

these systems. Also, the use of a dynamic/semi dynamic gastric digestion model has been reported to shed more light on the complexities and nuances of gastric digestion compared to a static system.

The research objectives as follows:

- To study the effect of low methoxy pectin (LMP) on the formation and physical characteristics (microstructure, rheological properties) of whey protein emulsion gels.
- To study the *in vitro* gastric digestion behaviour of emulsion gels formed at neutral pH (pH 7), favouring segregative interactions between the whey proteins and LMP.
- To study the *in vitro* gastric digestion behaviour of emulsion gels at acidic (pH 4) favouring associative interactions between the whey proteins and LMP.

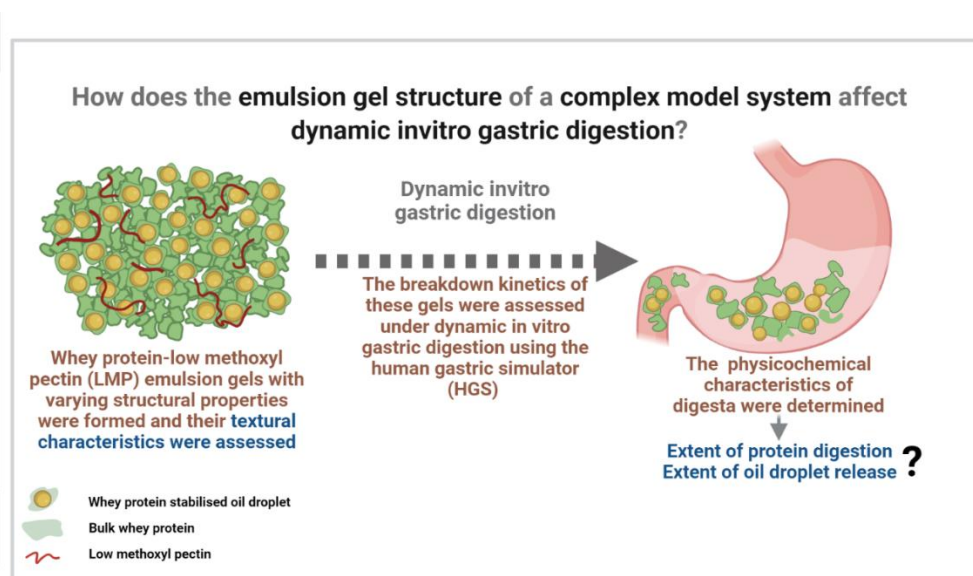


Figure 1-1 Rationale of the study

2 Review of literature

This chapter provides a brief review of protein-polysaccharide interactions in food systems, basic concepts of the mixing behaviour of biopolymer solutions and the factors contributing to their formation and their various functionalities. It also covers properties of whey proteins and low methoxyl pectin (LMP). Current protein-based emulsion systems, both natural and model systems, are also reviewed. It also covers design of protein-based emulsions of identical composition but different structures to study the effect of matrix structure on protein and lipid digestion kinetics. In addition, possible mechanisms of gastric colloidal destabilisation for simple and complex structured systems are discussed. The research gaps are identified i.e., lack of information on protein polysaccharide solid/semi-solid emulsion-based systems and the effect of the matrix on its digestion behaviour. Part of the literature review is published with permission from Nayak, N., & Singh, H. (2019).

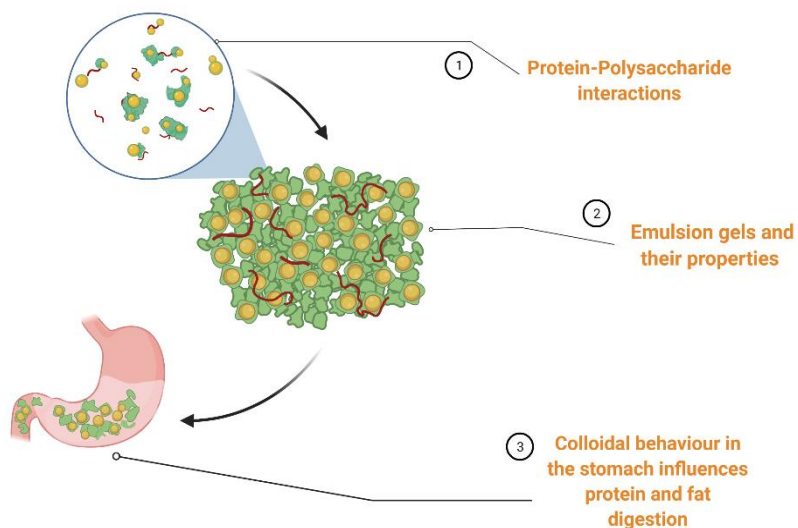


Figure 2-1 Review of literature summary

2.1 Biopolymers and their functionality in food systems

Proteins and polysaccharides are commonly used as ingredients in food formulations. These biopolymers confer vital functionality, such as thickening, stabilizing, gelling, and emulsifying properties, to food products. The functional properties of individual biopolymers (either used naturally or added as ingredients) add to the complexity of the multi-component food system. The overall stability and the microstructure of the food system depend on the individual functionalities of the proteins and polysaccharides and also on the nature and the strength of interactions between them.

Milk proteins, namely caseins and whey proteins, have different characteristics depending on the type of system in which they are present. Casein exists in different states, ranging from small, dissolved macromolecules to stable colloidal particles. It exists mostly in the colloidal state in commercial dairy products, whereas whey proteins are present as dissolved polymers of low molecular weight unless temperature/high pressure treatments are used, which lead to unfolding and aggregation. Aggregates of whey proteins that are formed by thermal and high-pressure processing have their own functional properties. The interaction of polysaccharides with milk proteins leads to the formation of a ternary 'milk protein–polysaccharide–water' polyelectrolyte solution. An understanding of the basic concepts of the mixing behaviour of biopolymer solutions and the factors contributing to their formation and their various functionalities is important in the elucidation of this rather complicated system.

2.2 Protein-polysaccharide interactions

2.2.1 Liquid systems

When aqueous solutions containing proteins and polysaccharides are mixed, one of four phenomena can occur: (1) co-solubility, i.e., the components mix well and the solution is stable; (2) thermodynamic incompatibility, i.e., the polymers repel each other and two phases appear, one abundant in polysaccharide and the other abundant in protein; (3) depletion interaction, which occurs in colloidal dispersions in the presence of non-interacting polymers (e.g., polysaccharides in an emulsion, or polysaccharides and colloidal casein micelles); (4) complex coacervation, i.e., electrostatic interaction occurs, giving rise to a concentrated protein–polysaccharide phase and a dilute phase (Figure 2-2).

It is important to consider the influence of the biopolymer concentration on the enthalpic interactions occurring in the system. For mixed polymer systems at high dilutions, the system becomes homogeneous regardless of whether thermodynamic incompatibility or coacervation occurs. However, coacervation can occur in dilute solutions whereas thermodynamic incompatibility cannot. Some terms associated with mixed biopolymer systems are listed below.

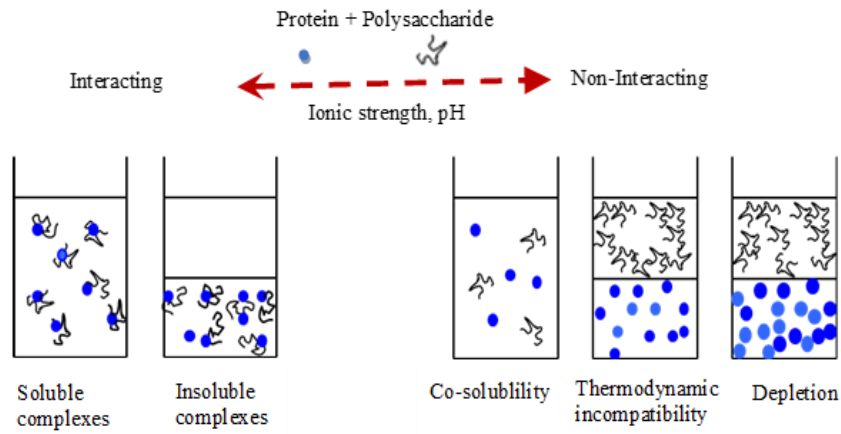


Figure 2-2 Different types of interactions between protein and polysaccharide in aqueous solutions.

2.2.2 Co-solubility

This phenomenon is based on the thermodynamic principle that the Gibbs free energy of mixing (ΔG_{mixing}) is negative when the entropy of mixing favorably exceeds the enthalpy term. The highest entropy is achieved when different kinds of molecules are randomly distributed throughout the system.

The expression for the Gibbs free energy accompanying mixing under standard conditions is given by.

$$\Delta G_{\text{mixing}} = \Delta H_{\text{mixing}} - T\Delta S_{\text{mixing}} \quad \text{Equation 1}$$

where ΔG_{mixing} , ΔH_{mixing} , and $T\Delta S_{\text{mixing}}$ are the free energy, enthalpy (interaction energy), and entropy changes, respectively, between the mixed and unmixed states.

As the entropy of a mixed biopolymer system is much lower than that for smaller molecules, the system tends to become less co-soluble because of thermodynamic incompatibility. Also, given the polymeric nature of proteins and polysaccharides and the presence of various functional groups in their macromolecules, co-solubility is the least typical situation.

2.2.3 Thermodynamic Incompatibility

This occurs when two dissimilar non-interacting macromolecular species separate into two different phases because the enthalpy of mixing exceeds the entropy difference. Such phenomena are also observed when the two biopolymers have different affinities towards the solvent. For mixed systems, molecular and structural differences between the same biopolymers also give rise to thermodynamic incompatibility (polysaccharides with different structures, proteins of different classes, e.g., proteins of different solubilities, native and denatured forms of the protein, and aggregated and non-aggregated forms of the same protein).

2.2.4 Depletion Interaction

Depletion interaction occurs in systems containing depletants such as nonadsorbing polysaccharides. It occurs by entropically driven exclusion of the depletant by an osmotic pressure gradient, ultimately leading to flocculation of the system. This type of flocculation is considered to be weak or reversible as the flocs are easily broken down on remixing. However, in most food systems, this weak flocculation may lead to extensive aggregation, resulting in creaming and instability of the system.

2.2.5 Complex Coacervation/Complexation

This phenomenon occurs because of the formation of electrostatic complexes between the protein molecules and the polysaccharide molecules, resulting in a two-phase system. One phase is rich in both biopolymers that represent the complex, whereas the other phase contains the excluded solvent and is depleted in biopolymers. This is observed when two oppositely charged biopolymers interact. These reactions are highly dependent on the ionic nature of the system. Coacervates are formed when proteins interact with polysaccharides that have a low charge density and/or a very elastic backbone, e.g., gum arabic, gelatin, dextran, pectin etc.

2.2.6 Semisolid/solid food systems

For structured food systems, similar thermodynamic interactions occur as in liquid systems with the addition of a gelation or aggregation step that gives structure and helps in partially arresting the thermodynamic interactions. In a system where protein-polysaccharide do not interact, gelation of either one or both components will result in arresting the thermodynamic incompatible system depending on the rates of phase separation and gelation. These systems might appear homogenous at a macroscopic scale but will be heterogeneous at a more microscopic level. In addition, interactions occurring between proteins and polysaccharides might also add to the functionality of the gelled/aggregated system. For example, electrostatic interactions occurring between whey protein-pectin lead to the formation of soluble complexes which has shown to improve water-holding capacity and gel strength of acid –induced gels (Zhang, Zhang et

al. 2014) and heat-induced gelation properties of the whey protein (Benichou, Aserin et al. 2002).

2.3 Factors that influence protein-polysaccharide interactions

Factors that affect the nature of protein-polysaccharide interactions and the corresponding structures formed can be classified as extrinsic, intrinsic, and processing factors (Table 2-1). These factors can be varied to obtain desired functionalities for tailored applications (Ye, 2008).

2.4 Flocculation in protein-polysaccharide emulsion systems

Protein stabilized emulsions generally flocculate under certain conditions, depending on the interactions of proteins among themselves and the nature of the bulk system. Flocculation is induced by numerous factors, for example at pH values close to pI, increasing ionic strength, addition of divalent cations, addition of polysaccharides etc. (Figure 2-3).

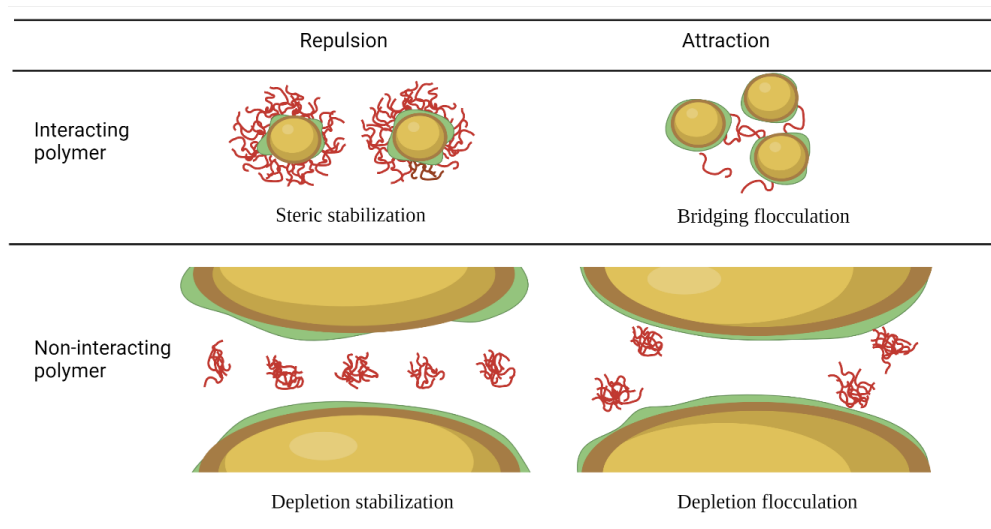


Figure 2-3 Flocculation in protein-polysaccharide emulsions

Processing conditions such as heat, pressure or enzyme action allow proteins to cross-link also leading to droplet flocculation. Characteristic flocculation that occurs in protein-stabilized emulsions on addition of polysaccharide is what contributes to the texture and mouthfeel of many food products, e.g., chocolate milks and low fat dairy products. Under associative conditions, interactions between adsorbed protein and polysaccharide (in the continuous phase) lead to bridging flocculation of emulsion droplets. Under segregative conditions at neutral pH, protein- polysaccharides interaction can lead to depletion flocculation; however, due to the high viscosity of the polysaccharide the system may form a gel-like network preventing creaming. Different extents of flocculation lead to different textures and mouthfeel of these products. For emulsion gels, the extent of pre-induced flocculation in emulsions before gelling will influence the final properties of the gels.

Table 2-1 Factors that influence protein–polysaccharide interactions.

Factor	Observations
Extrinsic Mixing ratio (<i>r</i>)	Affects structure of complexes or coacervates formed. Lower <i>r</i> results in the formation of coacervates that coalesce quickly, whereas higher <i>r</i> results in more stable coacervates.
Molecular concentration	Coacervation can occur in very dilute solutions, whereas thermodynamic incompatibility is favored in more concentrated systems.
pH	At a pH > the isoelectric point (pI) of the protein, there is repulsion between the protein and the polysaccharide. Near the pI, soluble complexes are formed, whereas a further reduction in the pH results in the formation of coacervates.
Ionic strength	At high salt concentration, micro-ions cause a decrease in electrostatic interaction, whereas, at low ionic strength, interference to the formation of the protein–polysaccharide complex is minimal.

Charge density		Coacervation does not occur at low charge densities, whereas precipitation of the inter-polymeric complexes occurs at very high charge densities. The nature of the charge group (carbonyl versus sulfated) influences the interaction strength.
Intrinsic	Molecular conformation	Increased chain flexibility and increased charge mobility result in stronger binding.
Charge distribution		Evenly charged chains form large homogeneous phases, whereas an uneven charge distribution leads to the formation of a meso-phase with a micellar structure.
Molecular weight		The internal structure and the final size of the complexes/coacervates can be controlled by adjusting the molecular weight of the polyelectrolyte.
Processing	Shear	Shear either can cause restructuring of the complexes formed or can stabilize coacervates against flocculation.

Pressure	Pressure causes partial denaturation of the protein, which strengthens the interaction during complex formation.
Temperature	Heat denaturation increases the molecular flexibility, which leads to stronger electrostatic interactions, yielding more stable complexes.
Acidification	The type of acidification method used, e.g., hydrochloric acid or glucono-delta-lactone, influences the structure of the complexes formed.

2.5 Emulsions

The term "emulsion" refers to a colloidal dispersion in which discrete droplets are suspended in a continuous phase in which they are immiscible. Between the two phases, there is an interfacial layer where the surfactant material is adsorbed. Oil-in-water (O/W) emulsions, such as milk and salad dressing, are made of oil droplets dispersed in water, whereas water-in-oil (W/O) emulsions, such as butter and margarine, are made of water droplets dispersed in oil. There is another type of emulsion known as a double emulsion, in which water droplets are encapsulated in oil droplets and then dispersed in continuous water phase (water-in-oil-in-water or W/O/W emulsions) or oil droplets are encapsulated

in water droplets and dispersed in continuous oil phase (oil-in-water-in-oil or O/W/O emulsions) (Dalglish, 2003; Luo, N., 2021).

Depending on their thermodynamic stabilities, emulsions can be divided into two categories: conventional and micro-emulsions. Because conventional emulsions are thermodynamically unstable, they eventually separate into an oil layer on top of a water layer. During emulsion formation, they require energy input. On the other hand, micro-emulsions are thermodynamically stable and, under the correct circumstances, can form spontaneously (McClements, 2012; Luo, N., 2021). Unless otherwise stated, only conventional O/W emulsions are mentioned in this work.

2.5.1 Emulsion formation

Oil and water are mixed in a specific proportion to make emulsions, after which energy is supplied to the system to break up the oil or water phase and form tiny droplets. Typically, mechanical shearing or sonication provides the energy. In order to stabilize the droplets and stop them from fusing together, emulsifiers are added during emulsion formation to lower the interfacial tension, by forming a protective layer around the droplets to stabilize and prevent them from merging with each other.

Emulsifiers are a category of amphiphilic chemicals that can bind to the interface and lower interfacial tension between oil-water or air-water (Krog & Vang Spars, 2003). Depending on their molecular weights, they can be divided into two categories: small-molecule surfactants (such polysorbates, sugar esters, and monoglycerides); and proteins (like casein and lactoglobulin). During emulsification, small-molecule surfactants can

readily adsorb to the interface, where their hydrophobic parts will stick to the oil and their hydrophilic components to the water. The phase where the surfactant is more soluble becomes the continuous phase, according to Bancroft's rule. Small-molecule surfactants are characterized by their HLB (hydrophilic-lipophilic balance) values, which range from 3 (more soluble in oil) to more than 10 (more soluble in water) (Dalglish, 2003).

In comparison to small-molecule surfactants, emulsifying mechanisms of protein are more complex. Normal native protein solubility in water occurs at pH levels far from their isoelectric points. For instance, native β -lactoglobulin is soluble at neutral pH, and the hydrophobic parts of β -lactoglobulin are hidden inside its globular structure while the hydrophilic parts are exposed to water. The β -lactoglobulin, however, undergoes a conformational shift during emulsification that exposes its hydrophobic components during and/or immediately after adsorption. Adsorbed proteins are consequently partially denatured. After adsorption, their stabilizing mechanisms at play are typically electrostatic and/or steric repulsion. Protein adsorption to the interface, on the other hand, is reversible and can be replaced by small-molecule surfactants when present in adequate concentrations (Dalglish, 1997). This is due to the fact that small-molecule surfactants, in general, may lower interfacial tension to a greater extent than proteins, and can adsorb to the interface much easier and faster. The degree to which small-molecule surfactants desorb and displace proteins is determined by the surfactant/protein ratio (Luo, N., 2021).

2.5.2 Emulsion stability

Creaming, sedimentation, flocculation, coalescence, Oswald ripening, and phase inversion (REF) are all phenomena that destabilize emulsions. They behave independently and can have an impact on one another (McClements, 2009). Temperature, pH, ionic strength, and the addition of other molecules like polysaccharides can all cause emulsion destabilization.

Creaming or sedimentation happens when the density of the continuous and scattered phases differs. The velocity of moving droplets depends on the variations in gravitational, buoyancy, and friction forces. The Stock's law equation below explains this:

$$v_{droplet} = \frac{2R^2g}{9\mu_c}(\rho_c - \rho_d) \quad \text{Equation 2-2}$$

Where, $v_{droplet}$ is the velocity of creaming or sedimentation; R is the emulsion droplet radius; μ_c is the viscosity of the continuous phase; ρ_c and ρ_d are the densities of continuous and dispersed phase respectively; g is the gravitational acceleration.

According to this equation, creaming or sedimentation can be decelerated by decreasing emulsion droplet size, and/or increasing the viscosity of the continuous phase, and/or decreasing the density difference between the continuous and dispersed phases.

Flocculation is the process whereby two or more droplets aggregate into larger units but do not merge into larger droplets (Tadros, 2013). Droplet-droplet interactions help explain the mechanism of flocculation. Evans and Wennerström (1994) proposed the

following equation to describe droplet flocculation in colloidal systems containing monodispersed spherical particles:

$$\frac{dn_t}{dt} = -\frac{1}{2}EF \quad \text{Equation 2-3}$$

Where, n_t is the total number of particles per unit volume; t is the time; dn_t/dt is the flocculation rate; E is the collision efficiency; F is the collision frequency.

The collision frequency, defined as the total number of droplets encountered per time per unit volume, is mostly determined by Brownian motion. The collision efficiency, represented as the fraction or likelihood of droplet flocculation contacts, is affected by the nature of the interfacial films and the forces (attractive vs. repulsive) between droplets. Van der Waals contacts, depletion interactions, hydrophobic interactions, hydrogen bonds, and electrostatic interactions between oppositely charged ionic groups all contribute to attractive forces. Electrostatic repulsion, steric repulsion, and Born repulsion are the repulsive forces. By modulating droplet-droplet interactions, flocculation can be prevented (McClements, 2015; Luo, N., 2021.).

2.5.3 Emulsion gels

An emulsion gel is a complicated colloidal system that may exist as both an emulsion and a gel (Dickinson, 2012). As a result, it requires emulsifiers as well as gelling or thickening agents during formation. They can be the same or different components, each of which has a significant impact on the emulsion gel characteristics. Whey proteins as a gelling agent is discussed here.

Emulsion gels are classified into two categories based on their structural arrangements: (Dickinson, 2012): emulsion-filled protein gels (Fig. 2-4 a); protein-stabilized emulsion gel (Fig. 2-4 b). In actuality, an emulsion gel is often a combination of the two. Because emulsion oil droplets are embedded in the protein gel matrix in emulsion-filled protein gels (Fig 2-4 a), their solid-like rheological properties are mostly determined by the protein gel matrix. However, the size of the oil droplet has a significant impact on the gel's strength: if the oil droplet is small, it can be incorporated into the protein gel network, making the gel stronger; if the oil droplet is large, it disrupts the gel network, making the gel weaker.

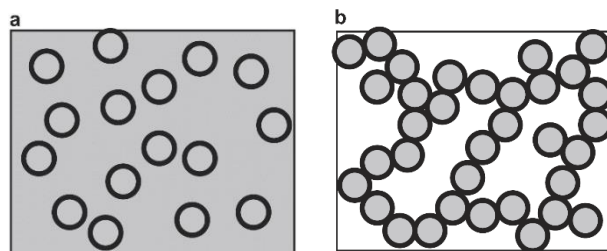


Figure 2-4 Schematic representations of two proposed emulsion gel models: an emulsion-filled protein gel and an emulsion gel stabilized by protein (Dickinson, 2012).

Protein-coated oil droplets aggregate randomly or at a specific angle to create a space-spanning network in protein-stabilized emulsion gels. Since they are a particulate gel, their rheological characteristics are primarily influenced by the network properties of aggregated oil droplets (Dickinson, 2012). For instance, changes in pH or ionic strength will alter the surface charge of oil droplets stabilised by protein. Therefore, it will have an impact on how oil droplets approach one another and consequently have an impact on the network thickness and strength: when the surface charge is low, electrostatic repulsion between oil droplets is low, allowing them to easily approach one another at a random angle, the network is closely packed and strong. Conversely, if the surface charge is high, electrostatic repulsion between oil droplets is strong, and they can only approach each other at a specific angle; the network is weaker since there are fewer oil droplets aggregated per unit volume.

2.5.4 Emulsion gel formation

The initial step in the development of an emulsion gel is the preparation of a liquid emulsion, which is typically accomplished through high-pressure homogenization or high-shear mixing. The emulsion is characterised by its oil content, droplet size distribution, emulsifier type, and concentration (Dickinson, 2012). A protein emulsifier, such as sodium caseinate or whey protein isolate, or a small-molecule surfactant, such as polysorbates, sugar esters, or monoglycerides, can be used as an emulsifier.

Then, the emulsion gel is produced by either aggregating the oil droplets, gelling the continuous phase, or combining both (Dickinson, 2012). Even centrifugation of the emulsion oil droplets is enough to generate a dense protein-stabilized emulsion with solid-

like characteristics (Dimitrova & Leal-Calderon, 2001). It is well known that for whey proteins, their native confirmation, heat/chemical denaturation, interfacial absorption, and amenability to environmental conditions (pH, ionic strength) affects their gelation properties. Emulsion gel systems can be carefully designed by varying the properties of the gel matrix, properties of oil phase and interactions between the matrix and oil droplets (Figure 2-5). These systems can also be designed to deliver either lipophilic or hydrophilic bioactives where the gel matrix regulates it release and stability.

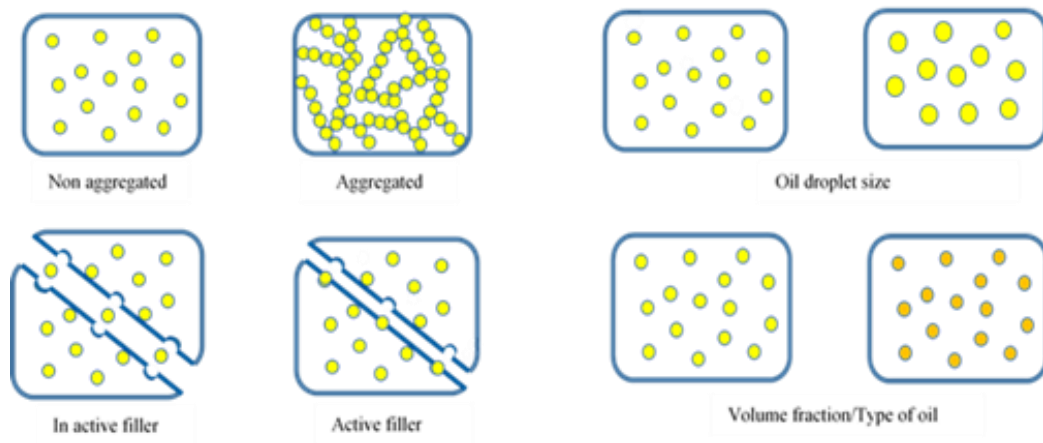


Figure 2-5 Emulsion gels formed by varying different properties.

2.5.5 Rheological properties of emulsion gels

An emulsion gel is a soft solid with an elastic response to applied force; it can store energy and does not yield immediately (Walstra, 2002). Thus, an emulsion gel has a loss tangent value less than one ($\tan \delta = G''/G' < 1$, where G' is the shear storage modulus and G'' is the shear loss modulus). The rheological qualities of an emulsion gel (such as yogurt, cheese,

jelly, etc.) are crucial in its manufacturing, storage, and consumption. Shear storage and shear loss moduli, for example, vary during gel formation. G' is lower than G'' when starting with a liquid emulsion; following gel formation, G' is higher than G'' . It transitions from a thick liquid to a soft solid at one point. To have a better understanding of the transition mechanisms, the values of both moduli must be measured as a function of time (through small strain oscillatory shear rheometry).

Large deformation characteristics, in addition to small deformation properties, are crucial for sensory perception and oral processing behaviour, particularly during consumption. Typically, uniaxial compression is used to compress emulsion gel samples while measuring a number of variables. Then, these mechanical characteristics can simulate or predict the sensory texture properties. Fracture stress reflects the firmness (hardness) of the gel, and the corresponding strain is representative of gel deformability. A higher Young's modulus is attributed to thickness of strands in networks and is usually observed for more coarser networks as thicker strands are more difficult to bend than less stiff thin strands (Munialo et al., 2014).

2.5.6 Effect of protein-polysaccharide matrices on digestion and postprandial responses

The three-dimensional network in which nutrients are encompassed play a key role in controlling digestion and postprandial responses associated with it. Many *in vivo* studies have reported how the physical state of food regulates satiety and a whole range of postprandial responses (Marciani, Hall et al. 2012, Mackie, Rafiee et al. 2013, Camps, Mars et al. 2016).

2.6 Influence of structure of gastric chyme on satiety and gastric emptying

Satiety responses arise partly due to differences in the structure changes of gastric chyme after food ingestion. Liquid and semi-solid foods can undergo sedimentation and phase separation under gastric pH. For solid samples, its effective particle size and properties of the matrix decide the rate of gastric emptying. Mackie, Rafiee et al. (2013) studied how the physical structure and spatial arrangement of nutrients in a food system affect digestion kinetics. More structured meals were reported to induce satiety as compared to liquid meals. An understanding of meal emptying requires assessment of both the sieving function of the stomach and the strength of contractions that can be used to break down materials into small particles before exiting via the pylorus. Research suggests that increased viscosity of gastric chyme allows for better antral grinding, prevents sedimentation, facilitates rapid disintegration and gastric emptying of indigestible particles (Marciani, Gowland et al. 2001). Gastric emptying depends on estimating how the antrum breaks down systems of defined fracture strength before being emptied. The stomach contractions act upon the food bolus, and it undergoes an elastic deformation and breaks down into smaller particles after crossing the threshold value. Some studies suggest that that the force exerted by the antral walls in grinding food is between 0.53 and 0.78 N (Marciani, Gowland et al. (2001) or are mostly <1 N (Vassallo, Camilleri et al. 1992) and the matrices with a fracture strength greater than that exerted by antral contractions would be retained in the stomach for longer (Marciani, Gowland et al. 2001). Gel strength of chyme would be an appropriate indicator for determining gastric emptying times, as weak gels would tend to break up into tiny fragments during antral grinding while stronger gels would be retained for longer periods.

2.7 Influence of protein-polysaccharide systems on gastric emptying, intragastric gelation and satiety

Intragastric gelation refers to the mechanism where the consumed liquid food forms a gel under highly acidic conditions which is hypothesised to cause gastric distention and promote satiety. Many studies on simulated gastric digestion for mixed protein-polysaccharide systems employ the pH range of 1.2 - 2, which is typically the pH of the fasted state. At this pH, below the pI of the protein, liquid mixtures containing negatively charged polysaccharides complex with protein leading to intra-gastric gelation. Zhang, Zhang et al. (2014) reported that intragastric gelation depends on the biopolymer ratio, biopolymer concentration, charge density of the polysaccharide, initial pH of the sample, and pH of the SGF. They suggested that a mixture of WPI-polysaccharides resulted in a stronger gel that could resist gastric degradation, and this could be used to delay gastric emptying and promote satiety. However, no corroborations were made relating intragastric gelation and satiety. Other observations suggest that high viscosity and not intragastric gelation of the food matrix imparts satiety (Marciani, Gowland et al. 2001, Hoad, Rayment et al. 2004, Wee, Yusoff et al. 2017). Unfortunately, many of these studies fail to consider the dynamic changes in pH and effect of contractions of the stomach as these drastically affect the structure of the food matrix.

2.8 Effect of protein-polysaccharide interactions on protein digestion

Regulating protein digestion kinetics in the gastrointestinal tract helps control neuro-hormonal and immune responses like gastrointestinal motility, gastric emptying time, secretion of acid and pepsinogen, and total protein and energy intake (Dangin, Boirie et

al. 2002; Sah, McAinch et al. 2016). Matrices fabricated from protein-polysaccharides help restrict interactions between the secreted digestive enzymes and food material. Zhang, Zhang et al. (2017) reported the use of calcium alginate microgels to encapsulate whey protein isolate. They reported that when the attraction between the protein and polysaccharide is weak, the native protein easily escapes from the polysaccharide matrix because of its size being smaller than the microgel pore size. To remedy this, they used thermally aggregated protein for better retention and encapsulation in the polysaccharide matrix and found that the denatured proteins had better retention in the matrix thus leading to a considerably lower hydrolysis in the stomach.

Borreani, Llorca et al. (2016) studied the effect of adding neutral or anionic polysaccharides on digestion of dairy protein ingredients. They reported that neutral konjac glucomannan-dairy protein aggregates had a viscosity modifying effect and were broken down into smaller aggregates over time in the GIT. However, aggregates formed on complexation with alginate were larger and remained unchanged throughout their passage in the GIT. This was attributed to the strong interaction between the oppositely charged protein and alginate at the gastric pH thus limiting pepsin accessibility to the protein. Other methods include a gastro-retentive floating delivery system employing the use of protein-polysaccharides in an effervescent and non-effervescent system (Sarojini & Manavalan 2012). The main objective of both systems is to form a floatable buoyant gelatinous mass at gastric pH that allows sustained release of proteins.

2.9 Effect of protein-polysaccharide interactions on lipid digestion

Most food emulsions are stabilized by proteins as they are highly surface active and adsorb at fluid interfaces. These interfaces and structures can be engineered in a way so as to control lipolysis (Singh, Ye et al. 2009). Polysaccharides on their own cannot adsorb to interfaces but adsorption is possible by forming a phase-separated interfacial layer or by electrostatic interaction with the protein at the interface. This leads to improved stabilization due to the thicker interfacial layers of protein-polysaccharide complexes and structural reinforcement of the protein layer by the polysaccharide. In addition, micro or nano-scale structures/particles formed through protein-polysaccharides can be used to stabilize emulsions. Additional modifications such as the use of indigestible polysaccharides or the use of gelling biopolymers can further delay lipid digestion.

2.9.1 Gastric colloidal behaviour of milk protein in dairy products under gastric conditions

Many natural and processed foods are typically oil-in-water emulsion systems. These are either simple or complex depending on their structure and their constituents. The colloidal behaviour of these emulsions during gastric digestion can be tailored, to manipulate the extent of lipid digestion by modifying the rate of gastric emptying and delivery of gastric digesta with different compositions to the duodenum (Golding et al., 2011; Singh et al., 2009). There is enough evidence to suggest that preceding gastric protein digestion influences the kinetics of subsequent lipid digestion for protein stabilised/containing emulsion systems (Mackie, 2020; Singh et al., 2009; Ye et al., 2020).

The state of the proteins adsorbed to the emulsion interface and the properties of the environment surrounding it dictates the physico-chemical characteristics of the emulsion droplets such as size, charge, and aggregation state. For a system containing protein-polysaccharides, the polysaccharides influence structural changes in the protein, thus altering its digestibility by impacting the accessibility of digestive enzymes to the protein. The colloidal stability of emulsions in the gastro-intestinal tract depends on various factors such as the properties of the biopolymer on the surface (molecular weight, charge density etc.), the properties of the gastric fluid (pH, digestive enzymes, and electrolyte content) and the environmental conditions prevailing during gastric digestion (temperature, mechanical force due to peristalsis).

After oral processing and on entering the stomach, emulsions undergo chemical and mechanical destabilization. Gastric fluid is made up of primarily hydrochloric acid and digestive proteins, enzymes, and electrolytes. This along with the mechanical forces of the gastric walls leads to destabilization of the emulsion leading to flocculation, coalescence, and creaming (Singh et al., 2009). Emulsions that are gastric-unstable usually consist of emulsions stabilised with emulsifiers that are ionizable surfactants or proteins (Golding et al., 2011). These are highly prone to proteolysis or destabilisation once in contact with gastric fluids. Emulsions made using non-ionic surfactants are highly stable in the gastric environment and are said to be gastric-stable.

In vivo studies have shown that gastric-stable emulsions have a slow rate of passage from the gastric lumen into the duodenum while gastric unstable emulsions undergo flocculation and creaming. This phase separation results in a biphasic emptying pattern

of the gastric digesta (Foster & Norton, 2009; Liu et al., 2016; Marciani et al., 2007; Parker et al., 2017; Steingoetter et al., 2015). This biphasic destabilisation leads to an accelerated release of the lower aqueous phase of the stomach and its contents and a gradual and slow emptying of the top cream layer. As a result, nutrients dissolved in the bottom aqueous layer, or the top cream layer follow the same pattern of emptying. This was corroborated by blood tests and magnetic resonance imaging of the stomach, where for gastric-unstable emulsions, significant rate of emptying, lower levels of postprandial CCK plasma levels, and less gall bladder contractions were observed (Marciani et al. 2007). The researchers stated that emulsion stability in the gastric environment considerably alters the emptying/secretion rates of both the stomach and the duodenum (Foster & Norton, 2009; D.; Liu et al., 2016; Marciani et al., 2007; Parker et al., 2017). This further affects the rates of absorption and metabolization of nutrients, resulting in changes in the bioavailability of nutrients, especially lipophilic bioactive compounds present in the lipid component of the emulsions (Araiza-Calahorra, Akhtar, & Sarkar, 2018; McClements et al., 2009; Sarkar & Mackie, 2020).

2.9.2 Mechanism of gastric colloidal destabilisation

There is extensive literature on droplet flocculation caused by the acidic gastric pH and consecutive coalescence caused by proteolysis of the surface layer (Li, Ye, Lee, & Singh, 2012, 2013; Sarkar et al., 2009; Ye, Wang, Lin, Han, & Singh, 2020) resulting in changes in droplet size and microstructure. These changes occurring during gastric digestion have shown to impact subsequent intestinal digestion (Li et al., 2012).

For milk protein stabilized emulsions, in addition to low pH, the coagulating property of pepsin also leads to flocculation by destabilisation of the casein that is present on the emulsion surface. For MPC-stabilized emulsions, flocculation occurred during the early stages of digestion (at pH > 6) by pepsin, leading to formation of large closely knitted flocs that were difficult to dissociate and were persistent throughout *in vitro* dynamic gastric digestion along with creaming of the oil to the top of the stomach (Wang et al. 2019). The persistence of these large clots during digestion is said to be because the dense structure hinders pepsin diffusion through the flocs.

In contrast, for emulsions stabilised by calcium depleted MPC or sodium caseinate, flocculation occurred within 40 mins of digestion, due to the low pH resulting in flocs that were relatively small and that disintegrated with further digestion. The particle size data and oil content data of the digesta suggested that the MPC emulsion showed a relatively slower release of oil droplets to the small intestine compared to the calcium depleted MPC and sodium caseinate emulsions. This indicates that the composition of surface proteins of the emulsion, dictates its sensitivity to pepsin which in turn affects its colloidal stability in the gastric phase.

For emulsions stabilized by caseinate or calcium depleted MPC, flocculation did not occur at this pH, despite SDS-PAGE results demonstrating that κ -casein was also hydrolysed by pepsin (Wang et al., 2019). These emulsions could undergo flocculation at longer digestion times due to the pH reaching the isoelectric point (pH ~ 5) of the proteins, but the resultant clot structure formed were smaller and looser, that broke down further into a fine emulsion with further digestion due to the increased activity of pepsin as pH

decreased to < 3 . Wang et al., (2018) suggested that the difference in the microstructure and the size of the flocculated emulsions, were due to low pH or proteolysis as reflected by the difference in the structural properties of the protein clots formed during digestion. The type of flocculation occurring and the time it takes to occur, influence creaming of the oil layer, in turn, modulating the delivery of oil and consequent lipid digestion in the small intestine. This was further corroborated by work done by Ye et al., (2020), where gastric colloidal stability of whey-protein-stabilized emulsions and its effects on the lipolysis of the emulsions was investigated using the *in vitro* dynamic HGS and a subsequent small intestinal model. It was observed that heated whey-protein-stabilized emulsions, under gastric conditions, flocculated to a greater extent with the formation of larger flocs as compared to unheated emulsions, which were more prone to coalescence. For the former, the greater extent of flocculation, resulted in a lower amount of oil being delivered to the small intestine during the initial phase of digestion. The differences in the extent of flocculation led to a greater rate and extent of intestinal lipolysis for the heated emulsion as compared to the unheated emulsion.

The same mechanism of flocculation and destabilisation observed for milk-protein-stabilized emulsions also occurs for other natural and processed protein-based emulsion food systems such as plant-based milks, which influences the delivery of oil/fat for digestion for these systems (Wang, Ye, Dave, & Singh, 2021).

2.9.3 Mechanism for complex structured systems

Oil destabilisation during gastric digestion has been attributed mainly to proteolysis of the interfacial layer rather than exposure to low pH or ionic strengths of the SGF (Nik et

al., 2010). Changes in WPI-stabilized emulsion interfacial properties in relation to lipolysis and β -carotene transfer during exposure to simulated gastric–duodenal fluids of variable composition. For emulsion gels, the gel matrix contains protein making up the bulk gel phase and interfacial gelled protein stabilizing the oil droplets. Oil destabilization in semi-solid emulsion systems may occur due to the follow factors, 1) mechanical breakdown of gel breakdown due to shear 2) better accessibility of pepsin to cleavage sites due to mechanical shear 3) destabilisation of oil droplets within the gel due to ingress of acid and SGF. Therefore, the structural properties of the gel matrix modulate the stability of the oil droplets in the gel matrix. For a system containing protein-polysaccharides, the polysaccharides in the system could lead to differences in the physiochemical and properties protein, thus affecting the digestibility of protein because the accessibility of cleavage sites to protease on protein could be altered through electrostatic interactions with polysaccharides. For semi-solid emulsion systems, degradation/ dissolution of the matrix would result in release of the enclosed emulsion droplets. The stability of the released droplets would then be dependent on the properties of the interfacial layer and its likely interactions with other components in the gastric environment. For emulsion systems, dynamic gastric *in vitro* systems are better at simulating the complex biochemical and colloidal changes occurring in the emulsion, released components and the gastric environment, as they account for factors such as gradual acidification, sample dilution and continual mechanical shear.

During dynamic gastric digestion, the pH and ionic strength of the gastric contents keep changing. Also, due to period gastric emptying, the contents also undergo dilution by continual addition of SGF. During oral processing and the initial stages of gastric

digestion, the pH is near neutral, which is above the pI of WPI (~ pH 4.8). At pH close to/at pH 7, both WPI and LMP carry opposite charges, which may result in repulsion of both biopolymers. As digestion progresses, gradual acidification leads to a drop in pH. Under associative conditions, released emulsion droplets may interact with oppositely charged polysaccharides dispersed in the digestion fluid leading to bridging flocculation. However, if the concentration of the polysaccharide is sufficient, the emulsion droplets may be completely coated by a secondary charged layer, conferring some protective effects against proteolysis during gastric digestion (Wackerbarth et al., 2009). Nik et al (2010) reported that WPI emulsions made with a higher protein concentration than that required for optimum surface coverage of droplets, was more stable during gastric digestion and the authors attributed this to the presence of intact protein and higher concentration of surface-active peptides after pepsin hydrolysis that confer stability to the emulsion system. However, these peptides are also said to have weak emulsifying properties and insufficient sufficient charge to prevent droplet flocculation/coalescence (Mao, L., & Miao, S. (2015).

Polysaccharide release from the emulsion gel will depend on the microstructure of the gel i.e., the amenability of the gel to mechanical shear and proteolysis and the strength and nature of interactions between the pectin and the gel matrix. Remondetto, G. E., et al. (2004). reported that fine gels facilitated faster release of iron as compared to particulate whey protein gels. This was attributed to iron localisation within the different microstructures where it was suggested that iron was bound more tightly in aggregated particulate gels but was located at the outer surface of fine gels, thus facilitating its release. The interactions that could occur between proteins and polysaccharides, depends

on multitude of factors such as the pH and ionic strength of the gastric environment, along with factors such as charge density, degree of ionisation, structure and concentration of the both the biopolymers. Polysaccharides are thought to influence the viscosity of the gastric digesta which possibly also causes the enzyme–substrate from binding or direct interactions between pectin and enzymes (Nacer S, A., Sanchez, C., Villaume, C., Mejean, L., & Mouecoucou, J. (2004).

Some of these approaches seem inadequate as most of these systems are unstable under gastric conditions and allow lipid droplets to be emptied in the duodenum and their subsequent access to lipase (McClements and Li 2010). A more feasible approach as proven by results obtained under static *in vitro* conditions is the use of gel matrices that modulate the diffusion of enzymes. The gel matrix could be tailored depending on the functionality and targeted site of release. Gel matrices formed can be digestible, e.g., using proteins (Goh, Sarkar et al. 2009, Dekkers, Kolodziejczyk et al. 2016) or using indigestible polysaccharides (Corstens, Berton-Carabin et al. 2017, Zhang, Zhang et al. 2017). Many non-digestible matrices include chitosan, nano-cellulose or starch. These components when heated form an indigestible shell that prevents access of lipase to oil droplets.

2.10 Conclusions

Emulsion gels are structured systems which are often referred to as complex colloidal material that may exist as both an emulsion and a gel (Dickinson 2012). These serve as good models for structured foods where heat/acid/enzyme processing leads to gelation giving structure to the liquid emulsion. These systems can be carefully designed by

varying the properties of the gel matrix, properties of oil phase and interactions between the matrix and oil droplets. These systems can also be designed to deliver either lipophilic or hydrophilic bioactives where the gel matrix regulates its release and stability.

There has been extensive research on digestion of single and mixed biopolymer systems (Boirie, Dangin et al. 1997, Hall, Millward et al. 2003, Macierzanka, Böttger et al. 2012, Peram, Loveday et al. 2013, Singh, Øiseth et al. 2014, Luo, Boom et al. 2015). Whey protein model systems have been extensively studied and previous studies have highlighted the effect of different colloidal matrices of whey protein emulsion gels produced by varying ionic strength and oil droplet size on the *in vitro* gastro-intestinal digestion of lipids (Guo 2015).

To sum up, the main gaps in literature pertaining to use of protein-polysaccharide emulsion systems were as follows:

There is a need to develop multicomponent complex model systems with different structures and physical properties and to understand how these complex food structures break down in the GIT.

- To understand how the rate of protein digestion is affected by segregative or associative interactions in a protein-polysaccharide emulsion gel system.
- To understand how protein-polysaccharide segregative or associative interactions in an emulsion gel system affect lipid release kinetics and digestion.

3 Materials and Methods

3.1 Materials

Whey protein isolate 895 (WPI) was purchased from Fonterra Co-operative Group Limited, Auckland, New Zealand. Refined soybean oil was purchased from Davis Trading Company, Palmerston North, New Zealand. Low methoxyl pectin (GENU® pectin type LM-22 CG, low ester non-amidated pectin having a low calcium reactivity) was supplied by CP Kelco (Axieo, Auckland, New Zealand). Water purified by Milli-Q apparatus (Millipore Corp., Bedford, MA) was used for all experiments. Pepsin from porcine gastric mucosa, ≥ 250 units/mg solid was procured from Sigma Chemicals (St. Louis, MO, USA). All other chemicals used were of analytical grade and were purchased from Sigma Chemical Co. (St. Louis, MO) or Thermo Fisher Scientific New Zealand Ltd (Auckland, North Shore City, New Zealand) unless otherwise specified.

3.1.1 Emulsion preparation

WPI-stabilized emulsions were prepared by mixing 250 g soybean oil with 750 g of 16.66 wt.% WPI protein solution using a high shear mixer (L4RT, Silverson, Massachusetts, USA) at 9000 rpm for 3 min to reach final concentrations of 12.5 wt% WPI and 25 wt% soybean oil. No adjustments to pH were made prior to homogenisation. Coarse emulsions were homogenized using four passes through a two-stage valve homogenizer (APV 2000, Albertslund, Denmark) operated at 280 bars for the first stage and 40 for the second stage. The average oil droplet size $d_{4,3}$ of the emulsions was $\sim 0.5 \mu\text{m}$ (Guo et al., 2014). This emulsion was divided into two subsamples, which were then diluted with either deionised

water or LMP stock solution (2.5 wt%) respectively to obtain control emulsion (CO emulsion) and emulsion containing 0.5 wt% LMP in the aqueous phase (PE emulsion). The pH of freshly prepared emulsions was 6.80 ± 0.05 for CO emulsion and 6.52 ± 0.05 for PE emulsion. The pH was adjusted to 7 or 4.5 by the addition of 6M NaOH or 3M HCl respectively. All emulsions had final concentrations of 10 wt% WPI and 20 wt% soybean oil. Ionic strengths of 10 mM and 100 mM were achieved by adding required quantities of NaCl to pH-adjusted emulsions and these were then gently stirred for 1 h at room temperature to facilitate complete dissolution. For clarity, high ionic strength (100 mM of added NaCl) and low ionic strength (10 mM of added NaCl) refers to amount of added NaCl respectively.

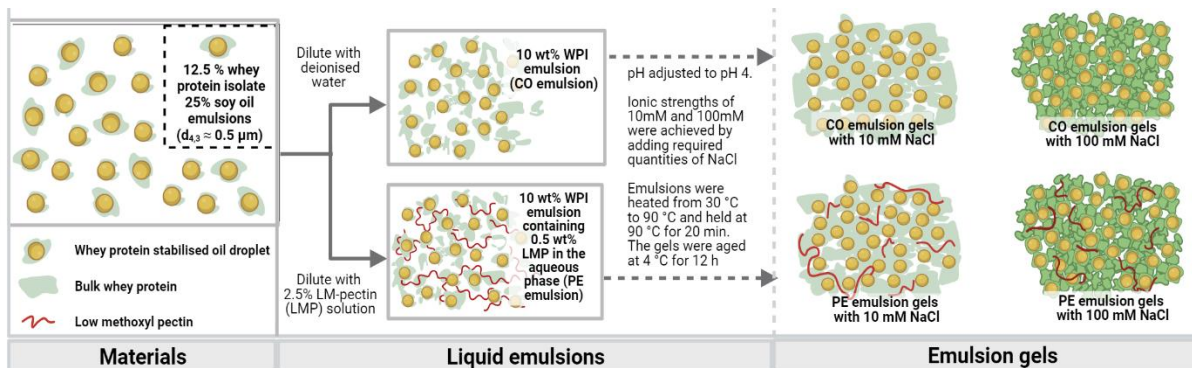


Figure 3-1 Emulsion preparation and emulsion gel formation

3.1.2 Emulsion gel formation

25 g of liquid emulsion was transferred into 30 ml flat base polystyrene vials (27mm wide x 82mm high, LabServ, Thermo Fisher Scientific), and heated in a water bath from 30 °C to 90 °C and held at 90 °C for 20 min. After heating, the gels were kept at 4 °C for 16 h prior to analysis to ensure complete gel formation. The emulsions gels made from CO emulsion and PE emulsion with different ionic strengths are hereafter designated as CO gels or PE gels respectively (Fig. 3-1).

3.2 Properties of liquid emulsions and emulsion gels

3.2.1 Zeta potential measurements

Zeta potential measurements of the emulsions at varying pH and ionic strength were carried out using a ZetaSizer (Nano-ZS, Malvern Instruments Ltd., Malvern, Worcestershire, UK). Dilution buffers were prepared using deionised water with required amounts of NaCl to give final ionic strengths of 10 mM and 100 mM. Approximately, 100 µl of the emulsion was diluted 1000 times with appropriate ionic strength diluent and its pH was checked before analysis. The pH did not change on dilution with water or ionic strength diluent. The Smoluchowski approximation was used to convert electrophoretic mobility to zeta potential (mV). All measurements were carried out at 25 °C and are averages of triplicate runs.

3.2.2 Particle size characterization by laser diffraction

Particle size distributions of emulsions and emulsion gels were measured using MasterSizer2000 (Malvern Instruments Ltd., Malvern, UK). The refractive index of oil droplet was set at 1.47 and that of water was set to 1.33. The particle size of the liquid emulsion droplets was determined by diluting the emulsions 10-fold in SDS (5 wt%) and gently mixing for a few seconds to break down the flocs and yield the actual droplet size of emulsion droplets. For the emulsion gel, 2 g gel was added to 20 ml dissociating buffer (SDS 5 wt% and 50 mM 2-mercaptoethanol and shaken overnight until totally dissolved. The buffer solubilises the protein component of the gel, allowing the release of oil droplets which were measured the same way as that for the liquid emulsions. The obscuration value was kept between 12% to 15%. Each sample was measured two times and the results were averaged. The volume-to-surface diameter ($d_{3,2}$, μm) and weight-to-volume diameter ($d_{4,3}$ μm) were used as the average oil droplet sizes.

3.2.3 Confocal microscopy

Visualization of emulsion and gel microstructure at the micrometre length scale was done using confocal laser scanning microscopy (Leica, Heidelberg, Germany) equipped with a 63 \times oil immersion objective lens. The oil phase was stained using 0.1 w/v% of Nile Red (in acetone) while the protein phase was stained using 1 w/v % (in water) Fast Green. The excitation wavelength was set at 488 nm for Nile Red and 633 nm for Fast Green.

For the emulsions, 500 μL of the emulsion was stained with 20 μL of Nile Red and Fast Green respectively. For the emulsion gels, a thin section of emulsion gel (roughly about

3mm x 3mm) was cut using a surgical scalpel and stained using 20 μl of Nile red and 20 μl fast green and incubated for 30 min at 4 $^{\circ}\text{C}$ prior to visualisation. Gastric digesta (approx. 2 mL) collected during the experimental runs was stored in centrifuge tubes in an ice bath and were stained in a similar manner to that of the emulsion gels. Digital image files were acquired in lif file format at a resolution of 1024×1024 pixels using LAS AF software (version 2.7.3.9723) and were processed using ImageJ software.

3.2.4 Oscillatory rheology

Rheological properties during heat-induced gelation were determined using a stress-controlled rheometer (MCR 302, Anton Paar Physica, Stuttgart, Germany) with a concentric-cylinder (cup and bob) geometry (CC27). Each run involved pouring 19 mL of emulsion into the cup and covering it with a thin layer of low-viscosity silicone oil to prevent evaporation. Heat-set gelation was induced in situ by (1) heating the sample at a constant rate of 3 $^{\circ}\text{C}/\text{min}$ from 30 to 90 $^{\circ}\text{C}$, (2) holding at 90 $^{\circ}\text{C}$ for 30 min, (3) cooling at a rate of 1 $^{\circ}\text{C}/\text{min}$ from 90 to 30 $^{\circ}\text{C}$, and (4) holding at 30 $^{\circ}\text{C}$ for 20 min (Guo et al., 2014). Both storage (G') and loss (G'') modulus were recorded throughout the temperature sweeps as a function of time. All measurements were made in the linear viscoelastic region (0.5% strain) and at a constant frequency of 1 Hz. The data reported are the means of five replications.

3.2.5 Large deformation properties

Uniaxial compression tests on emulsion gel pieces (20 mm in height and 25 mm in diameter) were performed using a texture analyser (TAXTPlus, Stable Micro Systems

Ltd., Surrey, England) equipped with a 50 kg load cell using a 60 mm diameter cylindrical acrylic plate geometry. The top and bottom side of the gel samples were lubricated with mineral oil to minimize friction between sample and the probe during compression. The gels were allowed to equilibrate at room temperature before compression testing. All tests were carried out at room temperature. The gels were compressed to 80% of their original height using a crosshead speed of 4 mm/s. Stress (σ_t) and Hencky strain (ϵ_H) were calculated at each point from time at zero to time at final deformation using the following equations (Truong & Daubert, 2000). The Young's modulus, E (Pa), was calculated from the slope of the linear region in the stress-strain curve up to 0.5% strain. The apparent Young's modulus is representative of the stiffness of the gel. At least fifteen gel emulsion gel samples were tested for each pH and ionic strength variation and each treatment was replicated three times.

$$\text{Stress: } \sigma_t = \frac{F}{A_i} \times \frac{(L_i - \Delta L)}{L_i} \quad \text{Equation 3}$$

$$\text{Strain: } \epsilon_H = \left| \ln \frac{L_i}{L_i - \Delta L} \right| \quad \text{Equation 4}$$

Where, F is the force measured during compression (N); A_i is the initial cross sectional area of the specimen (m^2); L_i is the initial specimen height (m); ΔL is the absolute deformation (m).

3.3 *In vitro* dynamic digestion

3.3.1 Simulated oral processing.

3.3.2 Particle size simulation during mastication

Emulsion gels were cut into cylindrical pieces (20 mm in height and 25 mm in diameter). At a given time, eight gel pieces (approx. 12 g) were mixed in a food processor (Breville Mini Wizz, New Zealand) for different standardised durations to produce gel particles with a median size of 2.4 ± 0.5 mm as determined by the procedure of Jalabert-Malbos et al., (2007).

3.3.3 Simulated bolus preparation

Briefly, 125 g of ground gel was mixed with 95 g of preheated simulated saliva fluid (SSF) with no salivary α -amylase (Minekus et al., 2014). This ratio was chosen to ensure optimal bolus hydration and consistency for all the different emulsion gels prepared. After mixing, the oral phase was incubated at 37 °C for 2 min whilst continuous stirring before proceeding to the gastric phase.

3.3.4 *In vitro* gastric digestion using the Human gastric simulator (HGS)

In vitro gastric digestion was carried out using a human gastric simulator (HGS) developed by Kong and Singh (2010).

Simulated gastric fluid: The simulated gastric fluid and pepsin solution were prepared separately as they were to be delivered using separate pumps, so concentrations were adjusted accordingly but the concentrations in the final digestion mixture were according to Minekus et al., (2014) with modifications explicitly stated. The electrolyte composition and concentration for the simulated fluid gastric fluid (SGF) were according to Minekus et al., (2014) at a 1.25x concentration with the exception that the pH of the SGF was adjusted to pH 1.5 using 3 M HCl/NaOH. Pepsin required was prepared separately in MilliQ water to achieve a concentration of 1000 U/mL in the final digestion mixture. This had lower activity than that suggested by Minekus et al, 2014 to account for a higher dilution rate due to the solid nature of the food and dynamic nature of our simulation.

Setting up the HGS: The temperature of the HGS was maintained at 37 °C. Digestion was carried out for a period of 4 h. The total gastric secretions comprising of SGF (1.25X) and pepsin (kept chilled at 10 °C) were added at a rate of 2.0 and 0.5 mL/min respectively via two separate peristaltic pumps (Model LabV1, MC series, Shenchen, China). A mesh liner having a pore size of 1 mm was fitted on the inside of the HGS so that so that only liquid and solid mass of size ≤ 1 mm could be emptied through the spout fitted at the rear end of the HGS. The rates set up for gastric secretions and emptying were used as in our previous studies.

Gastric digestion run: The sample from the oral phase (220 g) was fed into the HGS after addition of the basal fasting fluid (30 mL SGF adjusted to pH 1.5 1X containing pepsin at 1000 U/mL). Since the emptied digesta contained liquid and small gel particles, emptying was done by weight, not volume, for the sake of accuracy. Emptying began

after 30 min to account for the solid nature of the food. Gastric emptying was simulated by taking samples (45 g) of digesta from the bottom of the stomach chamber at 15-min intervals, equalling an emptied digesta rate of 3 g/min.

Analysis: The '0 min' samples referenced in this manuscript refers to the sample from the oral phase with the basal fasting fluid. Measurement of the pH, particle size analysis, observation by confocal microscopy and pectin analysis was carried out right away without any pH adjustment. For the other analysis, pH was adjusted to pH 7.5 or pH 4.5 with 2 M NaOH and/or 1 M HCl to curb the activity of pepsin and stored at 4 °C or freeze dried till further analysis.

3.3.5 pH measurement

The initial pH in the HGS refers to the pH of the sample mixed with the oral phase along with the fasting SGF. As direct pH measurement inside the HGS was not possible due to mechanical constraints of the machine, the pH reported refers to the pH of the aliquot emptied at each time interval presumably representative of the pH inside the stomach chamber. Although the temperature inside the HGS was maintained at 37°C, the pH values reported are measured in the temperature range of $35 \pm 2.75^\circ\text{C}$, which is slightly lower than 37°C as some cooling is inevitable during sampling/pH measurement.

3.3.6 Apparent pectin content of the emptied gastric digesta

The pectin content in the emptied digesta was estimated as galacturonic acid content (GalA), as described by Melton and Smith (2001). Briefly, emptied digesta was collected and its pH was adjusted to 7.5. These were then weighed into a plastic centrifugation tube, capped, and centrifuged 4500 g for 30 min at 4 °C to separate the cream layer, middle aqueous layer, and small eluted gel particles. The middle aqueous layer obtained after centrifugation was carefully removed using a pipette and was used for pectin estimation. Absorbance was measured at 525 nm against a standard curve of galacturonic acid (50 to 150 µg/mL). Results are expressed as pectin content (mg/g) of the emptied gastric digesta at each time point. Some pectin may be still associated with the cream phase and present in the eluted small gel particles, which could lead to underestimation of the pectin content. Hence, the pectin content is reported as apparent pectin content. Based on this data, a cumulative percent of pectin release (%) over digestion time (min) was also plotted.

3.3.7 Measurement of the solid content of emptied gastric digesta

Samples of digesta emptied at each time point were subjected to gravimetric moisture content analysis to determine the solid matter content. Since emptying times were held constant, the measurement of solid content emptied is considered indicative of the extent of breakdown of the emulsion gels. Amount of dry matter is expressed as % of digesta emptied.

3.3.8 Measurement of the lipid content of emptied gastric digesta

The freeze dried digesta was used for determination of the oil content using the Mojonnier ether extraction method (AACC method 30–10; AACC, 2000) as previously described by Wang et al. (2019).

3.3.9 Determination of particle size distribution of emptied digesta

A MasterSizer 2000 (Malvern Instruments Ltd., Malvern, UK) was used to measure the particle size distribution of the digesta without any pH modification. The refractive index for the gel particles was set at 1.47. The samples were measured immediately after collection and the weight-to-volume diameter $d_{4,3}$ (μm) was used to denote the average gel particle size.

3.3.10 Determination of Oil Droplet Size Distribution

The oil droplet size distribution of the digesta was measured in a similar manner as that listed for the emulsion gels. Oil droplet size distributions of emulsions and emulsion gels were measured using MasterSizer2000 (Malvern Instruments Ltd., Malvern, UK). The refractive index of oil droplet was set at 1.47 and that of water was set to 1.33. The particle size of the liquid emulsions was determined by diluting the emulsions 10-fold in SDS (5 wt%) and gently mixing for a few seconds to break down the flocs and yield the actual droplet size of emulsion droplets. For measurements of the emulsion gel, 2 g gel was added to 20 ml solution containing SDS (5 wt%) and 2-mercaptoethanol (50 mM) and shaken overnight until totally dissolved.

The obscuration value was kept between 12% to 15%. Each sample was measured two times and the results were averaged.

3.3.11 Statistical Analysis

The t test distribution was used to compare the mean values of distinct samples at $P < 0.05$. Pearson correlations were calculated using SAS 9.4 software to examine the relationships between lipid release and gel disintegrations. The results were expressed as the correlation coefficient r and the probability level P . A complete positive correlation is shown by the symbol $r = 1$, a perfect negative correlation by the symbol $r = -1$, and a perfect zero correlation by the symbol $r = 0$. P stands for the correlation's significance. Using IBM SPSS Statistics 24, one-way analysis of variance was used to analyse additional data. Tukey tests were used to compare the means at $P < 0.05$.

4 The effect of gel structure on the *in vitro* gastric digestion of protein-polysaccharide emulsion gels formed at pH 7: effect of segregative interactions

Abstract

Understanding the relationship between food structures and their digestion is important in explaining the association between diet and health. Protein-polysaccharide emulsion gels serve as good models for multicomponent structures present in real foods. The pH and ionic strength of these systems determine the nature of interactions between proteins and anionic polysaccharides and contributes to the distinct structural properties and functionalities of these systems. In the present study, heat-set whey protein emulsion gels ($d_{4,3} \sim 0.5 \mu\text{m}$) with and without low methoxyl pectin (LMP) were formed at pH 7. Additionally, the impact of low and high ionic strength (achieved by 10 mM and 100 mM NaCl addition) on gel structure was studied. These systems were characterized in terms of rheology, microstructure, and fracture properties. Gels made at high ionic strength had a higher fracture stress compared to gels made at lower ionic strength. Confocal micrographs of PE gels at low ionic strength showed the presence of LMP depletion zones within the gelled protein emulsion matrix, which were not evident at high ionic strength.

The breakdown kinetics of these gels were assessed under dynamic *in vitro* gastric digestion using the human gastric simulator and the physicochemical characteristics of digesta were determined. Emulsion gels formed at high ionic strength, irrespective of

LMP addition, had a much lower extent of matrix disintegration and showed minimal oil droplet coalescence. In comparison, gels formed at low ionic strength disintegrated faster and showed a greater degree of oil droplet coalescence. Regardless of ionic strength used, PE emulsion gels at low ionic strength showed less oil droplet coalescence compared to the control gels. These results indicate that addition of LMP and ionic strength seem to influence the structural properties of the emulsion gel matrix, which impacts their gastric digestion kinetics and would likely modulate the subsequent delivery of lipids in these systems.

4.1 Properties of liquid emulsions prior to heat-induced gelation

The influence of ionic strength on the stability of CO and PE emulsions was investigated. The behaviour of the emulsions was characterized based on their ζ -potential (Figure 4-1), particle size distributions (Figure 4-2) and through confocal laser scanning microscopy before and after gelation (Figure 4-3).

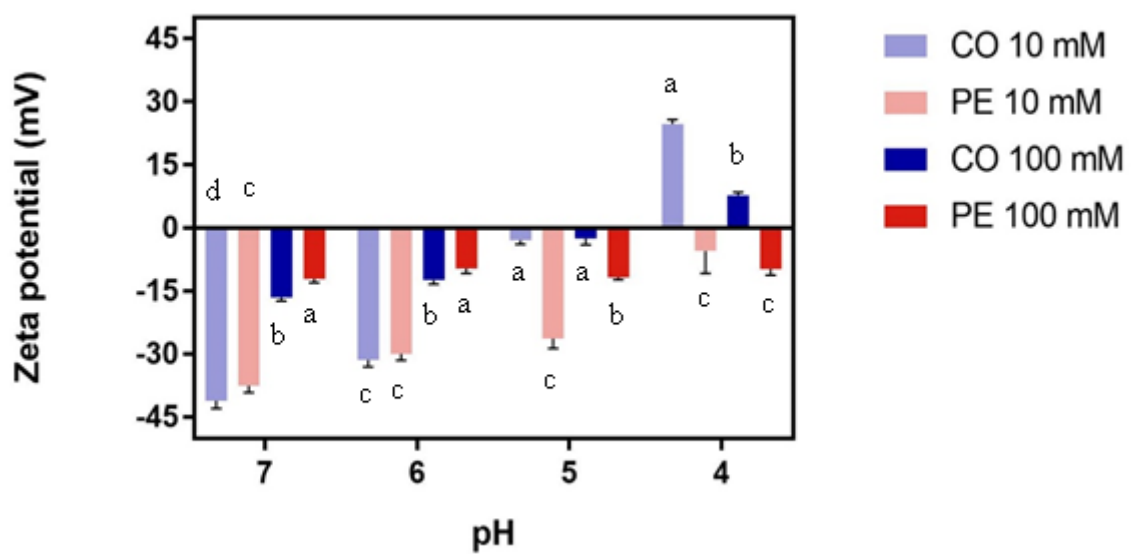


Figure 4-1 Zeta potential measurements of whey protein emulsions (CO) with 10 mM NaCl, Whey protein-LMP emulsions (PE) with 10 mM NaCl, Whey protein emulsions (CO) with 100 mM NaCl and Whey protein-LMP (PE) with 100 mM NaCl as a function of pH. Stock emulsion refers to primary emulsion (12.5 wt% WPI and 25 wt% soybean oil, $d_{4,3} \sim 0.5 \mu\text{m}$) used to formulate the various treatments. The measurements were replicated at least six times. Error bars represent standard deviations. For Figure 4-1, columns with different letters are significantly different ($P < 0.05$) for each pH.

4.1.1 ζ -potential of liquid emulsions

The ζ -potential values provide valuable information about how bulk environmental conditions, such as pH and ionic strength, modulate the electrostatic potential of the emulsion droplet surface. The pH-dependent ζ -potential values of CO and PE emulsions at low and high ionic strengths were compared (Fig. 4-1). At low ionic strength, the ζ -potential of the CO emulsion was -41.11 at pH 7.0 and changed to $+24.71$ mV at pH 4.0, with a point of zero charge around pH 4.9, which corresponds to the isoelectric point (pI) of whey proteins (Fig. 4-1). At high ionic strength, the overall magnitude of the ζ -potential of CO emulsions decreased with values ranging from -16.56 mV to 7.79 mV on decreasing pH from 7 to 3, which could be attributed to electrostatic screening/ion binding effects of salt addition (Kulmyrzaev & Schubert, 2004).

LMP solution presented negative zeta potential values over the pH range studied, with its electronegativity decreasing with decreasing pH ($pK_a \sim 3.5$), which is attributed to the protonation of the anionic carboxylic acid groups on the pectin backbone (Cho et al., 2010). For PE emulsions at low ionic strength, the ζ -potential values range from -5.45 mV at pH 4 to -37.48 mV at pH 7. At pH between 6 and 7, irrespective of ionic strength, the ζ -potential values for PE emulsions were slightly less negative and fairly similar to that of the CO emulsions which might be due to the anionic character of LMP and the proportion in which they were added to the continuous phase (0.5 wt% LMP to 10 wt% WPI). At pH 5, the ζ -potential of PE emulsions formed at low ionic strength became considerably more negative (i.e. -26.3 mV compared to -2.85 mV obtained for CO emulsion). This effect was less pronounced at high ionic strength which may indicate screening of charges.

4.1.2 Particle size distribution of liquid emulsions

The effects of low (10 mM) and high (100 mM) ionic strength and addition of LMP on the particle size of emulsions at pH 4-7 was evaluated and compared (Fig. 4-2). At pH 7, the mean particle size of the WPI emulsions used to make CO and PE emulsions was $d_{4,3} \sim 0.5 \mu\text{m}$. For CO emulsions at low ionic strength, at near neutral pH, the particle size distribution was similar to that of the stock emulsion. This is likely attributed to the relatively strong electrostatic repulsion between the emulsion droplets at neutral pH. At lower pH, the size distribution shifted to a slightly higher diameter range, possibly indicative of droplet flocculation due to a reduction in electrostatic repulsion between the emulsion droplets at a pH near the isoelectric point of WPI. At higher ionic strength, CO emulsions showed similar behaviour as that observed at low ionic strength, the only exception being that at pH 4, a slightly smaller droplet diameters were observed. Previous work on whey protein emulsions made under similar conditions indicated that varying ionic strength did not influence the particle size of the emulsions (Guo, 2015). Changes in pH and ionic strength often lead to flocculation in protein-stabilized emulsions (Hunt & Dalgleish, 1994). However, dilution effects occurring during particle size measurement in the Mastersizer might undermine changes caused by ionic strength or pH. Also, for flocculated emulsion samples, stirring of samples during measurements along with changes in the refractive index and the morphology of droplets affect the accuracy of the measurement.

LMP containing emulsions also did not seem to be affected by changes in ionic strength, but the distributions appeared to be slightly broader (Fig. 4-2B and 4-2D). This may be indicative of likely droplet flocculation in the protein-stabilised emulsion due to addition

of LMP and changes in ionic strength. For all the emulsions, irrespective of LMP addition or varying ionic strength, dispersing in 2.0 % SDS solution led to the distributions to revert to that of the initial stock emulsions, indicating that the aggregation observed was due to droplet flocculation (data not shown).

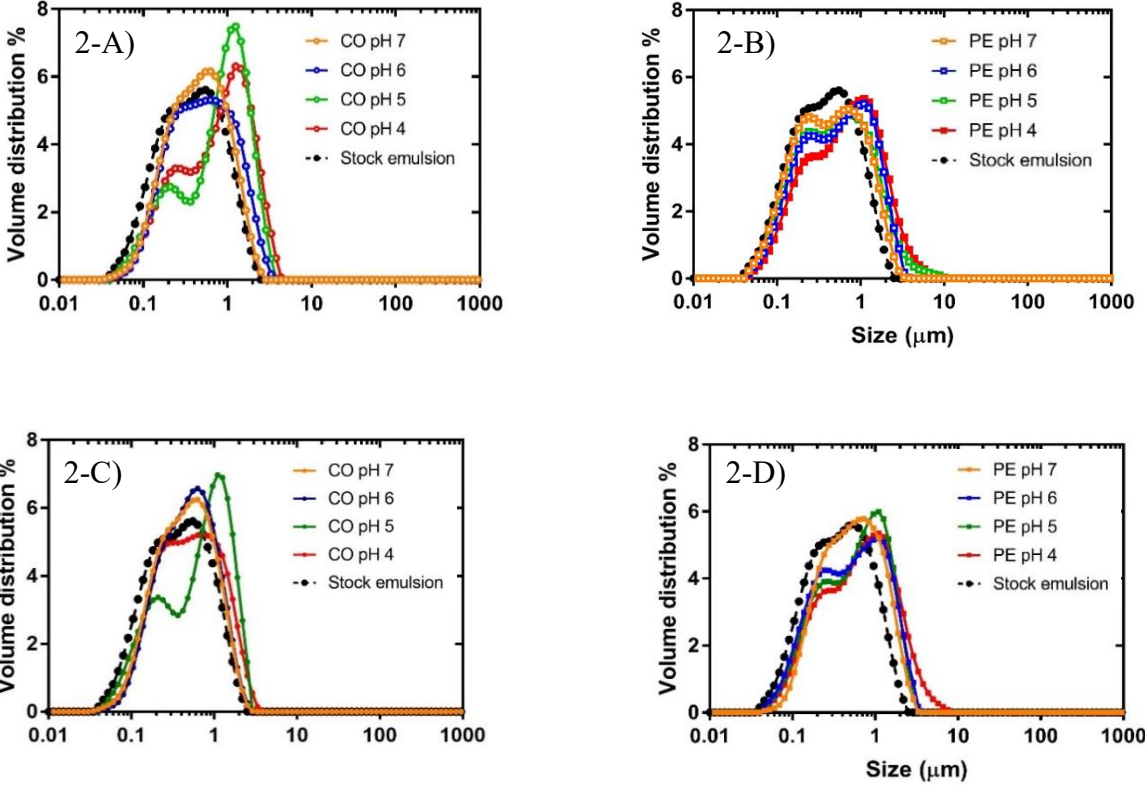


Figure 4-2 Particle size distributions ($d_{4,3}$) of (2-A) Whey protein emulsions (CO) with 10 mM NaCl, (2-B) Whey protein-Low methoxyl pectin emulsions (PE) with 10 mM NaCl, (2-C) Whey protein emulsions (CO) with 100 mM NaCl and (2-D) Whey protein-Low methoxyl pectin emulsions (PE) with 100 mM NaCl as a function of pH. Stock emulsion refers to primary emulsion (12.5 wt% WPI and 25 wt% soybean oil, $d_{4,3} \sim 0.5 \mu\text{m}$) used to formulate the various treatments. The measurements were replicated at least six times. Error bars represent standard deviations.

4.1.3 Confocal microscopy of liquid emulsions

Confocal laser scanning microscopy (CLSM) was used to visually compare the extent of protein aggregation and oil droplet morphology and distribution (Figure 4-3) prior to gelation. The composite images represent the green stained protein network and red stained oil droplets. The dark areas are representative of regions devoid of protein and oil, most likely indicative of the pectin network; however, it might also represent trapped water or air.

As shown in Fig. 4-3A and 4-3C, prior to gelation, CO emulsions show a fine non-aggregated microstructure, and the oil droplets appear to be homogeneously distributed in the protein-containing medium irrespective of ionic strength. LMP containing emulsions (Fig. 4-3B and 4-3D) showed the presence of dark zones or ‘depletion regions’ sandwiched between a network of protein aggregates containing the oil droplets. The area of the depletion zones seemed to decrease with an increase in ionic strength. This was probably due to charge screening possibly leading to a decreased thermodynamic incompatibility between the protein and the polysaccharide. Interestingly, despite depletion, the oil droplets within the protein network in PE emulsions did not seem to be aggregated.

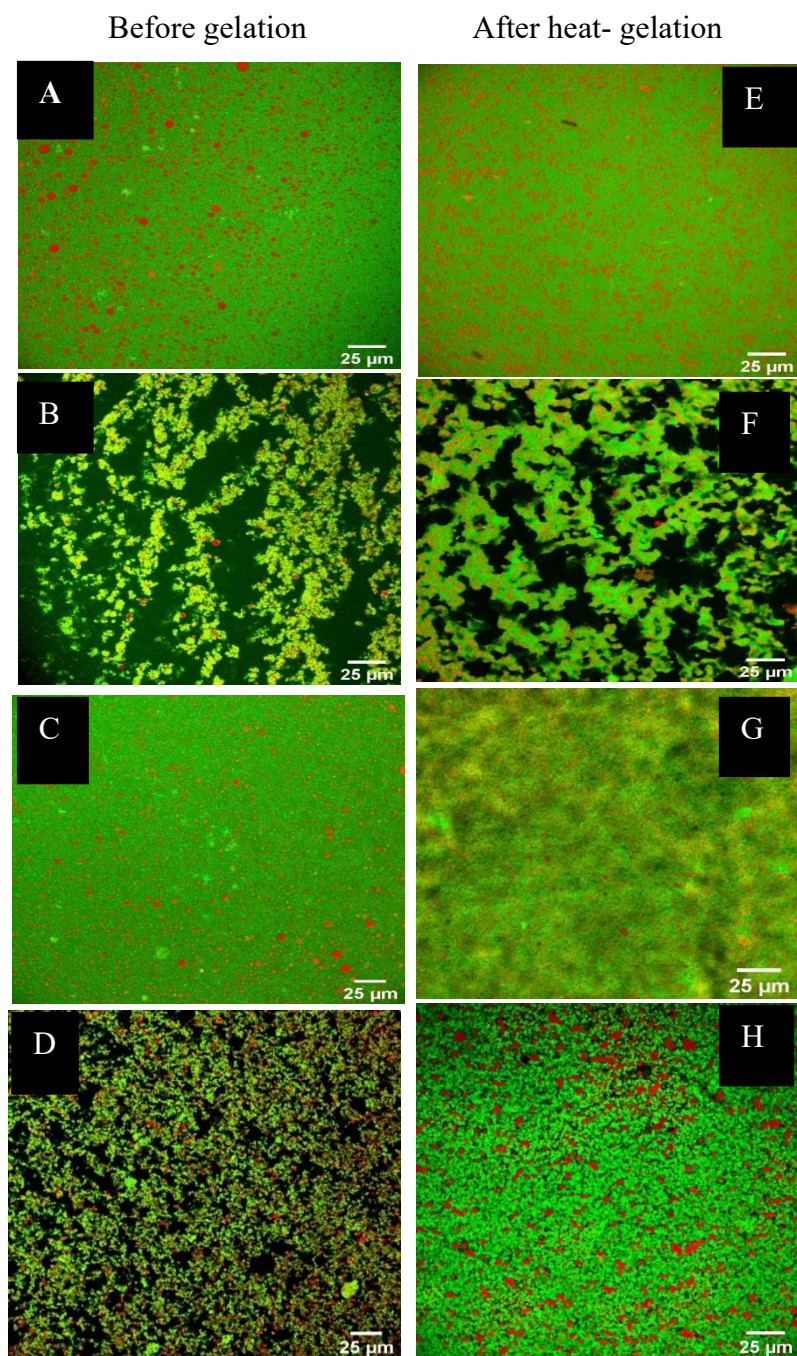


Figure 4-3 Confocal micrographs of emulsions before (A-D) and after heat gelation (E-H). Micrographs on the left represent liquid emulsions. A) whey protein emulsions (CO) with 10 mM NaCl, B) Whey protein-Low methoxyl pectin emulsions (PE) with 10 mM NaCl, C) Whey protein emulsions (CO) with 100 mM NaCl D), Whey protein-Low methoxyl pectin emulsions (PE) with 100 mM NaCl. The micrographs on the right represent the corresponding emulsions after heat gelation, namely E) Whey protein emulsion gel (CO) with 10 mM NaCl F), Whey protein-Low methoxyl pectin emulsion gel (PE) with 10 mM NaCl, G) Whey protein emulsion gel (CO) with 100 mM NaCl H), Whey protein-Low methoxyl pectin emulsion gel (PE) with 100 mM NaCl. Red represents the oil and green represents the protein. The scale bar corresponds to 25 μm .

4.2 Properties of heat-induced emulsion gels

4.2.1 Confocal micrographs of emulsion gels

After gelation, visible differences in the microstructure between CO gels made at low or high ionic strength could be observed (Fig. 4-3 E-H). For protein-based emulsion gels, the resulting microstructure depends on the properties of the protein adsorbed at the interface and the bulk unabsorbed protein in the continuous phase. The way these emulsion droplets are arranged prior to gelation affects how they become structured after gelation. It has been reported that if the droplets are in proximity prior to gelation this supposedly increases the likelihood of aggregation after gelation (Euston et al., 2002). At low ionic strength, CO gels showed characteristic ‘fine stranded’ structure (Fig. 4-3E) whereas at high ionic strength, the protein gel matrix appeared ‘particulate’ (Fig. 4-3G) as protein micro phase separation occurred (Nicolai et al., 2011). The state of the oil droplets in CO emulsions after gelation did not appear to be significantly affected by ionic strength, which has also been reported previously (Guo et al., 2014).

For PE gels at low ionic strength, it seemed the protein network became fused around the depletion zones (Fig. 4-3F). However, LMP does not form a gel at the concentration used in this study and exists as a viscous liquid at either low or high ionic strength (data not shown). By contrast at high ionic strength, a cohesive densely aggregated protein network was observed where LMP seemed to be buried amongst small pores in the network (Fig. 4-3H). At high ionic strength, charge screening might have led to a reduction in the net repulsive forces, leading to a decreased incompatibility between the protein and polysaccharide. PE gels at high ionic strength appear to be extensively flocculated. This

may be due to the combined effect of aggregation of the protein phase at high ionic strength and depletion flocculation induced by the polysaccharide.

Different extents of flocculation were evident for most gels as coalescence was ruled out after obtaining the same monomodal volume size distribution (data not shown) of oil droplets as that of the original emulsion after dissolving the gels in SDS buffer. Although gels appeared to be phase separated and flocculated at a microscopic length scale, macroscopically they were homogenous and self-supporting.

4.2.2 Rheological properties

The evolution of the storage modulus (G') during heat-induced gel formation of CO and PE emulsions at varying ionic strengths is shown in Figure 4-4. All the emulsions prior to gelation showed behaviour typically observed for liquid systems having a dominant viscous character (high $\tan \delta$ values) with very low values for G' (data not shown).

As the temperature increased, an increase in G' was observed which corresponded to the onset of gelation. Initial network formation was assessed by estimating the critical temperature corresponding to the onset of gelation. Defining the gelling temperature during dynamic rheological test is complicated due to the kinetic effects associated with protein gelation; for this study, the gelation temperature was determined by an increase of 10 Pa in G' during heating. In addition, the corresponding time at onset of gelation is reported in Table 4-1.

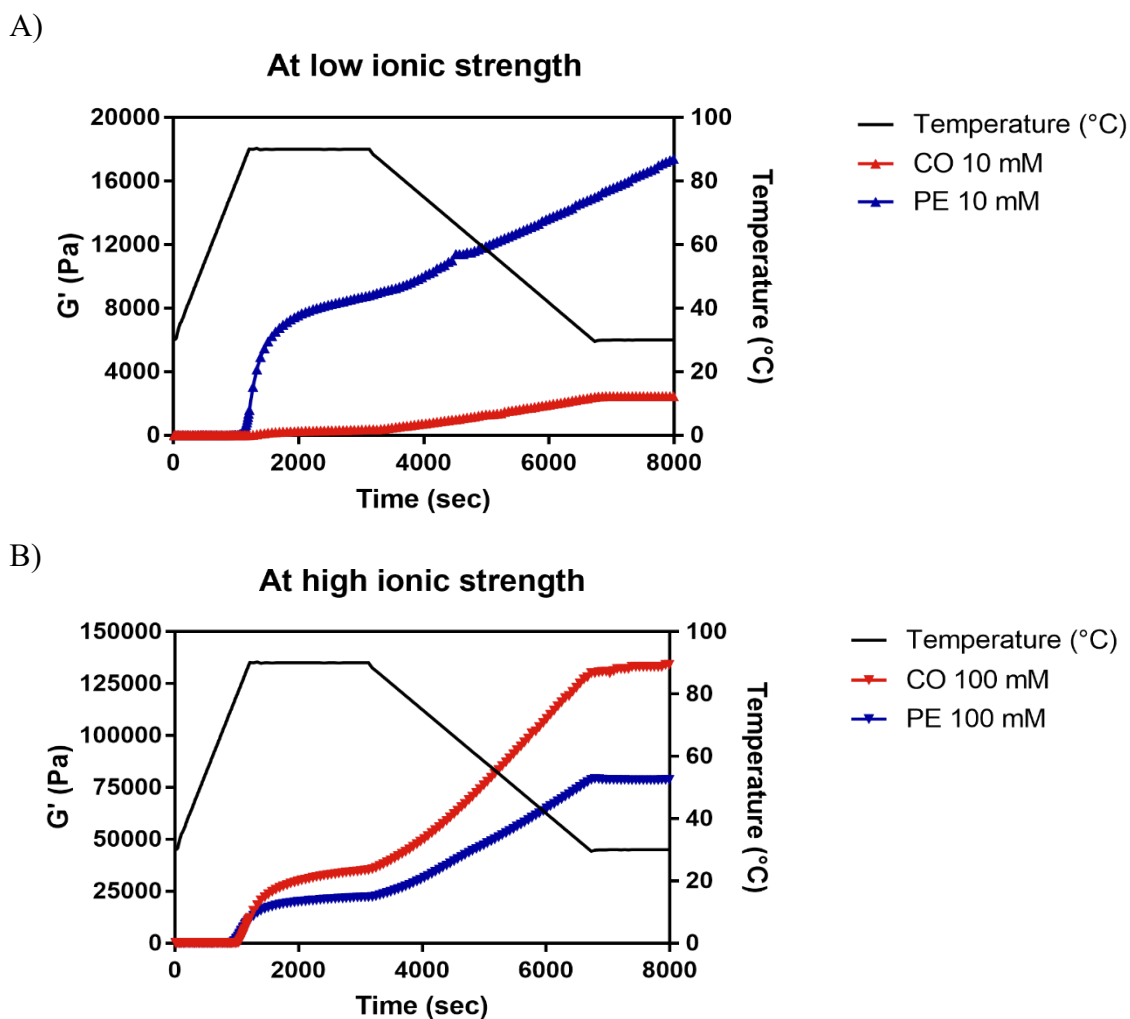


Figure 4-4 Change in storage modulus (G') during heat induced gelation of emulsions (0.5% strain, 1 Hz) at pH 7: (A) CO (whey protein) and PE (pectin and whey protein) emulsion gels formed at low ionic strength (10 mM); (B), CO (whey protein) and PE (pectin and whey protein) emulsion gels formed at high ionic strength (100 mM). The straight black line denotes the time-dependence of heating at temperature ($^{\circ}\text{C}$).

Table 4-1 Gelation properties during heat-induced gelation for CO (whey protein) and PE (pectin and whey protein) emulsion gels formed at low ionic strength (10 mM) and high ionic strength (100 mM). Gelation time (sec) and gelation temperature (°C) correspond to the time and temperature when an increase of 10 Pa in G' during the heating step was observed. Final storage modulus (KPa) corresponds to the final G' after the cooling step measured at 30 °C. Error bars represent standard deviation (n=5).

Gelation property	Low ionic strength		High ionic strength	
	CO	PE	CO	PE
Gelation time (sec)	1130 ± 5.774 ^a	918 ± 5.774 ^c	978 ± 5.774 ^b	887 ± 10 ^d
Gelation temp (°C)	86.1 ± 0.289 ^a	75.5 ± 0.289 ^c	78.6 ± 0.5 ^b	74 ± 0.289 ^d
Final storage modulus (KPa)	2.45 ± 0.98 ^d	17.9 ± 2.27 ^c	134 ± 7.87 ^a	78.7 ± 4.86 ^b

^{a-d}Values with different letters differ significantly ($P < 0.05$).

The onset of gelation was around 86.1 ± 0.289 °C and 75.5 ± 0.289 °C for CO and PE respectively at low ionic strength. At high ionic strength, the onset of gelation was around 78.6 ± 0.5 °C and 74 ± 0.289 °C for CO and PE respectively. Comparing CO emulsions at varying ionic strength, the decrease in the gelation temperature observed at high ionic strength is likely due to an increase in protein-protein interactions and aggregation due to reduction in the intermolecular repulsion of unfolded protein molecules as a result of charge screening effects (Lorenzen & Schrader, 2006).

The results clearly indicate that LMP addition led to a decrease in the gelation temperature of CO emulsions, and this effect was more pronounced at low ionic strength. Increase in

ionic strength also led to a decrease in gelation temperature particularly for CO emulsions whereas for PE emulsion it only led to a minor decrease. The earlier onset of gelation for PE emulsions at low ionic strength might be due to depletion flocculation on addition of LMP in concentrated protein emulsions promoting enhanced protein-protein aggregation resulting in formation of a gel at a lower temperature. This finding agreed with Çakır and Foegeding (2011) who reported similar results for mixed gels made using WPI/ κ -carrageenan. For PE emulsions at high ionic strength, screening of the charges would likely result in an increase in the protein-protein aggregation in addition to the depletion caused due to LMP. Changing the ionic strength would affect the strength of the interactions between protein-polysaccharide systems thereby modifying the extent of association/segregation in these systems due to charge shielding effects.

Changes in the storage modulus (G') during heat induced gelation of the CO emulsion gels followed the general behaviour typically observed for WPI emulsion gels formed at varying ionic strength (Guo et al., 2014; Ikeda et al., 1999; Luo et al., 2019b). At low ionic strength, the final storage modulus (G') was 2.45 ± 0.98 KPa and 17.9 ± 2.27 KPa for CO and PE respectively. At high ionic strength, a relatively higher final G' of 134 ± 7.87 KPa and 78.7 ± 4.86 KPa was obtained for CO and PE gels respectively (Table 4-1). The results show that ionic strength and LMP addition led to differences in the final storage modulus after cooling, the results seemed to imply that ionic strength had a more prominent effect, probably because the gels was predominately made of WPI. The influence of LMP addition on the final gel strength of the gels would depend on the extent of phase separation prior to gelation and the extent of depletion by the polysaccharide as affected by ionic strength reflecting the differences in G' values upon cooling. For

emulsion gels, the extent of pre-aggregation state of the oil droplets prior to gelation might also affect the rheological properties and the functionality of the gels formed.

4.2.3 Large deformation properties

Table 4-2 shows mean values for Young's moduli (stiffness of gels), fracture stress (gel strength), and fracture strain (brittleness of the gels) for the emulsion gels as measured by uniaxial compression.

Table 4-2 Mechanical properties of emulsion gels measured by uniaxial compression, CO (whey protein) and PE (pectin containing whey protein) emulsion gels formed at low ionic strength (10 mM) and high ionic strength (100 mM). Results are shown as mean \pm standard deviation of $N = 10$ independent experiments.

Mechanical property	Low ionic strength		High ionic strength	
	CO	PE	CO	PE
Fracture stress (KPa)	7.1 ± 1.9^c	15.9 ± 2.2^c	210.3 ± 13.5^a	180.7 ± 11.8^b
Fracture strain	1.56 ± 0.12^a	1.24 ± 0.08^b	0.89 ± 0.04^d	0.97 ± 0.04^c
Young's Modulus (KPa)	4.3 ± 0.4^c	6.8 ± 0.9^c	222.4 ± 19.1^a	196.7 ± 11.7^b

^{a-d}Values with different letters differ significantly ($P < 0.05$).

Gels formed at low ionic strength showed an overall lower values of Young's (elasticity) modulus as compared to gels made at high ionic strength. For gels made at low ionic strength, CO gels were less stiff (4.3 ± 0.4 KPa) as compared to PE gels (6.8 ± 0.9 KPa). At high ionic strength, CO gels (222.4 ± 19.1 KPa) were stiffer as compared to PE gels (196.7 ± 11.7 KPa). A higher Young's modulus is attributed to thickness of strands in networks and is usually observed for more coarser networks as thicker strands are more

difficult to bend than less stiff thin strands (Munialo et al., 2014). This may be possible given that increasing ionic strength gives rise to more coarser networks as observed in the confocal micrographs.

Fracture stress reflects the firmness (hardness) of the gel, and the corresponding strain is representative of gel deformability. Gels formed at low ionic strength showed lower fracture stress values compared to gels made at high ionic strength. In contrast, higher fracture strain values were obtained at low ionic strength whereas lower fracture strain values were obtained at high ionic strength. At low ionic strength, addition of LMP increased shear stress values at fracture (15.9 ± 2.2 KPa) of PE emulsion gel compared to CO gels (7.1 ± 1.9 KPa). However, at high ionic strength, opposite trends were seen where PE gels demonstrated lower fracture stress values (180.7 ± 11.8 KPa) compared to CO gels (210.3 ± 13.5 KPa). In terms of fracture strain, at low ionic strength, LMP addition led to a decrease in fracture strain values (1.24 ± 0.08) compared to CO gels (1.56 ± 0.12), whereas at high ionic strength, PE gels demonstrated higher fracture strain values (0.97 ± 0.04) compared to CO gels (0.89 ± 0.04). This indicates that under conditions where a fine stranded emulsion gel network is formed, addition of LMP caused the gels to become stronger and less elastic (increased fracture stress and decreased fracture strain) whereas addition of LMP under conditions where a particulate gel is formed causes the emulsion gels to become weaker and less brittle (decreased fracture stress and increased fracture strain). As observed in the confocal micrographs, PE gels showed the presence of large depletion zones at low ionic strength, which added discontinuity to the overall gel matrix thus making the emulsion gel brittle but increasing the overall strength of the gel matrix. However, at high ionic strength, the presence of depletion zones in PE gels considerably

decreased and the gel matrix appeared to be more particulate thus explaining its weaker network as compared to CO gels. High ionic strength also shields the effective charges between protein and polysaccharides, which may lead to changes in the extent of interactions between the biopolymers.

The overall higher fracture stress observed at high ionic strength was probably due to the higher amount of salt (100 mM) which increases the rigidity of the protein gel network (Hussain et al., 2012; Ikeda et al., 1999). It has been stated that increase in ionic strength may promote cross-links between whey proteins through both disulfide bridges and hydrophobic interactions and thus accelerating the aggregation of proteins (Macierzanka et al., 2012). In addition, the flocculation of oil droplets within the emulsion gel might also influence the mechanical properties of the emulsion gels in addition to LMP addition and varying ionic strength. The results imply that varying the ionic strength largely influences the mechanical properties of these gels. Although distribution of oil droplets and LMP addition and its interaction with the protein emulsion gel matrix does contribute to the overall strength of the network, the gels are predominately made up of protein, which are amenable to changes in ionic strength and seems to be the dominant factor contributing to overall mechanical properties of the mixed system.

4.3 Behaviour of emulsion gels during dynamic gastric digestion

4.3.1 pH profile of emptied digesta

The HGS simulates the dynamics of human gastric digestion process; there is a continuous addition of SGF (pH 1.5), and pepsin accompanied by shear and progressive

gastric emptying. This leads to gradual acidification of the stomach contents along with a continual sample dilution. The changes in pH of the emptied gastric digesta for the various gels as a function of digestion time are shown in Fig. 4-5A-B.

The initial pH values depict the pH of the sample from the oral phase when mixed with the basal fasting fluid. The initial pH values for gels were 6.10 and 6.15 for CO and PE gels made at low ionic strength (Fig. 4-5A), whereas for gels made at high ionic strength, pH values were 5.47 and 5.67 for CO and PE gels respectively (Fig. 4-5B). The pH profiles of CO and PE gels at both low and high ionic strengths were not significantly different ($P > 0.05$). After 240 min, gels made at low ionic strength dropped to pH about 2.68 which was slighter higher than gels made at high ionic strength which decreased to about pH 2.34.

Dynamic structural breakdown of the gel leads to changes in the pH as different extents of released material in the gastric fluid have different buffering capacities as affected by gradual acidification. In addition, the buffering capacity of the food, dilution by gastric emptying of food, and the increasing volume of enzyme/acid secretion also affects pH.

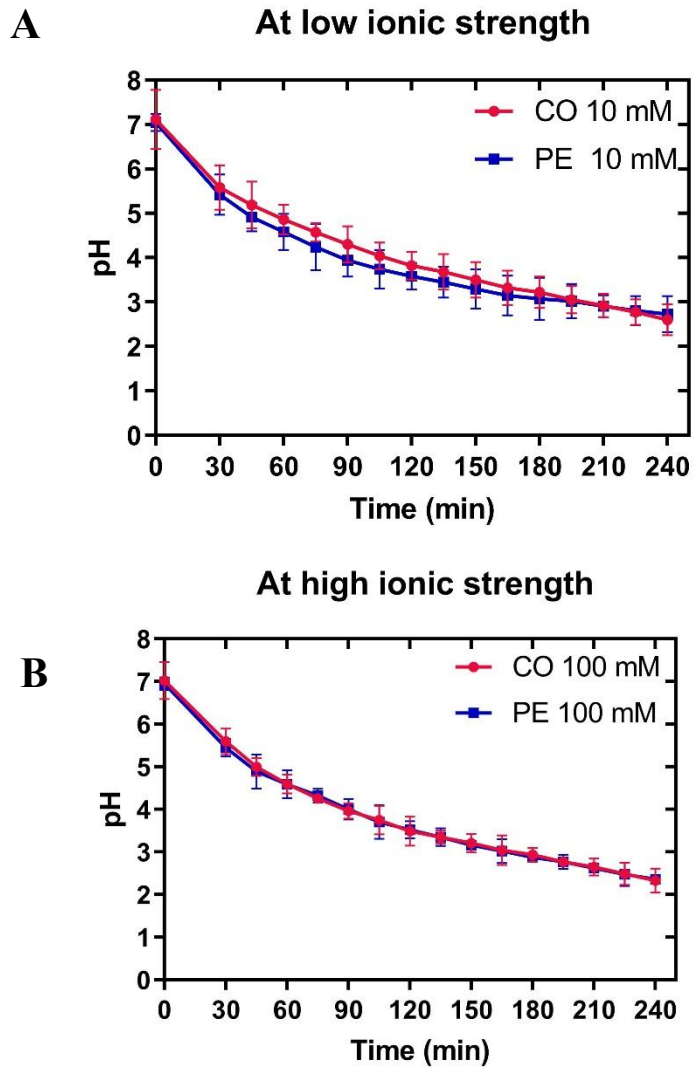


Figure 4-5 Changes in pH of the emulsion gels during dynamic gastric digestion in the HGS: A, CO (whey protein) and PE (pectin containing whey protein) emulsion gels formed at low ionic strength (low ionic strength-10 mM); B, CO (whey protein) and PE (pectin containing whey protein) emulsion gels formed at high ionic strength (low ionic strength- 100 mM). Error bars represent standard deviation (n=5).

One caveat during pH measurement for digestion of soft solids is that emptied gastric digesta is mainly the liquid containing some undigested gel particles that pass through ≤ 1 mm sieve. Therefore, the measured pH value mainly reflects the liquid portion of the digesta and might not necessarily be indicative of the pH changes inside the main stomach chamber containing intact undigested gel pieces (above 1mm) along with the gastric fluids. However, our results indicate that the presence of LMP or varying the ionic strength did not lead to significant changes in pH profiles of the gels during digestion ($P > 0.05$).

4.3.2 Changes in the solid content of emptied digesta

The solid content (dry matter %) of the emptied digesta is shown in Figure 4-6. The dry matter content for both sets of gels showed a slow increase till 150 min of gastric digestion after which it increased rapidly. For the first 150 min, compared to the control, LMP containing gels showed a lower degree of dry matter loss at low ionic strength whereas at high ionic strength, a slightly higher extent of dry matter loss was observed. Post 150 min, dry matter losses increased progressively for all the gels, and this increment was greater for gels made at low ionic strength than at high ionic strength. There seemed to be a considerable difference in the rate of dry matter content post 150 min for gels made at low and high ionic strength, possibly indicating different extents of gel breakdown during digestion.

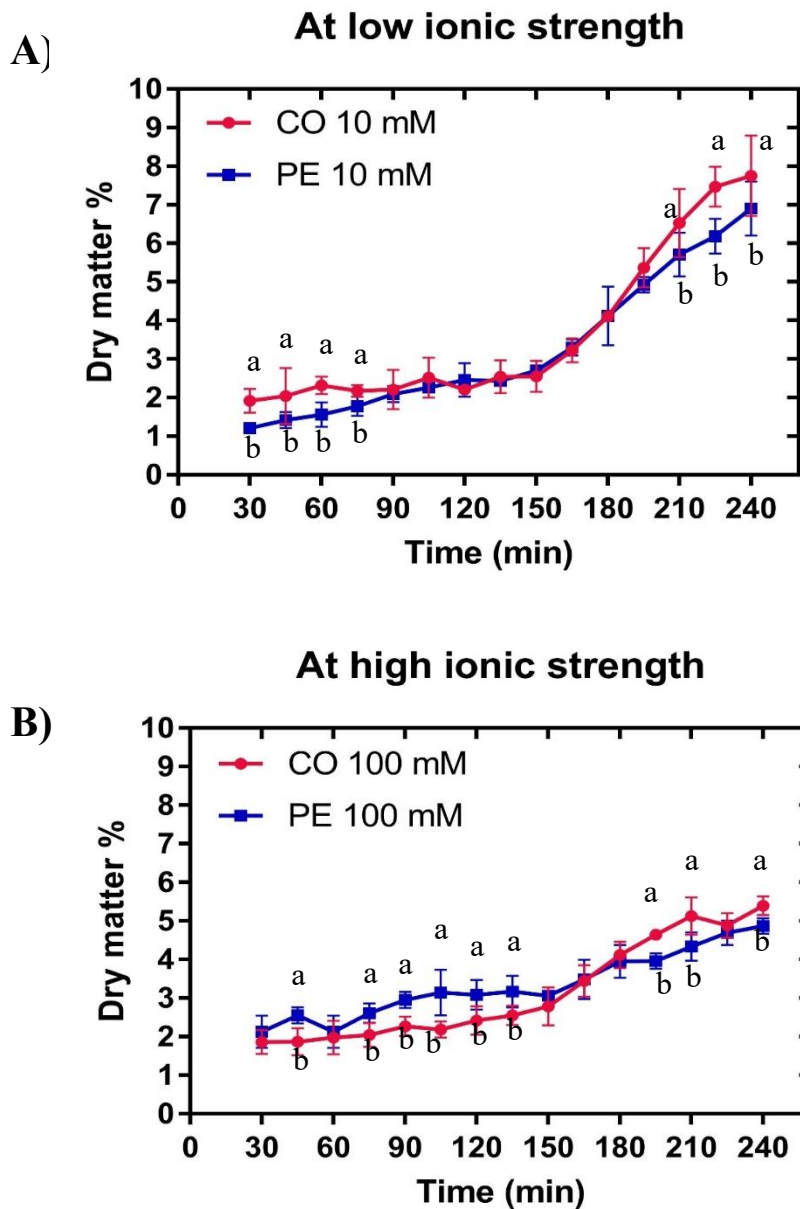


Figure 4-6 Changes in dry matter of the emulsion gels during dynamic gastric digestion in the HGS as a function of digestion time: A, CO (whey protein) and PE (pectin containing whey protein) emulsion gels formed at low ionic strength (low ionic strength-10 mM); B, CO (whey protein) and PE (pectin containing whey protein) emulsion gels formed at high ionic strength (low ionic strength-100 mM). Error bars represent standard deviation ($n=5$).

The slight lag in the dry matter loss during the initial period might be because gastric pH was above the optimal pH for pepsin activity. Therefore, the initial differences might be a result of the mechanical disintegration of these gels. Overall, the results imply that gels made at high ionic strength disintegrated to a lesser extent than gels made at low ionic strength. These results indicate that the effect of pepsin accompanied by mechanical shear was greater for the gels made at low ionic strength than gels made at high ionic strength.

To ascertain the rate of bio-accessibility of nutrients during gastric digestion from a given food system, it is important to measure the dry matter loss as this would be made up of soluble and insoluble nutrients which have been emptied out of the stomach and made available for absorption in the small intestine. Disintegration of a food matrix depends on the rate of diffusion of gastric fluid, which is dependent on the particle size, pH of the fluid, the structure of the food matrix and its resistance to mechanical shear. For these experiments, emptying times were held constant at 3ml/min and differences in solid emptied are indicative of different extents of breakdown during digestion. As stated in the previous section, particle sizes of the bolus were similar and pH values did not show considerable differences indicating that for these emulsion gels, their susceptibility to mechanical shear and their structural differences played an important role in their disintegration. However, it should be noted that solid loss does not necessarily imply hydrolysis, but mechanical disintegration does make the protein more accessible to pepsin.

As discussed in the previous section, for PE gels at low ionic strength, LMP was continually released into the surrounding gastric media. This along with the phase

separated structure of the PE gels may be expected to lead to a higher extent of disintegration as compared to control which is not in line with our observation. This might be due to an increase in the local concentration of gelled protein matrix in the gels resulting from depletion flocculation due to LMP during gel formation as corroborated by rheological and texture measurements. This increase in concentration is said to provide higher mechanical resistance and show a lower degree of hydrolysis during simulated gastric digestion (Luo et al., 2015). The slightly higher extent of disintegration for PE gels at high ionic strength for the first 150 min might be attributed to the combined effects of ionic strength and LMP on the structural properties of the gel network, where the decreased gel strength, brittle nature and high aggregated particulate network might explain differences observed.

4.3.3 Release of pectin from emulsion gel during digestion

LMP diffusion from the gels depends on factors such as its physico-chemical interaction with the bulk gel matrix and other factors, such as susceptibility to mechanical shear, extent of proteolysis, gel swelling, gel erosion and disintegration.

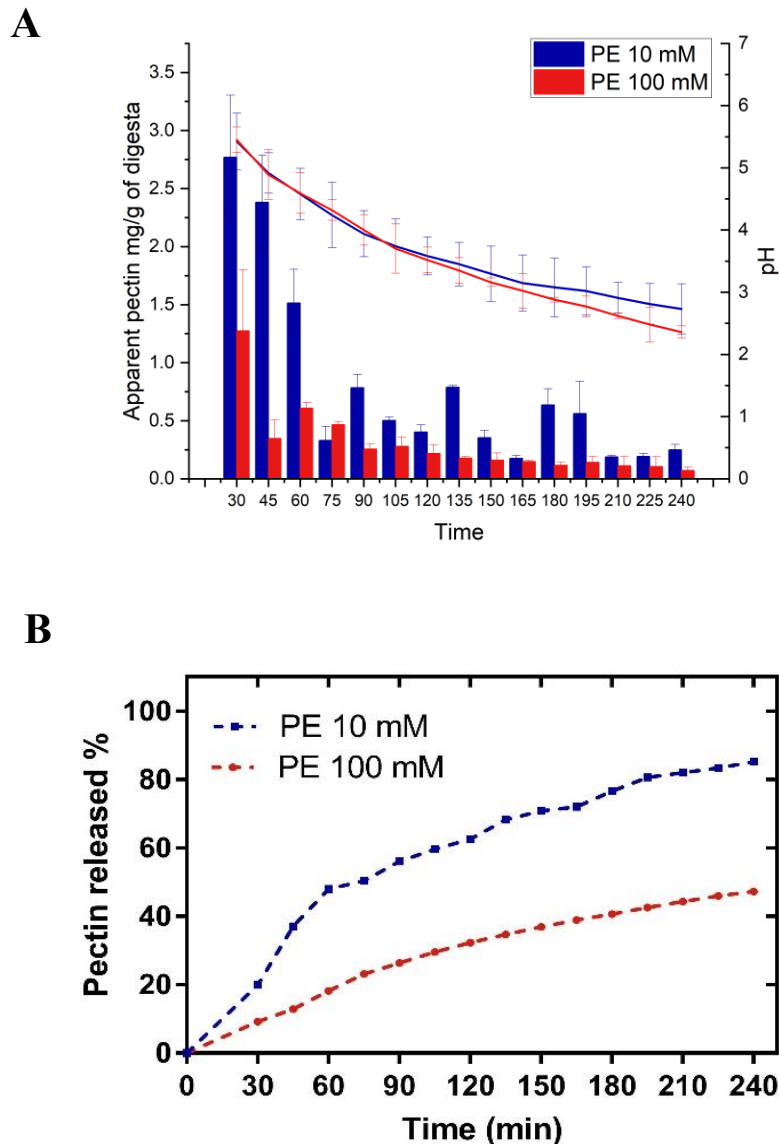


Figure 4-7 Low methoxyl pectin content of the gastric digesta (mg/ml) as a function of digestion time (A) and cumulative percent of pectin release (B) during gastric vitro digestion for the soft (gels made with 10 mM NaCl) and hard gels (gels made with 100 mM NaCl). Results are expressed as pectin content (mg/g) of the gastric digesta at each time point on dry weight basis. Based on this data, a cumulative percent of pectin released (%) over digestion time (min) was also plotted. This was calculated based on the release of pectin at specific digestion times.

To quantify the amount of LMP released into the surrounding gastric medium because of gel breakdown during gastric digestion, the amount of LMP in the emptied digesta was measured. Fig 4-7A and 4-7B shows the amount of LMP present in the gastric digesta (mg/mL) at each time point and the cumulative percentage of LMP released into the gastric fluid during gastric digestion of PE emulsion gels made at low and high ionic strength.

In general, LMP release from PE gels showed a trend having an initial higher rate of LMP release followed by a somewhat steady increase towards the latter stage of digestion (Fig. 4-7A). The cumulative amount of LMP release was considerably higher for PE gels made at low ionic strength compared to gels made at high ionic strength (Fig. 4-7B). This could be attributed to the phase separated gel structure of PE gels at low ionic strength; the presence of pectin rich regions in the gel could be considered as weak spots resulting in a greater susceptibility to mechanical shear the stomach and digestion process (Fig. 4-7B). As described in previous sections, PE gels made at high ionic strength were mechanically stronger and the gel matrix was coarser and more aggregated which may explain the differences observed. However, the overall disintegration of the bulk gel may also impact the overall release of pectin from the gels.

4.3.4 Particle size distribution of emptied digesta

Bulk gel strength of structured food systems is considered to be as a key factor influencing digestion (Guo et al., 2015, Luo et al., 2017). For the present study, the emulsions gels were ground to a similar particle size during simulated oral processing to discount the effect of higher-level structural order, therefore assessing if the inherent microstructural properties of the emulsion gel still play a role during digestion. To understand the different

extents of disintegration occurring during *in vitro* digestion of the emulsion gels, the particle size distributions (PSD) of the emptied digesta were characterised (Figure 4-8). The PSD can be generally divided into three different particle size ranges: large ($d_{4,3} \sim 100 - 1000 \mu\text{m}$), intermediate ($d_{4,3} \sim 1 - 10 \mu\text{m}$) and small ($d_{4,3} \sim 0.1 - 1 \mu\text{m}$). The peaks in the large size range ideally correspond to gel particles and the peak between 0.1 to 1 μm is representative of stable emulsion droplets that have been released from the gel matrix. After oral processing the average D50 of the emulsions gels was 2.5 mm. During gastric digestion particles <1 mm are emptied, thus we can expect that the peaks in the large size range are indicative of emptied intact gel particles of smaller size.

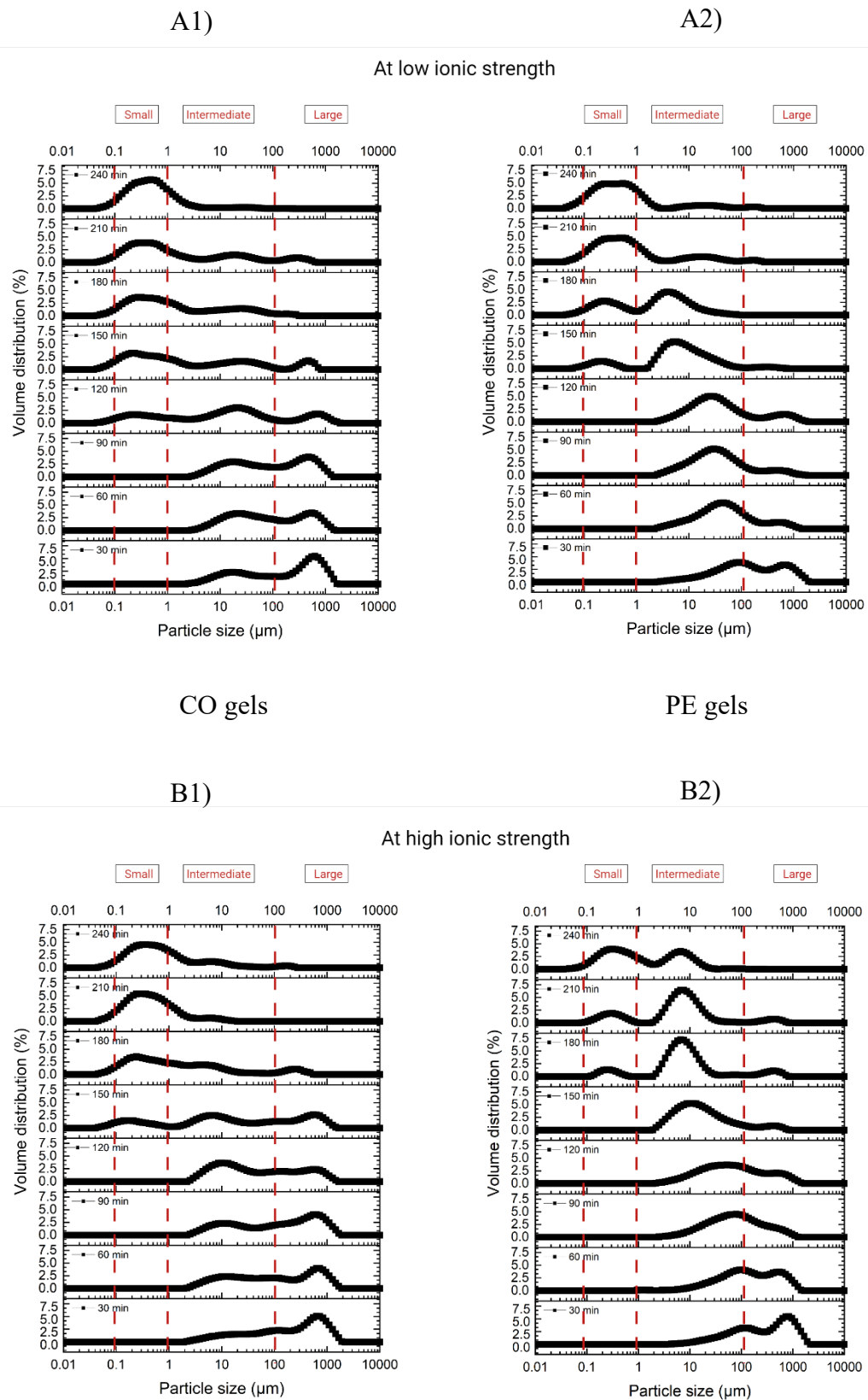


Figure 4-8 Changes in particle size distribution (volume-weighted average diameter $d_{4,3}$) of (A1 and A2) CO gels (whey protein) and PE gels (pectin and whey protein) emulsion gels formed at low ionic strength (10 mM); (B1 and B2), CO gels (whey protein) and PE gels (pectin and whey protein) emulsion gels formed at high ionic strength (100 mM) during gastric digestion in the human gastric simulator. The legends at the top left of each stack indicate the gastric digestion time.

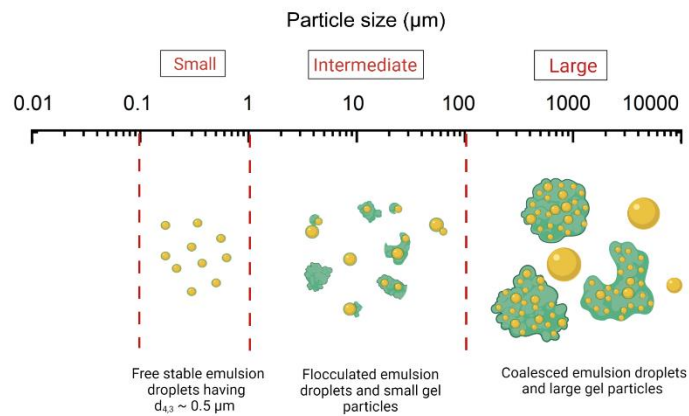


Figure 4-9 The schematic diagram represents possible contributors in the emptied gastric digesta that impact the particle size distribution of the emptied digesta at different length scales.

For the emulsion gels, during the initial stages of digestion, the emptied digesta comprised of particles in the intermediate and large size range. As digestion progressed, the peaks in the larger size range decreased and the size distribution post 150 min was dominated by the presence of larger peaks of smaller sizes (in the range $\sim 0.1\text{--}10\ \mu\text{m}$). The presence of peaks in the intermediate and large size range during the latter stages of digestion might be indicative of aggregation or possible coalescence (Fig. 4-9).

The emulsion gels differed in their breakdown patterns during digestion. Comparing gels made at low ionic strength, PE gels disintegrated more rapidly as compared to CO gels as evidenced by a decrease in the 100 -1000 μm peak during the initial stages of gastric digestion and shifting of the distribution to smaller sizes. Confocal micrographs corroborated these findings. Post 150 min, the peak between 0.1–1 μm became more prominent indicating the presence of stable emulsion droplets in the digesta. For PE gels,

appearance of this peak was in conjunction with an increase in the peak in the $\sim 10 \mu\text{m}$ range during 150-180 min, which then decreased towards the end of digestion. The volumes of the peaks in the small and intermediate region varied for the CO and PE gels indicating differences in extents of free stable emulsion droplets and presence of coalesced oil droplets in the digesta.

For gels made at high ionic strength, the 0.1–1 μm peak was observed to appear at 150 min for CO gels, whereas for PE gels it was observed around the 180 min mark. Additionally, there were clear differences in volume percent of the 0.1–1 μm peak indicative of different extents of stable emulsion droplets released from these gels. After 150 min of digestion, the $\sim 10 \mu\text{m}$ peak was more pronounced as compared the 0.1–1 μm peak for PE gels whereas for CO gels, the $\sim 10 \mu\text{m}$ peak was much smaller. This indicates for gels made at high ionic strength, CO gels broke down to a greater extent as compared to PE gels. This suggests that given no dissociating buffer was added to the samples during the measurement, results are more likely indicative of aggregation of the released droplets/small gel fragments.

4.3.5 Microstructure of emptied digesta

Oral and gastric digestion processes destroy the initial gel network structure and results in particles of different sizes dispersed in the gastric fluid. The behaviour of the disintegrated system is said to be dependent on the initial gel properties but, the disintegration process along with changes due to the gastric environment might lead to restructuring of the gastric contents at different structural levels. The microstructure of the emulsion gels during gastric digestion is shown in Fig. 4-10.

The overall pattern observed for emulsion gels was that as digestion progressed, the gel particles seemed to reduce in size. During the latter stages of digestion, it could be observed that the emptied digesta appeared to be more concentrated with the presence of small gel particles and released oil droplets. Comparing CO and PE gels formed at low ionic strength (Fig 4-10A), it could be seen that although they were ground to a similar particle size, their structural breakdown patterns differed. Differences in structural breakdown patterns might lead to differences in dissolution of the gel matrix, extents of proteolysis and oil droplet release. CO gels seemed to be broken down as large chunks as compared to PE gels which broke down into much smaller fragmented particles. This might be attributed to the phase separated gel structure of PE gels where disintegration leads to disruption of the gel network and hydrophilic LMP enclosed in the network, releases into the gastric fluid leaving behind fragments of the protein gel network.

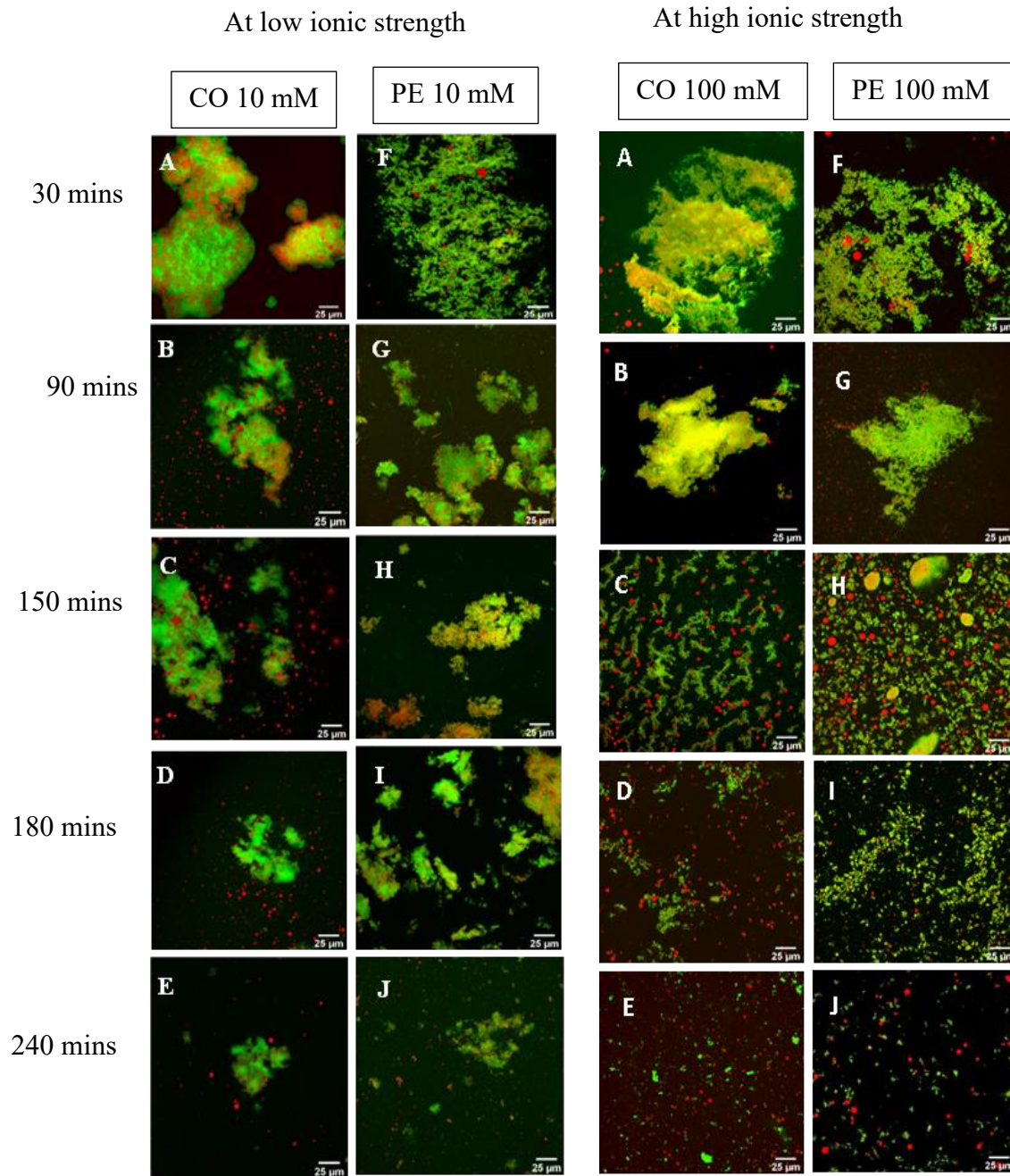


Figure 4-10 CLSM images of gastric digesta as a function of digestion time during dynamic gastric digestion in the HGS: Micrographs on the left represent gastric digesta of gels formed at low ionic strength, whey protein emulsions (CO) with 10 mM NaCl, Whey protein-Low methoxyl pectin emulsions (PE) with 10 mM NaCl at different digestion time points (30 min- 240 min), whereas micrographs on the right represent gastric digesta of gels formed at high ionic strength, whey protein emulsions (CO) with 100 mM NaCl, Whey protein-Low methoxyl pectin emulsions (PE) with 100 mM NaCl. Red represents the oil and green represents the protein. The scale bar corresponds to 25 μ m.

For CO gels at low ionic strength, as digestion progressed, the gel particle seemed to disintegrate, and coalescence of the oil droplets occurred as evidenced by presence of large droplets. Although PE gels appeared to have a more fragmented breakdown pattern, the oil droplets within the gel matrix appeared to be quite stable throughout the gastric digestion. The micrographs seem to suggest that oil droplets present within the emptied gel particles of PE gels remained structurally intact and released oil droplets may likely be due to surface proteolysis. The increased stability of PE gels was probably due to the slightly more aggregated protein gel network caused by depletion due to LMP during gel formation. Also, presence of LMP in the gastric fluid and gradual acidification might have an impact on the stability of PE gels.

For gels made at high ionic strength, a similar trend was observed where size reduction of the emptied gel particles was observed as digestion progressed (Fig 4-10B). The oil droplets in the emptied gel particles showed no visible sign of coalescence or flocculation even as size reduction occurred although a few free oil droplets were observed. This is well corroborated with results obtained for the oil droplet size. This is likely caused due to highly rigid particulate network formed at high ionic strengths that likely protects against mechanical shearing and proteolysis. Comparing CO and PE gels made at high ionic strength, it could be seen that during the initial stage, emptied gel particles in CO gels digesta seemed to be more resistant and emptied as large clumps whereas for PE gels the emptied gel particles seemed to fragment into smaller particle sizes. However, there was no discernible difference in oil droplet release was observed as corroborated by oil droplet size results.

4.3.6 Stability of oil droplets during gastric digestion

The changes in oil droplet size distribution of the emptied digesta, measured in a dissociating buffer, during gastric digestion are shown in Fig. 4-11 and Fig. 4-12. For the emptied digesta, mixing with the dissociating buffer solubilises the emptied gel particles and breaks down any flocs in the sample, allowing for the assumption that increases in droplet size due to coalescence. The peak between 0.1 to 1 μm is representative of stable emulsion droplets that have been released from the gel matrix or intact droplets that were present within the emptied gel particles.

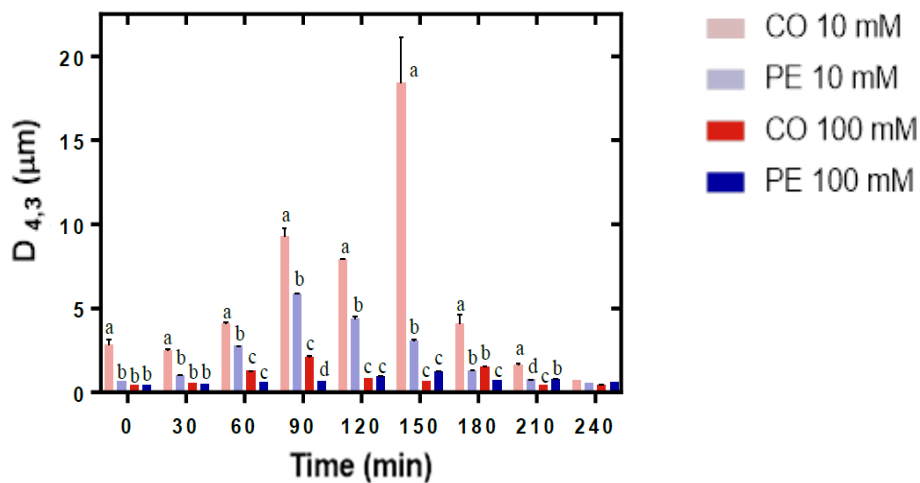


Figure 4-11 Changes in volume-weighted average diameter $d_{4,3}$ of CO (whey protein) and PE (pectin and whey protein) emulsion gels formed at low ionic strength (10 mM); (C1 and C2), CO (whey protein) and PE (pectin and whey protein) emulsion gels formed at high ionic strength (100 mM). The measurements were replicated at least six times. Error bars represent standard deviations. For Figure 4-11, bars without a common superscript letter differ ($P < 0.05$) as analyzed by one-way ANOVA and the Tukey test.

For all the gels, irrespective of LMP addition or ionic strength, the particle size and PSDs of the original emulsions, emulsion gels and the samples after exposure to oral phase and basal gastric fluid (0 min) were similar ($d_{4,3} \sim 0.45 \mu\text{m}$) indicating that the oil droplets were stable during heat-induced gelation and physical shear/ionic changes during simulated oral processing.

CO gels made at low ionic strength (Fig. 4-11), showed a distinct change in droplet size ($d_{4,3} \sim 2.86 \pm 0.87 \mu\text{m}$) after 30 min of gastric digestion with the distribution changing to multi-modal with the presence of smaller peaks of larger sizes (in the range $\sim 1\text{--}100 \mu\text{m}$). As digestion progressed, the peaks in the larger area became more pronounced, with $d_{4,3}$ reaching a value of 18.41 ± 1.27 at 180 min after which a decrease in the $d_{4,3}$ values were observed corresponding with a decrease in the peaks in the large size range $\sim 1\text{--}100 \mu\text{m}$. For PE gels, after 30 min digestion, the average droplet size slightly increased ($d_{4,3} \sim 0.682 \pm 0.22 \mu\text{m}$) and the size distribution was primarily bimodal with the peak at 10-100 μm size range increasing as digestion progressed. The average droplet size increased to $\sim 5.84 \pm 0.37 \mu\text{m}$ at 90 min after which it decreased with further digestion with the size reaching similar to that of the initial emulsions at 240 min ($\sim 0.569 \pm 0.17 \mu\text{m}$). These results suggest that for gels made at low ionic strength, CO gels were least stable to gastric digestion compared to gels containing LMP. For a system containing protein-polysaccharides, the polysaccharides in the system could lead to differences in the physiochemical properties of the protein, thus affecting the digestibility of protein because the accessibility of cleavage sites to protease on protein could be altered through interactions with polysaccharides. As digestion progresses, gradual acidification leads to a drop in pH. Under associative conditions, released emulsion droplets may interact with

oppositely charged polysaccharides dispersed in the digestion fluid leading to bridging flocculation conferring some protective effects against proteolysis during gastric digestion (Wackerbarth et al., 2009). Although at low pH the polysaccharide is known to be less ionised (Brejnholt, 2009), LMP used in this study is low calcium gelling, sufficiently charged at pH 3 (-14.96 mV) and is highly charge dense. Given that the amount of LMP used in this study is low, and considering gastric dilution, viscosity modifying effects and pectin-enzyme interactions are thought to at a minimum (Rinaldi et al., 2015, Nacer et al., 2004). The stability of oil droplets in PE gels during the latter stages of digestion might be because LMP has been found to reduce the hydrolysis of proteins (Mouécoucou et al., 2007).

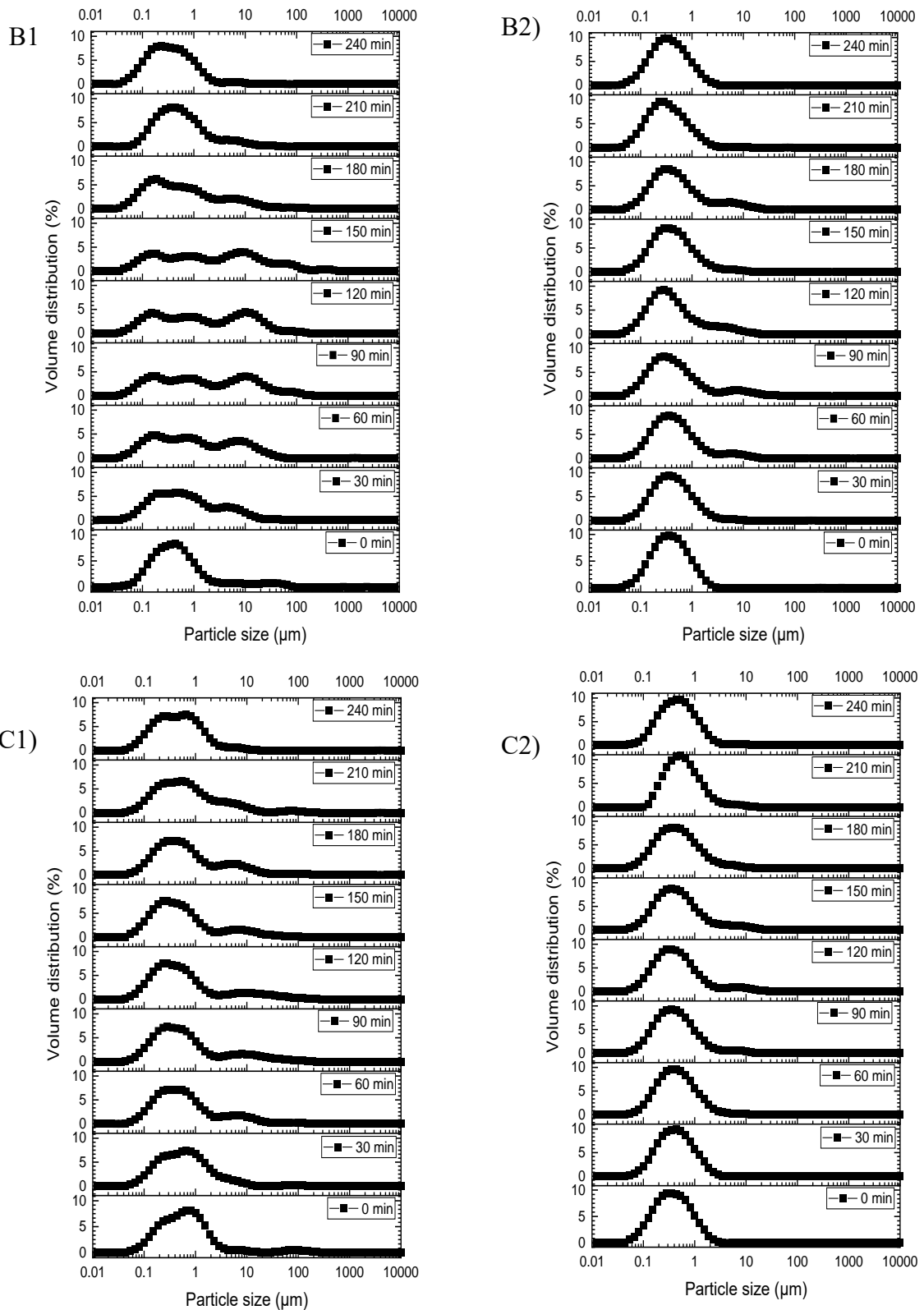


Figure 4-12 Changes in oil droplet size distribution of (B1 and B2) CO (whey protein) and PE (pectin and whey protein) emulsion gels formed at low ionic strength (10 mM); (C1 and C2), CO (whey protein) and PE (pectin and whey protein) emulsion gels formed at high ionic strength (100 mM). The measurements were replicated at least six times. Error bars represent standard deviations.

For gels made at high ionic strength, the average particle size did not change drastically, and they showed a primarily bimodal distribution, with a first peak around $\sim 0.5 \mu\text{m}$ and a small second peak in the larger size range ($\sim 3\text{-}10 \mu\text{m}$). The peak in the $\sim 3\text{-}10 \mu\text{m}$ range increased until about 150 min after which, particle size decreased until 240 min. The only difference for particle size for CO and PE being that the extent of this was discernibly less for PE gels as compared to CO gels. The size of the oil droplets in the emptied digesta for CO and PE gels only changed to about $0.434 \pm 0.22 \mu\text{m}$ and $0.629 \pm 0.31 \mu\text{m}$ after 240 min. The decrease in oil droplet size towards the latter stages of digestion might be due to the combined effect of gastric dilution, gastric emptying and presence of large, coalesced droplets not detected by the Mastersizer. However, no free oil or presence of large droplets was noticeable during measurements or during digestion.

Comparing gels made at low ionic strength and high ionic strength, gels made at low ionic strength showed an overall higher increase in droplet size with distributions being broader and more multimodal than for gels made at high ionic strength, clearly indicative of higher degree of droplet coalescence. This indicates that gel microstructure does play a role in the release of oil droplets. During the initial stages of gastric digestion, the onset of coalescence might be attributed to the release of oil droplets present near the surface of ground gel particles by hydrolysis and mechanical shear. This peak was more pronounced for gels made at low ionic strength than for gels made at high ionic strength which may mean that oil droplets in gels made at high ionic strength are more firmly bound to the gel matrix than gels made at low ionic strength. Similar results were for observed for fine and particulate whey protein gels.

Overall, the trends observed during particle size analysis indicate that for semi-solid emulsion systems, degradation/ dissolution of the matrix leads to a two-phase mixture consisting of the liquid phase containing released oil droplets and undigested gel particles. The stability of the released droplets then depends on the properties of the interfacial layer and its interactions with other components within the gastric environment. As digestion progresses, these droplets undergo further flocculation and coalescence and are emptied out, leaving behind undigested gel particles in the HGS chamber that are still being disintegrated and hydrolysed. This might explain the decrease in the extent of coalescence occurring during the latter stages of digestion, despite there being an increase in extent of solids emptied.

4.3.7 Impact of gel disintegration kinetics on lipid released during dynamic gastric digestion.

The structural properties of the chyme, such as its susceptibility to mechanical shear, extent of proteolysis, and gel disintegration affect the rate of lipid released in the emptied digesta. The amount of lipid released (%) during gastric digestion of the emulsion gels was measured (Fig. 4-13 A1 and A2). The rate of gel disintegration (expressed as solid % emptied) seemed to influence the rate of lipid emptied during gastric digestion. Therefore, the interrelationship between the extent of gel disintegration and lipid released was analysed to assess if the rate and extent of gel disintegration exerts a significant influence on lipid emptied during digestion. Results showed that, for all the samples there was a highly significant ($P < 0.01$) positive linear correlation (Table 4-3). For the gels made at low ionic strength, the correlation was higher than for the gels made at high ionic strength.

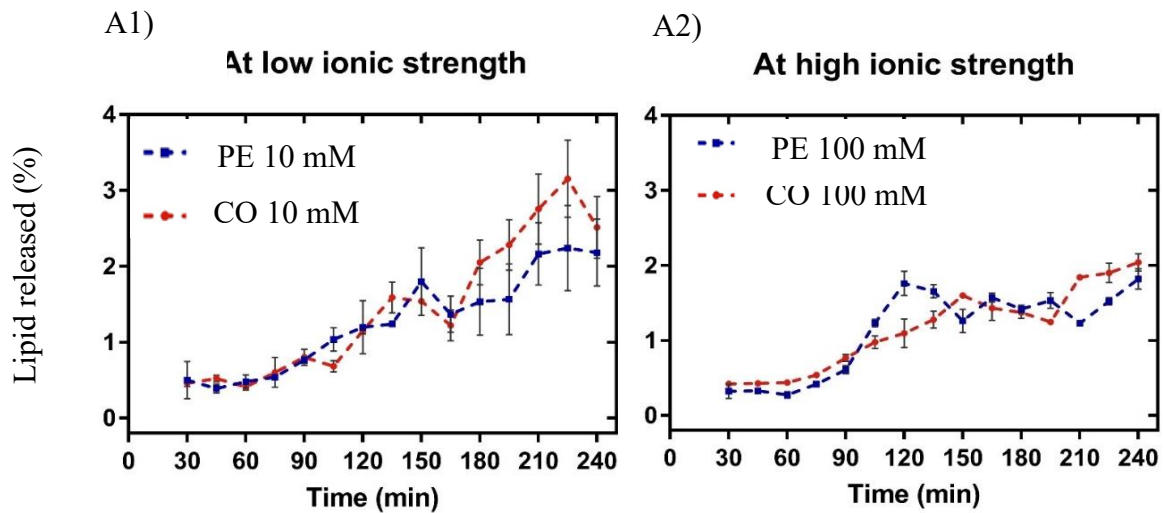


Figure 4-13 Changes in fat content (%) of the emptied digesta during dynamic gastric digestion in the HGS: A1, CO (whey protein) and PE (pectin containing whey protein) emulsion gels formed at low ionic strength (low ionic strength-10 mM); A2, CO (whey protein) and PE (pectin containing whey protein) emulsion gels formed at high ionic strength (low ionic strength- 100 mM). Error bars represent standard deviation (n=5).

Table 4-3 The relationship between the lipid released (%) and solid emptied (%) during gastric digestion for the different gels formed at pH 7, CO (whey protein) and PE (pectin and whey protein) emulsion gels formed at low ionic strength (10 mM) and high ionic strength (100 mM).. The Pearson correlation coefficient value (r), the R square are listed (P < 0.05).

Correlation between fat released (%) and solid emptied (%) at different digestion times			
	Pearson correlation r	R squared	P value (alpha = 0.05)
CO 10 mM	0.9023	0.8141	<0.0001
PE 10 mM	0.8869	0.7867	<0.0001
CO 100 mM	0.8739	0.7638	<0.0001
PE 100 mM	0.8009	0.6414	0.0003

For food containing oil droplets such as yoghurts, milk, cheese etc the fate of the structure of the surrounding matrix during gastric digestion dictates the extent and pattern of lipid release and oil droplet stability. Colloidal stability during gastric digestion also affects the rate of fat released, as phase separation, sedimentation or creaming of the gastric contents affect the release of fat during digestion (Singh, Ye et al. 2009, Acevedo-Fani & Singh, 2021). For this study, it was observed that the extent of lipid release was dependent on the extent gel breakdown as a linear positive correlation was observed for fat release and solid emptied.

The gels had similar fat contents prior to digestion, but the emulsion gels vastly differed in their kinetics of lipid release, which might have consequences for its consequent digestion. Since a highly significant positive correlation was observed for both CO and PE gels at low and high ionic strength (Table 4-3), our results suggest that the kinetics of lipid release during gastric digestion can be modulated by structural design of the emulsion gel.

4.4 Conclusions

Dynamic *in vitro* models like the HGS are able to simulate more closely the structural changes and physiologically relevant mechanisms that occur in structured foods like emulsions gels where the gastric phase plays an important role. This study demonstrated that addition of LMP and the ionic strength of the system influence the structural properties of the emulsion gel matrix, which impacts its gastric digestion kinetics and subsequently modulates the protein digestion and lipid release of these systems.

The results suggest that food matrix structural properties could be modified to alter resistance to gastric digestion which may have consequences on controlling the rate of gastric emptying and satiation. This study also provides for an increased understanding of the structure- digestion relationship and may help in the design of functional structures using complex emulsion-based matrices.

5 The effect of gel structure on gastric digestion of protein-polysaccharide emulsion gels formed at pH 4: Effect of associative interactions

Abstract

Mixed biopolymer emulsion gels are simplified models for multicomponent structures present in real foods. This chapter focussed on understanding how associative interactions between proteins and polysaccharides could generate a range of gel structures and textures.

Heat-set whey protein emulsion gels ($d_{4,3} \sim 0.5 \mu\text{m}$) with and without low methoxyl pectin (LMP) were formed at acidic pH (pH 4) favouring associative interactions. Additionally, the impact of low and high ionic strength (achieved by 10 mM and 100 mM NaCl addition) on gel structure was studied. Gels made at high ionic strength had an overall higher fracture stress compared to gels made at lower ionic strength. Confocal micrographs showed that these gels appeared to be aggregated irrespective of LMP or salt addition.

The breakdown kinetics of these gels were assessed under dynamic *in vitro* gastric digestion using the Human Gastric Simulator (HGS). LMP containing gels formed at low ionic strength showed a higher rate of matrix disintegration compared to control whereas at high ionic strength, a reverse trend was observed, i.e., the control gels disintegrated at a higher rate than the PE gels. Despite these observations, the emulsion gels did not show

any oil droplet coalescence. These results indicate that addition of LMP and ionic strength seem to influence the structural properties of the emulsion gel matrix, which impacts its gastric digestion kinetics and subsequently modulates the lipid release from these systems.

5.1 Properties of liquid emulsions prior to heat-induced gelation

The influence of ionic strength on the stability of CO and PE emulsions was investigated. The ζ -potential behaviour and particle size distribution have been discussed in the previous chapter (Chapter 4, Section 4.1.1 and Section 4.1.2). The changes in gel microstructure before and after gelation were assessed using confocal laser scanning microscopy.

5.1.1 Confocal microscopy of liquid emulsions

In Figure 5-1, A-D, the extent of protein aggregation and oil droplet distribution prior to gelation was compared using CLSM. The composite image shows the green-stained protein networks and red-stained oil droplets. Dark areas in the images are likely to be areas where protein or oil is absent, likely representing portions of the pectin network; however, they might also be water or trapped air.

CO emulsions at low ionic strength appeared as a dense compact network, whereas at high ionic strength, they appeared to have a disconnected aggregated network with the presence of dark regions. PE emulsions at both low and high ionic strength appeared to be highly aggregated having tight knit network. This aggregation for the emulsions is

probably because pH is close to IEP leading to microphase separation (Tuinier, Rolin et al. 2002, Tromp, de Kruif et al. 2004). At high ionic strength, charge screening might have led to the disconnected network of CO emulsions, whereas for PE emulsions, polysaccharide addition might prevent extensive flocculation near or at IEP, limiting protein aggregation (Tuinier, Rolin et al. 2002, Tromp, de Kruif et al. 2004).

5.1.2 Confocal micrographs of emulsion gels

At high ionic strengths, CO gels and PE gels appeared particulate irrespective of ionic strength changes or LMP addition (Figure 5-1E-H). Microstructures of protein-based emulsion gels are determined by the properties of the protein adsorbing at the interface and the bulk protein in the continuous phase. This arrangement of emulsion droplets prior to gelation impacts their subsequent structure. It has been reported that if droplets are in proximity before aggregation occurs, this increases the chance of aggregation after gelation (Euston et al., 2002)

CO gels, irrespective of ionic strength, appeared to be more flocculated than PE gels, which might be due to the combined effect of low pH and ionic strength. Flocculated emulsion oil droplets were unevenly distributed in the protein gel matrix; no droplet network was observed. Interestingly, PE gels appeared less flocculated, and the gel matrix appeared more cohesive (Figure 5-1 F-H). This effect can be attributed to the space filling effect of bulky polysaccharide chains in a particulate and permeable protein matrix. Although protein-polysaccharide binding under associative conditions is at a minimum, the presence of polysaccharide helps to prevent extensive flocculation via a steric mechanism.

Before gelation

After heat- gelation

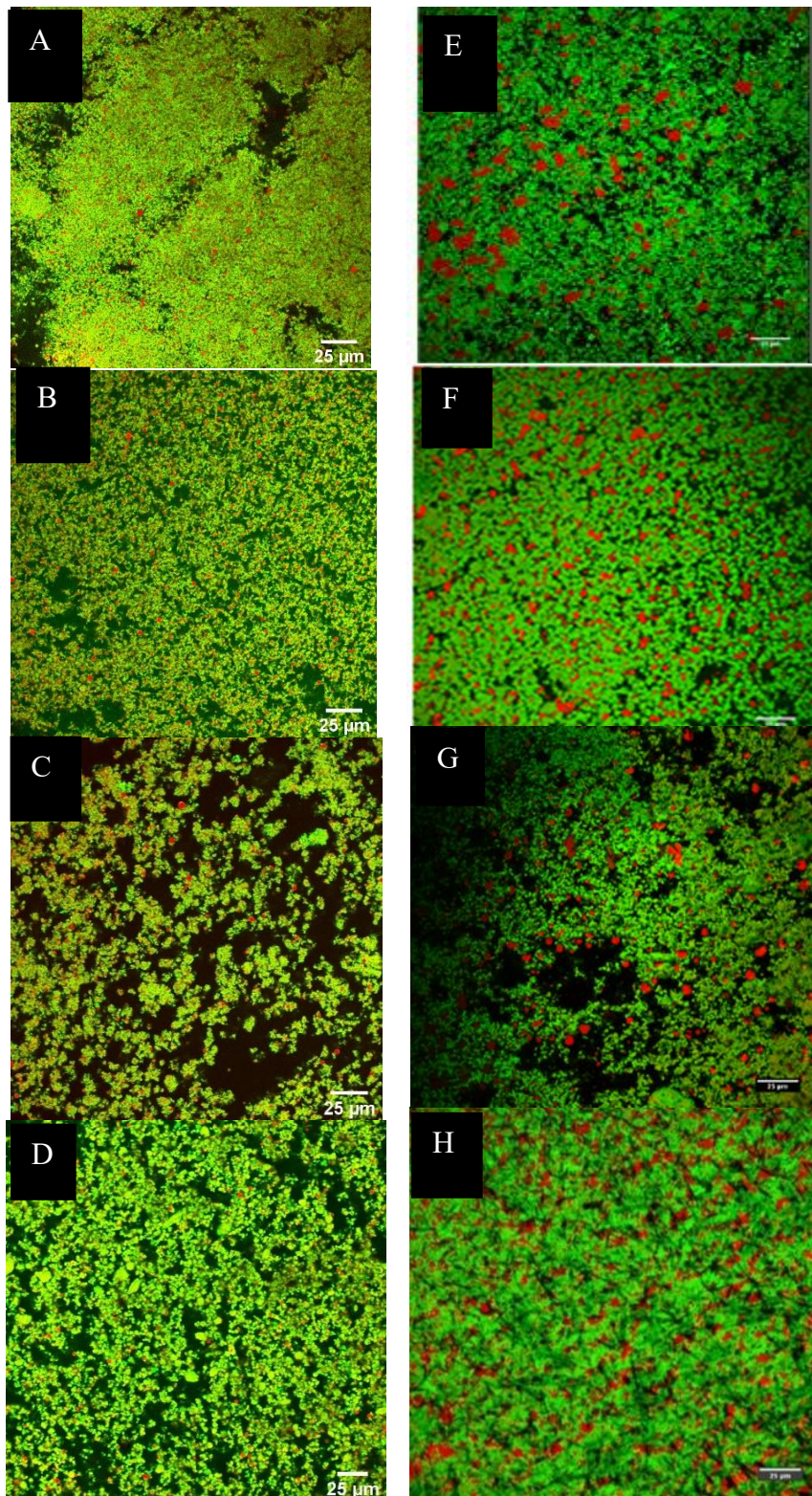


Figure 5-1 Confocal micrographs of emulsions before (A-D) and after heat gelation (E-H) formed at pH 4. Micrographs on the left represent liquid emulsions. A) whey protein emulsions (CO) with 10 mM NaCl, B) Whey protein-Low methoxyl pectin emulsions (PE) with 10 mM NaCl, C) Whey protein emulsions (CO) with 100 mM NaCl D), Whey protein-Low methoxyl pectin emulsions (PE) with 100 mM NaCl. The micrographs on the right represent the corresponding emulsions after heat gelation, namely E) Whey protein emulsion gel (CO) with 10 mM NaCl F), Whey protein-Low methoxyl pectin emulsion gel (PE) with 10 mM NaCl, G) Whey protein emulsion gel (CO) with 100 mM NaCl H), Whey protein-Low methoxyl pectin emulsion gel (PE) with 100 mM NaCl. Red represents the oil and green represents the protein. The scale bar corresponds to 25 μm.

Different extents of flocculation were evident for most gels as coalescence was ruled out after obtaining a monomodal volume size distribution (data not shown) of oil droplets having the same $d_{4,3}$ as that of the original emulsion after dissolving the gels in the SDS buffer. Although the gels appeared to be phase separated and flocculated at a microscopic length scale, macroscopically they were homogenous and self-supporting.

5.1.3 Rheological properties

The changes in the storage modulus (G') during heat-induced gel formation of CO and PE emulsions at varying ionic strengths is shown in Fig. 5-2. Prior to gelation, the emulsions despite being liquid had a dominant viscous nature as observed by high $\tan \delta$ values and low values for G' (data not shown). As the liquid emulsions were heated, the G' increased. The time at the onset of gelation, gelling temperature and final storage modulus was defined as described in the previous chapter (Section 4.4.2). These are reported in Table 5-1.

Table 5-1 Gelation properties during heat-induced gelation for CO (whey protein) and PE (pectin and whey protein) emulsion gels formed at low ionic strength (10 mM) and high ionic strength (100 mM). Gelation time (sec) and gelation temperature ($^{\circ}\text{C}$) correspond to the time and temperature when an increase of 10 Pa in G' during the heating step was observed. Final storage modulus (KPa) corresponds to the final G' after the cooling step measured at 30 $^{\circ}\text{C}$. Error bars represent standard deviation ($n=5$).

Gelation property	Low ionic strength		High ionic strength	
	CO	PE	CO	PE
Gelation time (sec)	964 ± 15.27^a	759 ± 15.27^{cd}	827 ± 20^{acd}	615 ± 10^b
Gelation temperature ($^{\circ}\text{C}$)	81.6 ± 0.5^a	72 ± 0.5^a	72.2 ± 1.21^a	63.6 ± 0.76^a
Final storage modulus (KPa)	17.4 ± 1.83^c	52.9 ± 4.26^d	88.4 ± 6.05^c	80.1 ± 5.51^c

^{a-d}Values with different letters differ significantly ($P < 0.05$)

The onset of gelation was around 81.6 ± 0.5 °C and 72 ± 0.5 °C for CO and PE respectively at low ionic strength. At high ionic strength, the onset of gelation was around 72.2 ± 1.21 °C and 63.6 ± 0.76 °C for CO and PE respectively. The results showed that irrespective of ionic strength, PE emulsions had a lower gelation temperature as compared to CO emulsions. Increase in ionic strength also led to a decrease in gelation temperature particularly for both CO and PE emulsions.

The earlier onset of gelation for PE emulsions at low ionic strength can be explained by the combined effects of polysaccharide addition, salt addition and low pH. As these emulsions were made at low pH, polysaccharide addition usually helps prevents aggregation of the protein as associative interactions between protein and polysaccharide are favourable. It is possible that low pH might lead to a decrease in the charge density of LMP (pKa~3.5) thus compromising the binding affinity of protein-polysaccharide. Changing ionic strength would affect the strength of the interactions between protein-polysaccharide systems thereby modifying the extent of association/segregation in these systems due to charge shielding effects.

Changes in the storage modulus (G') during heat induced gelation of the CO emulsion gels followed the general behaviour typically observed for WPI emulsion gels formed at varying ionic strength (Guo et al., 2014; Ikeda et al., 1999; Luo et al., 2019). At low ionic strength, the final storage modulus (G') was 17.4 ± 1.83 KPa and 52.9 ± 4.26 KPa for CO and PE respectively. At high ionic strength, a relatively higher final G' of 88.4 ± 6.05 KPa

and 80.1 ± 5.51 KPa was obtained for CO and PE gels respectively (Table 5-1). The results show that at low ionic strength, PE gels showed a comparatively high value of G' whereas at high ionic strength, the G' were almost similar. Since the polysaccharide used in this study is non-gelling, at low pH, associative interactions between WPI-LMP leads to the formation of coupled networks where the polysaccharide chains provide a framework upon which the protein molecules aggregate (Le, Rioux et al. 2017). This type of coupling prevents extensive protein aggregation and might explain the values observed. In addition, at low pH, this increased value in G' might be purely attributed to the viscosity or texture-modifying effects of LMP as interactions under these conditions is purely topological and not electrostatic.

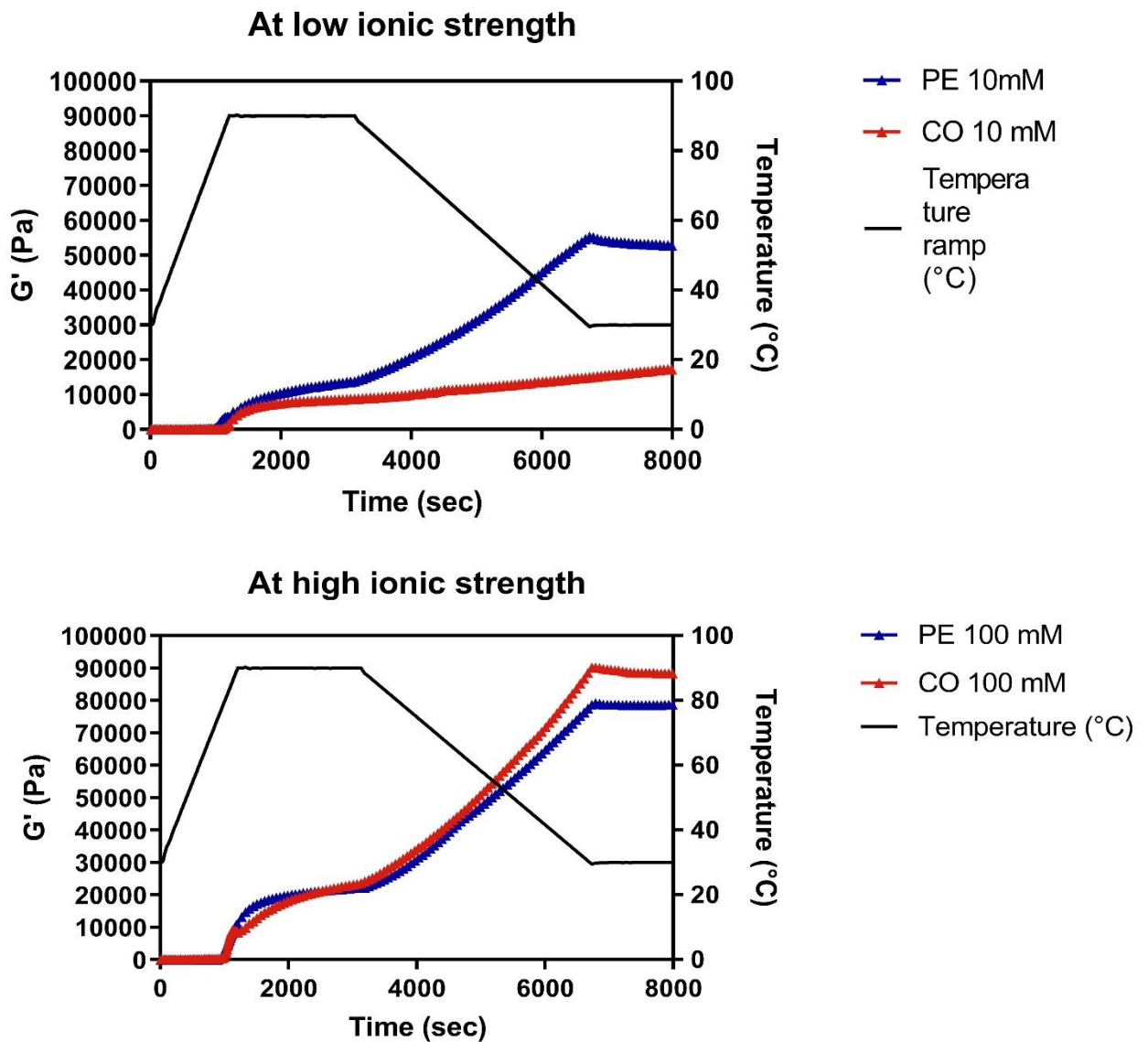


Figure 5-2 Change in storage modulus (G') during heat induced gelation of emulsions (0.5% strain, 1 Hz) at pH 7: (A) CO (whey protein) and PE (pectin and whey protein) emulsion gels formed at low ionic strength (10 mM); (B), CO (whey protein) and PE (pectin and whey protein) emulsion gels formed at high ionic strength (100 mM). The straight black line denotes the time-dependence of heating at temperature ($^{\circ}\text{C}$).

5.1.4 Large deformation properties

Table 5-2 presents mean values for Young's moduli (stiffness of gels), fracture stress (gel strength), and fracture strain (brittleness of the gels) for the emulsion gels as measured by uniaxial compression. Fracture properties of CO and PE gels were greatly affected by changes in microstructure induced by flocculation, pH and ionic strength.

Table 5-2 Mechanical properties of emulsion gels measured by uniaxial compression, CO (whey protein) and PE (pectin containing whey protein) emulsion gels formed at low ionic strength (10 mM) and high ionic strength (100 mM). Results are shown as mean \pm standard deviation of $N = 10$ independent experiments.

Mechanical property	Low ionic strength		High ionic strength	
	CO	PE	CO	PE
Fracture stress (KPa)	12.04 \pm 0.3 ^a	36.2 \pm 1.2 ^b	30.28 \pm 4.7 ^b	58.16 \pm 4.4 ^c
Fracture strain	0.84 \pm 0.06 ^a	1.54 \pm 0.12 ^b	0.97 \pm 0.02 ^a	0.88 \pm 0.06 ^a
Youngs Modulus (KPa)	14.33 \pm 2.2 ^a	24.1 \pm 3.6 ^b	39.41 \pm 8.5 ^c	58.16 \pm 5.2 ^d

^{a-d}Values with different letters differ significantly ($P < 0.05$).

Emulsion gels formed at low ionic strength were found to be more elastic (lower values of Young's modulus) compared to gels made at high ionic strength. For gels made at low ionic strength, CO gels were less stiff (14.33 \pm 2.2 KPa) as compared to PE gels (24.1 \pm 3.6 KPa). At high ionic strength, PE gels (58.16 \pm 5.2 KPa) were stiffer as compared to CO gels (39.41 \pm 8.5 KPa). A higher Young's modulus is attributed to thickness of strands in networks and is usually observed for more coarser networks as thicker strands are more

difficult to bend than less stiff thin strands (Munialo et al., 2014). Coarser networks might be due to the combined effect of low pH and ionic strength.

At low ionic strength, addition of LMP increased shear stress values at fracture (36.2 ± 1.2 KPa) of PE gels compared to CO gels (12.04 ± 0.3 KPa). At high ionic strength, similar results were obtained where PE gels demonstrated higher fracture stress values (58.16 ± 4.4) compared to CO gels (30.28 ± 4.7 KPa).

In terms of fracture strain, at low ionic strength, LMP addition led to an increase in fracture strain values (1.54 ± 0.12) compared to CO gels (0.84 ± 0.06), whereas at high ionic strength, PE gels demonstrated lower fracture strain values (0.89 ± 0.06) compared to CO gels (0.97 ± 0.02).

This indicates that addition of LMP at low ionic strength, caused the gels to become stronger and more elastic (increased fracture stress and increased fracture strain) whereas under conditions of high ionic strength, the emulsion gels is stronger but also more brittle (increased fracture stress and decreased fracture strain). These results can be explained by understanding the various factors that contribute to the bulk strength of the system i.e., oil droplet flocculation, addition of polysaccharide and strength of the protein matrix.

The high rigidity of the protein emulsion gel matrix and the screening of electrostatic interactions between protein-polysaccharide curtails any significant effect of LMP addition; therefore, under these conditions, LMP only confers a viscosity modifying effect resulting in gels having a more elastic character, which is reflected by the high strain

values for these gels. The higher fracture stress in PE gels at low pH may be attributed to a more pronounced effect of polysaccharide addition at conditions where protein micro phase separation is extensive due to the combined effect of high ionic strength and low pH.

The overall higher fracture stress observed at high ionic strength was probably due to the higher amount of salt (100 mM) which increases the rigidity of the protein gel network (Hussain et al., 2012; Ikeda et al., 1999). In addition, high ionic strength may also affect properties of the emulsions, prior to gelation such as extensive screening of electrostatic charges, which may hinder associative protein-polysaccharide interaction. The flocculation of oil droplets within the emulsion gel might also influence the mechanical properties of the emulsion gels in addition to polysaccharide addition and varying ionic strength. The results imply that LMP addition largely influences the mechanical properties of these gels. Although distribution of oil droplets and polysaccharide addition and its interaction with the protein emulsion gel matrix does contribute to the overall strength of the network, the gels are predominately made up of protein, which are amenable to changes in ionic strength and seems to be the dominant factor contributing to overall mechanical properties of the mixed system.

5.2 Behaviour of emulsion gels during dynamic gastric digestion

5.2.1 pH profile of emptied digesta

The changes in pH of the emptied gastric digesta for the various emulsion gels as a function of digestion time are shown in Fig. 5-3A-B. As a result of constant addition of simulated gastric fluid, and by continuous gastric emptying, the pH of the emptied gastric digesta, which is basically representative of the pH of the gastric contents, gradually decreased as digestion progressed.

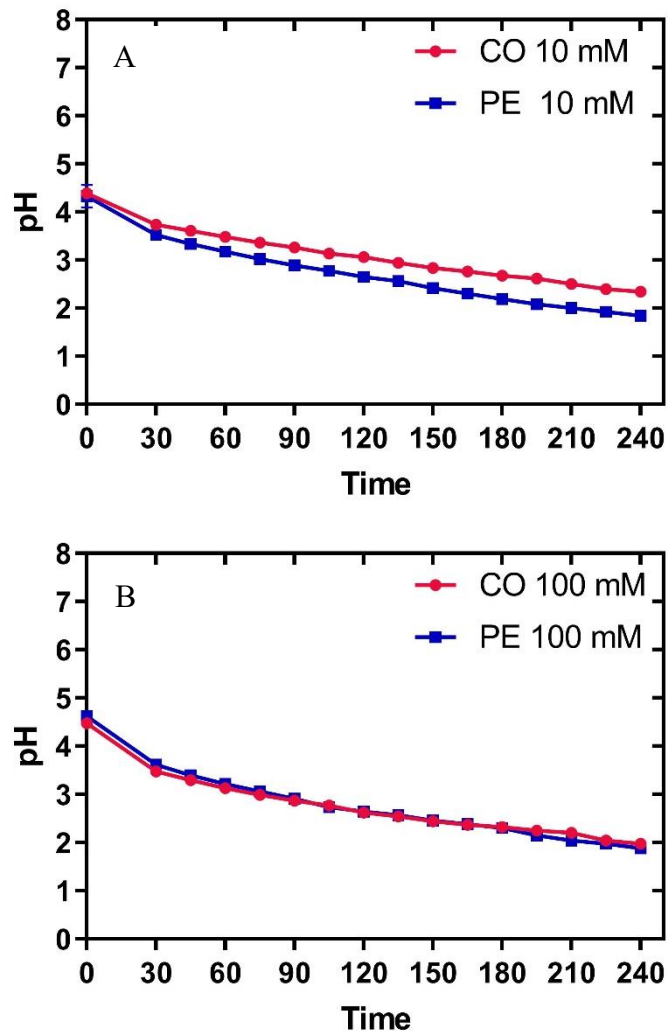


Figure 5-3 Changes in pH of the emulsion gels during dynamic gastric digestion in the HGS: A, CO (whey protein) and PE (pectin containing whey protein) emulsion gels formed at low ionic strength (low ionic strength-10 mM); B, CO (whey protein) and PE (pectin containing whey protein) emulsion gels formed at high ionic strength (low ionic strength- 100 mM) at pH 4. Error bars represent standard deviation (n=5). Error bars are smaller than the symbol size.

Initial pH values for CO and PE gels made at low ionic strength were 4.47 and 4.36, while for gels made at high ionic strength, pH values were 5.47 and 5.67, respectively. After 240 min of gastric digestion, the pH of the gels made at low ionic strength dropped to 2.68, a marginally higher pH than the pH of those made at high ionic strength, which fell to 2.34. There was little change in the pH profile of the different gels over the course of the experiment, indicating that the protein matrix structure had no significant ($P > 0.05$) impact on the buffering capacity of the emulsion gel.

5.2.2 Changes in solid content of emptied digesta

The solid content (dry matter) of the emptied digesta is shown in Fig. 5-4A-B. The solid content is reflective of the extent of chemical and mechanical disintegration of the gels during digestion.

There seemed to be a considerable difference in the rate of solid content emptied for CO and PE gels made at low and high ionic strength, possibly indicating different extents of gel breakdown during digestion. For gels made at pH 4, the gastric pH was at the optimal pH for pepsin activity throughout gastric digestion. For gels made at low ionic strength, for the first 150 min, compared to the control, PE gels showed a comparatively higher extent of solid loss compared to control. Post 150 min, the solid content emptied for PE gels decreased until the end of digestion. In comparison, CO gels showed a somewhat steady release of total solids throughout digestion.

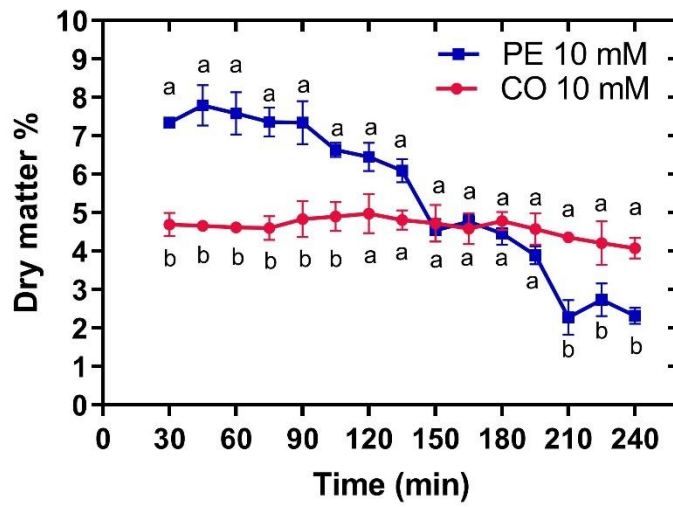
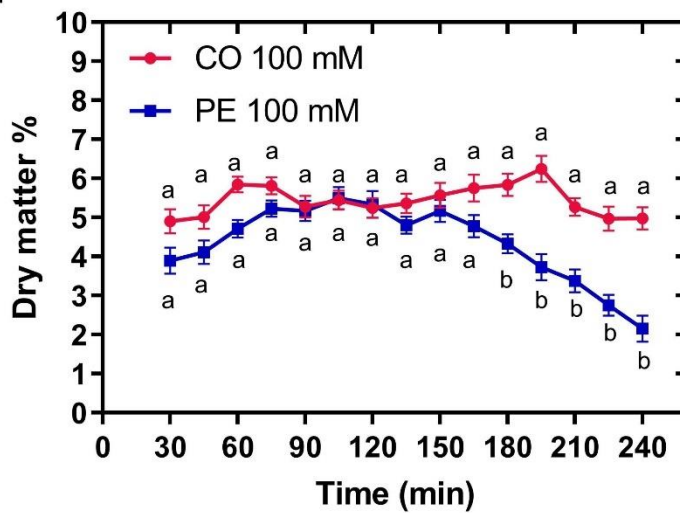
A**At low ionic strength****B****At high ionic strength**

Figure 5-4 Changes in dry matter of the emulsion gels during dynamic gastric digestion in the HGS: A, CO (whey protein) and PE (pectin containing whey protein) emulsion gels formed at low ionic strength (low ionic strength-10 mM); B, CO (whey protein) and PE (pectin containing whey protein) emulsion gels formed at high ionic strength (low ionic strength- 100 mM). Error bars represent standard deviation (n=5). Readings without a common superscript letter differ ($P < 0.05$) as analyzed by one-way ANOVA and the Tukey test.

This might be attributed to the particulate nature of PE gels as compared to CO gels, as corroborated by confocal images. In addition, large deformation results also show albeit the PE gels were stronger, coarser and less stiff, making them more prone to disintegration. CO gels on the other hand being less particulate and stiffer led to more consistent and steadier rate of solid emptying.

For gels made at high ionic strength, for the first 120 min of digestion both PE and CO gels had a somewhat similar rate of solid emptying, however, post 120 min, CO gels showed a slight increase in solid emptying until 195 min after which a decrease was observed. PE gels on the other hand showed a decreasing trend in solid emptying post 120 mins. The similar solid emptying rate for the initial period might be attributed to the particulate nature of the CO and PE gels made at high ionic strength. The slight phase separated nature of the particulate network of CO gels might explain the slightly higher rate of solid emptying as compared to the tight knit particulate network of PE gels formed at high ionic strength as corroborated by the higher fracture stress, higher Youngs Modulus of these gels and confocal images of these gels.

Overall, the results imply that PE gels made at high ionic strength disintegrated to a lesser extent than PE gels made at low ionic strength. Similarly for CO gels, gels formed at high ionic strength disintegrated to a higher extent as compared to gels formed at low ionic strength. These differences might be explained by the combined effects of ionic strength and pectin addition to the gel matrix of the gels. Though large deformation properties and confocal microscopy images can be used to explain some of these differences observed it should be noted that solid emptying depends on behaviour of the bulk gel matrix in the

gastric environment and its propensity to mechanical shear, extent of proteolysis, gel swelling, gel erosion and disintegration.

As stated in the previous section, particle sizes of the bolus were similar and pH values did not show considerable differences indicating that for these emulsion gels, their susceptibility to mechanical shear and their structural differences played an important role in their disintegration. However, it should be noted that solid loss does not necessarily imply hydrolysis, but mechanical disintegration does make the protein more accessible to pepsin.

5.2.3 Release of pectin from emulsion gel during digestion

The amount of pectin released into the surrounding gastric medium as a result of gel breakdown during gastric digestion was measured. Fig 5-5A and B shows the amount of pectin present in the gastric digesta (mg/mL) at each time point and the cumulative percentage of pectin released into the gastric fluid during gastric digestion of PE emulsion gels made at low and high ionic strength.

In general, pectin release from PE gels showed a trend having an initial higher rate of pectin release followed by a somewhat steady increase towards the latter stage of digestion (Fig 5-5A). The cumulative amount of pectin release was considerably higher for PE gels made at low ionic strength compared to gels made at high ionic strength (Fig 5-5B). This could be attributed to the weaker particulate network of the PE gels at low ionic strength as evidenced by the lower strength of the network (lower fracture stress) resulting in a greater susceptibility to mechanical shear the stomach and digestion process (Fig 5-5B). As described in previous sections, PE gels made at high ionic strength were mechanically stronger (higher fracture stress) and the gel matrix was coarser and more aggregated which may explain the differences observed. However, the overall disintegration of the bulk gel and solid emptying (as discussed in the previous section) may also impact the overall release of pectin from the gels.

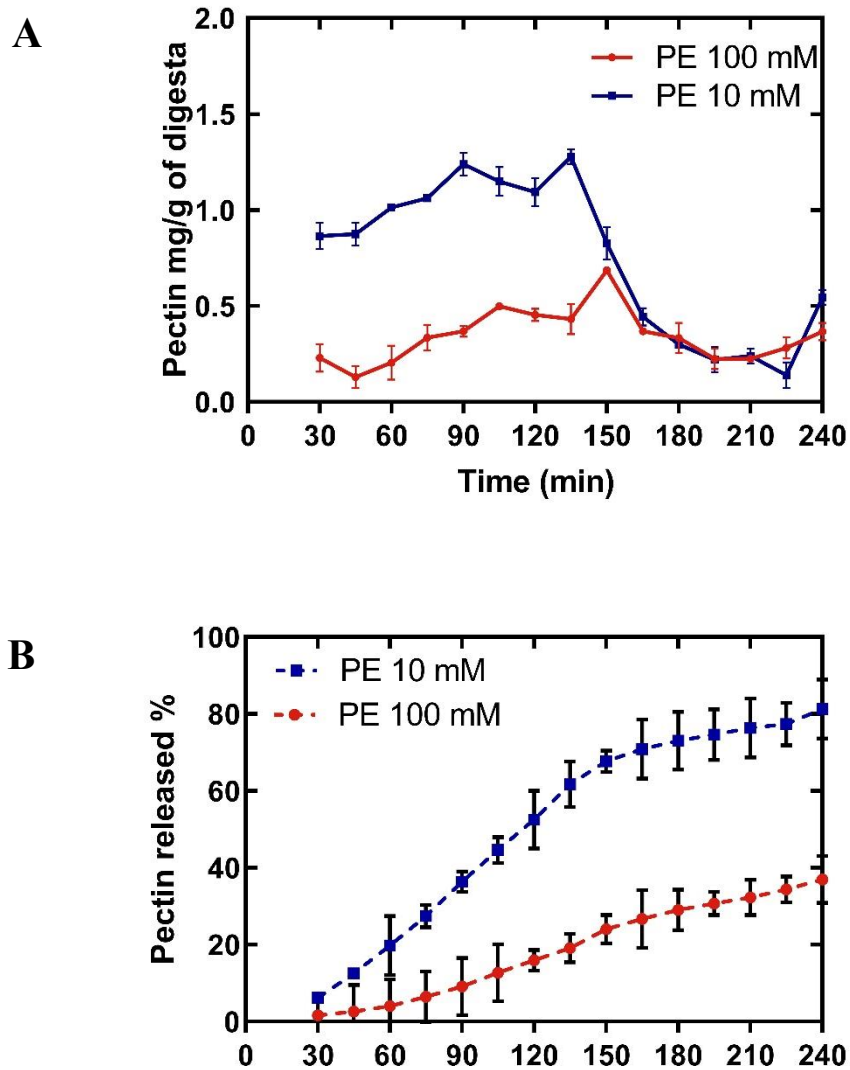


Figure 5-5 (A) The low methoxyl pectin content of the gastric digesta (mg/ml) during gastric digestion and (B) cumulative percent of pectin release during gastric vitro digestion for the soft (gels made with 10 mM NaCl) and hard gels (gels made with 100 mM NaCl). Results are expressed as pectin content (mg/g) of the gastric digesta at each time point on dry weight basis. Based on this data, a cumulative percent of pectin released (%) over digestion time (min) was also plotted. This was calculated based on the release of pectin at specific digestion times.

5.2.4 Particle size distribution of emptied digesta

The particle size distribution (PSD) of the emulsion gels during gastric digestion reflects the different extents of breakdown of the emulsion gels during *in vitro* digestion. The particle size distributions (PSD) of the emptied digesta were characterised (Fig. 5-6A-D).

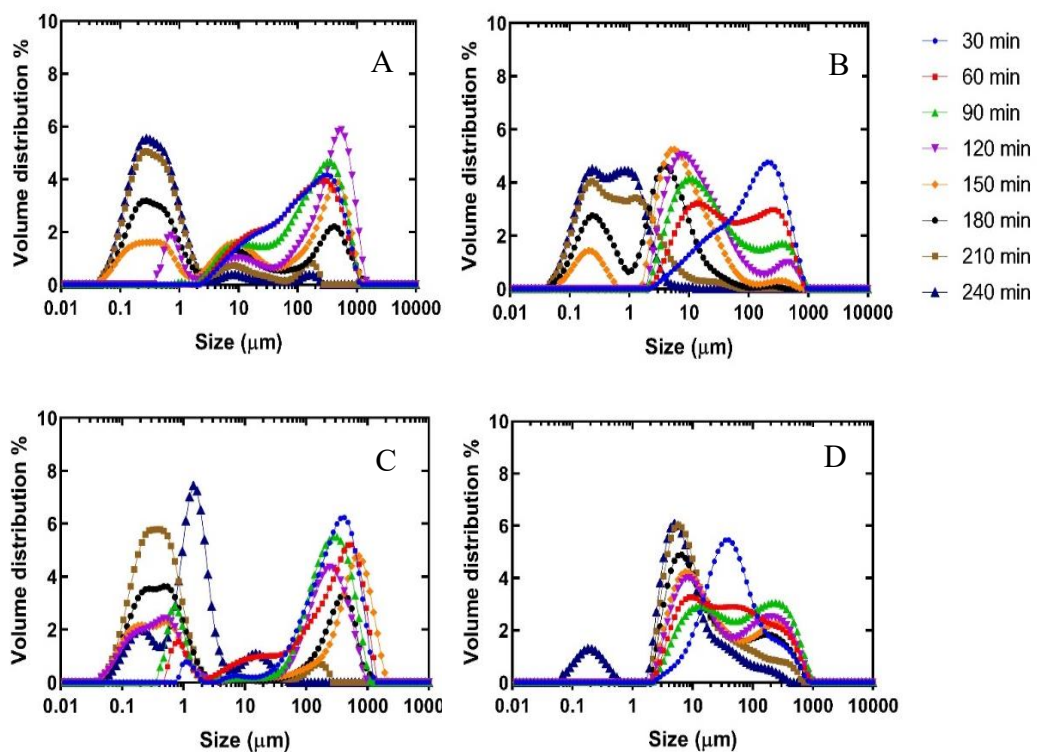


Figure 5-6 Changes in particle size distribution (volume-weighted average diameter $d_{4,3}$) of (A and B) CO gels (whey protein) and PE gels (pectin and whey protein) emulsion gels formed at low ionic strength (10 mM); (C and D), CO gels (whey protein) and PE gels (pectin and whey protein) emulsion gels formed at high ionic strength (100 mM) during gastric digestion in the human gastric simulator. The legends at the top left of each stack indicate the gastric digestion time.

The PSD can be generally divided into three different particle size ranges: large ($d_{4,3} \sim 100 - 1000 \mu\text{m}$), intermediate ($d_{4,3} \sim 1 - 10 \mu\text{m}$) and small ($d_{4,3} \sim 0.1 - 1 \mu\text{m}$). The peaks in the large size range ideally correspond to gel particles and the peak between 0.1 to 1 μm is representative of stable emulsion droplets that have been released from the gel matrix. Post oral processing the average D_{50} of the emulsions gels was 2.5 mm. Gastric sieving during digestion allows for particles $< 1 \text{ mm}$ to be emptied, thus the peaks in the large size range could be indicative of emptied intact gel particles of smaller size.

During the initial stages of digestion, the digesta emptied comprised of particle mostly in the intermediate and large size range. As digestion progressed, peaks in the larger size range decreased and the size distribution post 150 min was dominated by the presence of larger peaks of smaller sizes (in the range $\sim 0.1 - 10 \mu\text{m}$). Peaks in the intermediate and large size range during the latter stages of digestion might be indicative of aggregation or possible coalescence as these results were obtained without the use of dissociating buffer.

The emulsion gels showed considerable differences in their breakdown patterns during gastric digestion. For gels made at low ionic strength (Fig 5-6A-B), PE gels disintegrated more rapidly as compared to CO gels, wherein the 100 -1000 μm peak decreased and the distribution shifted to smaller sizes. The gastric digesta of PE gels indicated the presence of predominately larger peaks of smaller ($d_{4,3} \sim 0.1 - 1 \mu\text{m}$) and intermediate sizes ($d_{4,3} \sim 1 - 10 \mu\text{m}$), whereas for CO gels, the gastric digesta comprised predominately of intermediate peaks with a few smaller peaks during the end of digestion. The increase in smaller peaks between 0.1–1 μm towards the latter end of digestion probably indicates presence of stable emulsion droplets in the digesta. These breakdown patterns corroborate

well with highly particulate nature of PE gels which caused them to breakdown more rapidly as compared to CO gels as discussed in the previous section.

For gels made at high ionic strength (Fig 5-6C-D), the gastric digesta of PE gels appeared to be more predominant in intermediate ($d_{4,3} \sim 1-10 \mu\text{m}$) and large peaks ($d_{4,3} \sim 10 - 1000 \mu\text{m}$) as compared to the digesta of CO gels where a decrease in the volume of 100 -1000 μm peak during the initial stages of digestion and the distribution shifted to smaller sizes as digestion progressed. These results are in line with trends observed for solid emptying patterns observed for these gels. As discussed previously, the tight knit particulate nature of PE gels formed at high ionic strength made them less prone to breakdown and disintegration, whereas the weak particulate network of CO gels, given their lower strength caused them to breakdown at a faster rate. This also indicates that the gastric digesta of the CO gels formed at high ionic strength contained a higher percentage of released droplets/small gel fragments.

5.2.5 Microstructure of emptied digesta

The behaviour of the emulsion gels during gastric digestion depends on the structural properties of the emulsion gel but the dynamic changes occurring in the gastric environment might lead to restructuring of the gastric contents at different structural levels. The microstructure of the emptied digesta for the CO and PE emulsion gels made at low ionic strength and during high ionic strength during gastric digestion is shown in Fig. 5-7 and Fig. 5-8 respectively.

The overall pattern observed suggested that as digestion progressed, the gel particles seemed to reduce in size with the release of emulsion droplets. The initial stages showed the presence of large gel particles and during the latter stages of digestion, the emptied digesta appeared to be more concentrated with the presence of small gel particles and released oil droplets.

Despite being ground to a similar particle size prior to digestion, there were visible differences in the structural breakdown patterns of the gels. Comparing CO and PE emulsion gels formed at low ionic strength (Fig 5-7), PE gels seemed to be broken down at a faster rate compared to CO gels. This is corroborated by the solid emptying results and the particle size distribution data discussed in previous sections. Despite disintegration of the gels, the free oil droplets in the digesta and the emulsion gel fragments seemed to be structurally intact.

For gels made at high ionic strength (Fig 5-8), a different pattern was observed where CO gels seemed to disintegrate into much smaller particles compared to PE gels where the gastric digesta showed the presence of larger gel fragments for the initial stages of digestion. The solid emptying data shows that although for the first 150 min of digestion the gels disintegrated to a similar extent, the confocal images show that they differed in the disintegration patterns. This might be related to the structural properties of the emulsion gels where the slight phase separated nature of the particulate network of CO gels might explain the breakdown into smaller gel pieces compared to the tight knit particulate network of PE gels formed at high ionic strength, which broke down more as

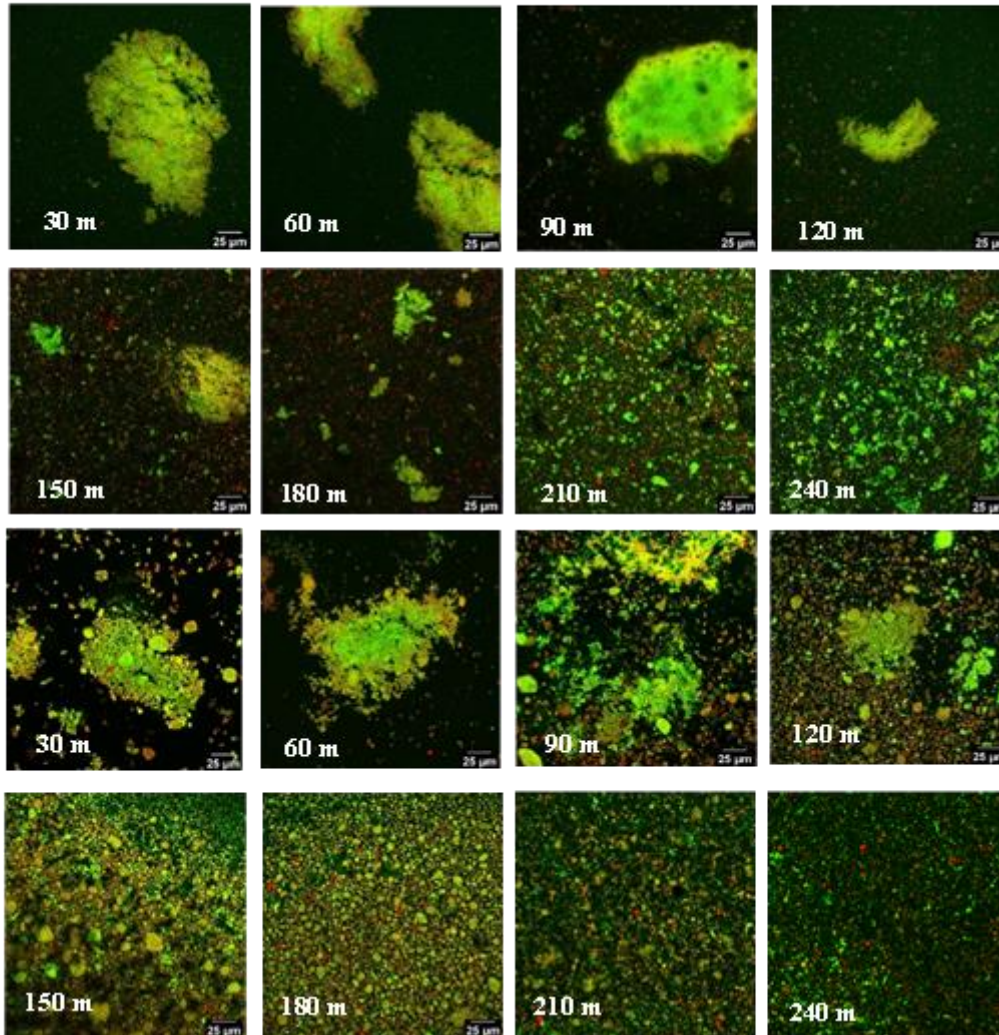
chunks. This is corroborated by the higher fracture stress and higher Youngs Modulus of these gels.

For the latter stages of digestion, the gastric digesta of CO and PE showed the presence of much smaller fragments with emulsion droplets. For CO gels, the gastric digesta seemed to be more concentrated with the presence of smaller gel fragments and emulsion droplets as compared to PE gels, which is in line with solid emptying data and size distribution data. The oil droplets in the emptied gel particles showed no visible sign of coalescence or flocculation even as size reduction occurred although a few free oil droplets were observed. This was well corroborated with results obtained for oil droplet size.

At low ionic strength

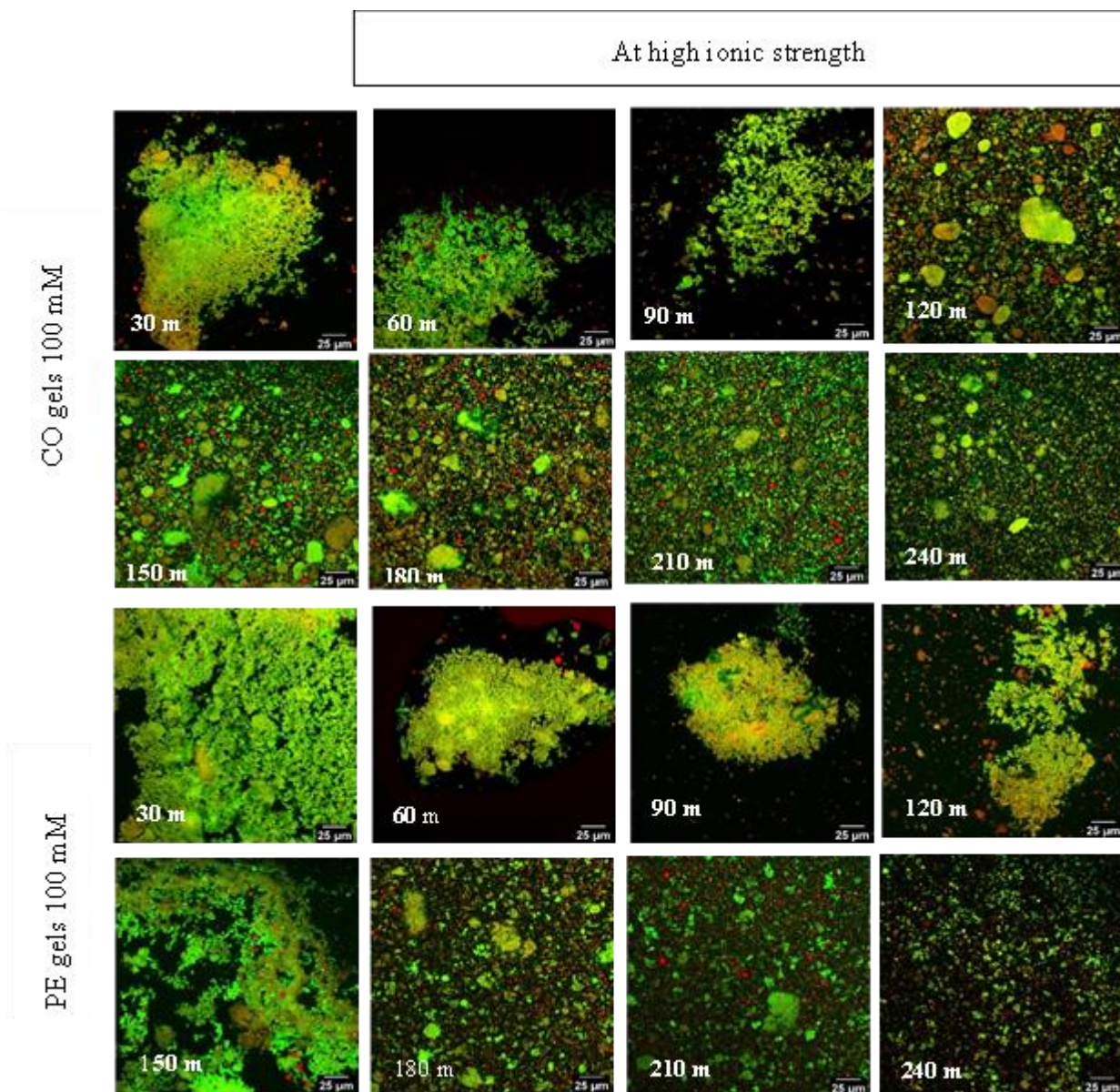
Figure 5-7 CLSM images of gastric digesta as a function of digestion time during dynamic gastric digestion in the HGS of gels formed at low ionic strength; CO (whey protein) and PE (pectin containing whey protein) emulsion gels formed at low ionic strength (ionic strength-10 mM); Red represents the oil and green represents the protein. The scale bar corresponds to 25 μm .

CO GELS 10 mM



PE GELS 10 mM

Figure 5-8 CLSM images of gastric digesta as a function of digestion time during dynamic gastric digestion in the HGS of gels formed at high ionic strength: CO (whey protein) and PE (pectin containing whey protein) emulsion gels formed at high ionic strength (ionic strength-100 mM); Red represents the oil and green represents the protein. The scale bar corresponds to 25 μm .



5.2.6 Stability of oil droplets during gastric digestion

The changes in oil droplet size distribution of the emptied digesta, measured in a dissociating buffer, during gastric digestion are shown in Figure 5-9. For the emptied digesta, mixing with the dissociating buffer solubilises the emptied gel particles and breaks down any flocs in the sample, allowing for the assumption that increases in droplet size due to coalescence. The peak between 0.1 to 1 μm is representative of stable emulsion droplets that have been released from the gel matrix or intact droplets that were present within the emptied gel particles.

For all the gels, irrespective of LMP addition or ionic strength, the particle size and PSDs of the original emulsions, emulsion gels and the samples after exposure to oral phase and basal gastric fluid (0 min) were similar ($d_{4,3} \sim 0.45 \mu\text{m}$) indicating that the oil droplets were stable against heat-induced gelation, physical shear/ionic changes during simulated oral processing and gastric digestion.

This indicates that gels formed at pH 4 were more stable during gastric digestion as compared to gels formed at pH 7. This might be attributed to the highly particulate and coarser gel network which conferred protection to the emulsion droplets during heat gelation, oral processing, and gastric digestion.

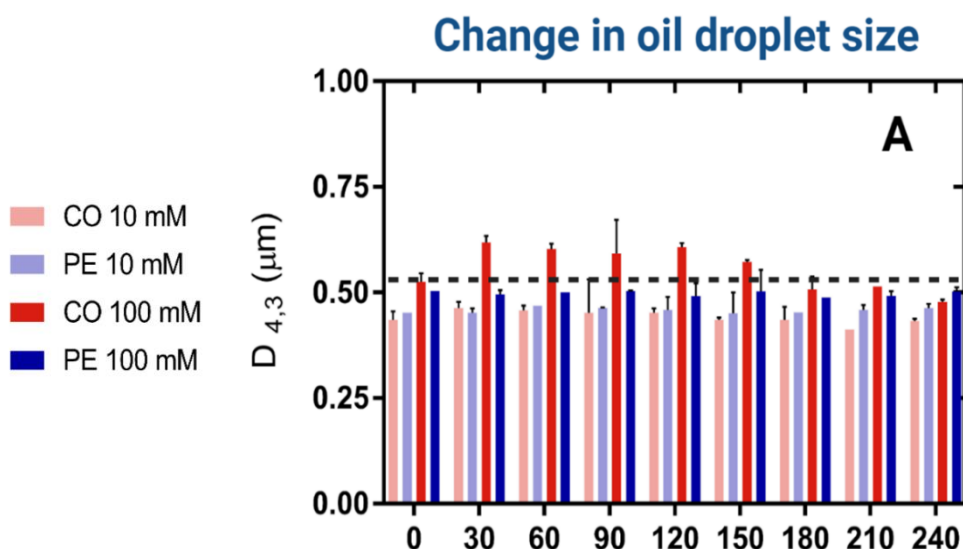


Figure 5-9 Changes in volume-weighted average diameter $d_{4,3}$ of CO (whey protein) and PE (pectin and whey protein) emulsion gels formed at low ionic strength (10 mM); (C1 and C2), CO (whey protein) and PE (pectin and whey protein) emulsion gels formed at high ionic strength (100 mM). The measurements were replicated at least six times. Error bars represent standard deviations. The values weren't significantly different ($P < 0.05$) as analysed by one-way ANOVA and the Tukey test.

5.2.7 Impact of gel disintegration on kinetics of lipid release during dynamic gastric digestion

The structural behaviour of the emulsion gels during gastric digestion affects the rate of lipid released in the emptied digesta. The extent of gel disintegration (expressed as solid % emptied) seemed to influence the rate of lipid released in the gastric digesta during digestion. The interrelationship between the solid emptying and fat released was assessed to see if there was significant correlation between the two.

Results showed that, for all the samples there was a highly significant ($P < 0.01$) positive linear correlation (Table 5-3). For foods containing oil droplets dispersed in a solid matrix, the structural fate of the matrix and its colloidal stability during gastric digestion affects the extent and sequence of lipid released during digestion (Singh, Ye et al. 2009, Guo, et al. 2017, Acevedo-Fani & Singh, 2021). As discussed in the previous section, the emulsion gels remained stable during gastric digestion and no coalescence of the emulsion was observed, but they differed in their extents of lipid release during gastric digestion. The results showed a linear positive correlation for the solid emptying data and the lipid released data suggesting that lipid released correlated with degradation of the gel matrix. Since the fat content of the gels were similar prior to digestion, the difference in the kinetics of lipid release during gastric digestion suggests that the structural design of the emulsion gels modulates the kinetics of lipid release during digestion.

Table 5-3 The relationship between the lipid released (%) and solid emptied (%) during gastric digestion for the different gels formed at pH 4, CO (whey protein) and PE (pectin and whey protein) emulsion gels formed at low ionic strength (10 mM) and high ionic strength (100 mM).. The Pearson correlation coefficient value (r), the R square are listed ($P < 0.05$).

Correlation between fat released (%) and solid emptied (%) at different digestion times			
	Pearson correlation r	R squared	P value (alpha = 0.05)
CO 10 mM	0.8217	0.6952	<0.0001
PE 10 mM	0.8571	0.7310	0.0002
CO 100 mM	0.8651	0.7284	<0.0001
PE 100 mM	0.8132	0.7414	0.0002

5.3 Conclusions

Dynamic *in vitro* models like the HGS can simulate more closely the structural changes and physiologically relevant mechanisms that occur in structured foods like emulsions gels where the gastric phase plays an important role. This study demonstrated that addition of LMP and the ionic strength of the system influence the structural properties of the emulsion gel matrix, which impacts its gastric digestion kinetics and subsequently modulates the protein digestion and lipid release of these systems.

The results of this study suggest that food matrix structural properties could be modified to alter resistance to gastric digestion which may have consequences on controlling the rate of gastric emptying and satiation. This study also provides for an increased understanding of the structure-digestion relationship and may help in the design of functional structures using complex emulsion-based matrices.

6 Overall conclusions and future recommendations

The aim of this thesis was to study the effect of food structure on the kinetics of food breakdown in a complex model emulsion system. This research aimed to develop heat-induced emulsion gels containing both proteins and polysaccharides. Salt and pH concentrations were varied to encompass most conditions present in real foods as they drive key interactions between proteins and polysaccharides. Structural properties of these gels and their *in vitro* dynamic gastric digestion behaviour was investigated.

Heat-set whey protein emulsion gels ($d_{4,3} \sim 0.5 \mu\text{m}$) with and without low methoxyl pectin (LMP) at low (10 mM NaCl) and high (100 mM NaCl) ionic strength were formed at pH 4 or pH 7. Microstructurally, confocal images showed these emulsions gel differed distinctly. The gel structures varied in appearance, ranging from being fine-stranded, particulate, phase separated or having a mixture of these microstructures depending on the polysaccharide addition, or pH and salt concentration. Different extents of flocculation were evident for most gels, and although the gels appeared to be flocculated at a microscopic length scale, macroscopically they were homogenous and self-supporting.

In terms of rheological properties, results clearly indicated that polysaccharide addition led to a decrease in the gelation temperature of the emulsions, and this effect was more pronounced at low ionic strength. At pH 7, the earlier onset of gelation for PE emulsions at low ionic strength might be due to depletion flocculation caused by LMP in concentrated protein emulsions promoting enhanced protein-protein aggregation resulting in formation of a gel at a lower temperature. At pH 4, a similar trend was

observed where irrespective of ionic strength, PE emulsions had a lower gelation temperature as compared to CO emulsions. Increase in ionic strength also led to a decrease in gelation temperature particularly for both CO and PE emulsions. This was attributed to effect of changing ionic strength on the strength of the interactions between protein-polysaccharide systems thereby modifying the extent of association/segregation in these systems due to charge shielding effects. The results showed that ionic strength and LMP addition led to differences in the final storage modulus after cooling, implying that ionic strength had a more prominent effect, probably because the emulsion gel was predominately made of WPI. The influence of LMP addition on the final gel strength of the emulsion gel would depend on the extent of phase separation prior to gelation and the extent of depletion by the polysaccharide as affected by ionic strength reflecting the differences in G' values upon cooling. For emulsion gels, the extent of aggregation state of the oil droplets prior to gelation might also affect the rheological properties and the functionality of the gels formed.

Emulsion gels with varying structural properties such as emulsion gels having an elastic or brittle nature, or gels having a weak or strong nature were affected by polysaccharide addition or ionic strength or the pH at which they were formed. The results imply that varying the ionic strength largely influences the mechanical properties of these emulsion gels. Gels formed at high ionic strength (100 mM) showed overall higher fracture stress. It has been stated that increase in ionic strength may promote cross-links between whey proteins through both disulfide bridges and hydrophobic interactions and accelerate the aggregation of proteins (Macierzanka et al., 2012).

For the present study, the emulsions gels were ground to a similar particle size during simulated oral processing to discount the effect of higher-level structural order, therefore assessing if the inherent microstructural properties of the emulsion gel still play a role during digestion.

Gastric digestion is a dynamic process where there is a continuous addition of gastric fluids and pepsin accompanied by shear and progressive gastric emptying. Gastric emptying only allows particles smaller than 1 mm to pass through to the duodenum. After oral processing the average D_{50} of the emulsions gels was 2.5 mm. The rate and extent of gastric emptying depends on the disintegration behaviour of the emulsion gels during gastric digestion.

The digestion and breakdown behaviour of the emulsion gels was studied in relation to their structural properties. For gels made at pH 7, PE gels made at high ionic strength disintegrated to a lesser extent than PE gels made at low ionic strength. This could be attributed to the phase separated gel structure of PE gels at low ionic strength; the presence of pectin-rich regions in the gel could be considered as weak spots resulting in a greater susceptibility to mechanical shear in the stomach. PE gels made at high ionic strength were mechanically stronger and the gel matrix was coarser and more aggregated which may explain the differences observed. For gels made at pH 4, a similar trend was observed where PE gels made at high ionic strength disintegrated to a lesser extent than PE gels made at low ionic strength. These results corroborate well with the findings of pectin released into the surrounding gastric medium because of gel breakdown, indicating

that pectin released into the gastric medium was dependent on the structural properties of the emulsion gel.

For semi-solid emulsion systems, degradation/ dissolution of the matrix leads to a two-phase mixture consisting of the liquid phase containing released oil droplets and undigested gel particles. The stability of the released droplets then depends on the properties of the interfacial layer and its likely interactions with other components in the gastric environment. As digestion progresses, these droplets undergo further flocculation and coalescence and are emptied out, leaving behind undigested gel particles in the HGS chamber that are still being disintegrated and hydrolysed. For all the gels, irrespective of LMP addition or ionic strength, the oil droplet size of the original emulsions, emulsion gels and the samples after exposure to oral phase and basal gastric fluid (0 min) were similar ($d_{4,3} \sim 0.45 \mu\text{m}$) indicating that the oil droplets were stable against heat-induced gelation and physical shear/ionic changes during simulated oral processing. Thus prior to digestion, all the emulsion gels were stable, and no coalescence was observed.

For gels made at pH 7, results showed that for gels made at low ionic strength, CO gels were least stable to gastric digestion compared to PE gels. Gels made at pH 4, irrespective of polysaccharide addition or ionic strength, were stable during gastric digestion and no coalescence was observed. This might be attributed to the highly particulate nature of gels made at low pH, making them less prone to proteolysis by pepsin.

The structural properties of the chyme such as its susceptibility to mechanical shear, the extent of proteolysis, and gel disintegration affects the rate of lipid released in the emptied

digesta. The interrelationship between the extent of gel disintegration and lipid released showed a highly significant positive linear correlation for gels made at pH 7 and pH 4, suggesting that rate and extent of gel disintegration exerts a significant influence on lipid emptied during digestion, despite having differences in structural properties.

Dynamic *in vitro* models like the HGS can simulate more closely the structural changes and physiologically relevant mechanisms that occur in structured foods like emulsions gels where the gastric phase plays an important role. This study demonstrated that addition of LMP and the ionic strength of the system influences the structural properties of the emulsion gel matrix, which impacts its gastric digestion kinetics and subsequently modulates the lipid release for these emulsion systems.

The study suggests that food matrix structural properties could be modified to alter resistance to gastric digestion which may have consequences on controlling the rate of gastric emptying and satiation. This study also provides for an increased understanding of the structure-digestion relationship and may help in the design of functional structures using complex emulsion-based matrices.

Recommendation for future work

- In vivo measurements of gastric emptying

The rate of gastric emptying depends on the nutrient composition of food and many other factors. Although the Human Gastric Simulator (HGS) can simulate, to an extent, the rate

of gastric emptying, more advanced measurements such as scintigraphy, sonography and MRI can be used to better understand gastric motility and emptying *in vivo*.

- Animal models and human studies

Digestion studies using the Human Gastric Simulator (HGS) has some limitations and is not able to simulate all aspects of the physiological digestion conditions in the human body. Digestion is a much more complex process modulated by many complex neural, physiological, and hormonal responses. For a better understanding and clarity, *in vitro* digestion methods should be validated by *in vivo* studies.

Human studies are the most preferred, but they are not always possible given ethical and financial constraints. Animal models such as pigs can be used as an excellent system to understand human digestion. These results can then be used to correlate with results from *in vitro* studies.

- Extent of gastric and intestinal lipid digestion

This study mainly focuses on structural properties of the emulsion gels and its behaviour during gastric digestion, but the extent of lipid digestion during gastric digestion and its effect on the consequent intestinal lipid digestion of these emulsion gels could be studied further.

- Using emulsion gel model systems for delivery of bioactive compounds

Emulsion-based gel model systems could be used for delivery of hydrophobic bioactive compounds. It will be important to understand the influence of structural properties of the emulsion gels on the bio accessibility of bioactive compounds during digestion could be investigated.

- Using these model systems for sensory studies and perception

The sensory properties of these emulsion gels were not investigated, but sensory properties and oral processing play a crucial role in food digestion. Further studies could be carried out to explore the sensory properties of these model emulsion systems.

- Using mathematical modelling to predict extent of food breakdown.

Mathematical modelling could be used in conjunction with *in vitro* or *in vivo* studies to understand if modelling could predict the extent of food breakdown and digestion in relation to its structural properties.

7 Bibliography

1. Acevedo-Fani, A., & Singh, H. (2021). Biopolymer interactions during gastric digestion: implications for nutrient delivery. *Food Hydrocolloids*, *116*, 106644. <https://doi.org/10.1016/j.foodhyd.2021.106644>
2. Acevedo-Fani, A., & Singh, H. (2022). Biophysical insights into modulating lipid digestion in food emulsions. *Progress in Lipid Research*, *85*, 101129. <https://doi.org/10.1016/j.plipres.2021.101129>
3. Araiza-Calahorra, A., Akhtar, M., & Sarkar, A. (2018). Recent advances in emulsion-based delivery approaches for curcumin: From encapsulation to bio accessibility. *Trends in Food Science & Technology*, *71*, 155-169. <https://doi.org/10.1016/j.tifs.2017.11.009>
4. Benichou, A., Aserin, A., & Garti, N. (2002). Protein-polysaccharide interactions for stabilization of food emulsions. *Journal of Dispersion Science and Technology*, *23*(1-3), 93-123. <https://doi.org/10.1080/01932690208984192>
5. Boirie, Y., Dangin, M., Gachon, P., Vasson, M. P., Maubois, J. L., & Beaufrère, B. (1997). Slow and fast dietary proteins differently modulate postprandial protein accretion. *Proceedings of the National Academy of Sciences*, *94*(26), 14930-14935. <https://doi.org/10.1073/pnas.94.26.14930>
6. Borreani, J., Llorca, E., Larrea, V., & Hernando, I. (2016). Adding neutral or anionic hydrocolloids to dairy proteins under *in vitro* gastric digestion conditions. *Food Hydrocolloids*, *57*, 169-177. <https://doi.org/10.1016/j.foodhyd.2016.01.030>

7. Brejnholt, S. M. (2009). Pectin. In *Food Stabilisers, Thickeners and Gelling Agents* (pp. 237–265). Wiley-Blackwell.
<https://doi.org/10.1002/9781444314724.ch13>
8. Çakır, E., & Foegeding, E. A. (2011). Combining protein micro-phase separation and protein-polysaccharide segregative phase separation to produce gel structures. *Food Hydrocolloids*, 25(6), 1538-1546.
<https://doi.org/10.1016/j.foodhyd.2011.02.002>
9. Camps, G., Mars, M., Graaf, C., & Smeets, P. A. (2016). Empty calories and phantom fullness: a randomized trial studying the relative effects of energy density and viscosity on gastric emptying determined by MRI and satiety. *The American Journal of Clinical Nutrition*, 104(1), 73-80.
<https://doi.org/10.3945/ajcn.115.129064>
10. Cho, Y. H., Decker, E. A., & McClements, D. J. (2010). Formation of protein-rich coatings around lipid droplets using the electrostatic deposition method. *Langmuir*, 26(11), 7937–7945. <https://doi.org/10.1021/la904823b>
11. Corredig, M., Sharafbafi, N., & Kristo, E. (2011). Polysaccharide-protein interactions in dairy matrices, control and design of structures. *Food Hydrocolloids*, 25(8), 1833-1841. <https://doi.org/10.1016/j.foodhyd.2011.05.014>
12. Corstens, M. N., Berton-Carabin, C. C., Elichiry-Ortiz, P. T., Hol, K., Troost, F. J., Masclee, A. A., & Schroën, K. (2017). Emulsion-alginate beads designed to control *in vitro* intestinal lipolysis: Towards appetite control. *Journal of Functional Foods*, 34, 319-328. <https://doi.org/10.1016/j.jff.2017.05.003>

13. Dalgleish, D. G. (1997). Adsorption of protein and the stability of emulsions. *Trends in Food Science and Technology*, 8(1), 1-6. [https://doi.org/10.1016/S0924-2244\(97\)01001-7](https://doi.org/10.1016/S0924-2244(97)01001-7)
14. Dalgleish, D. G. (2003). Food emulsions: Their structures and properties. In *Food Emulsions: CRC Press*. <https://doi.org/10.1201/9780203913222.ch1>
15. Dangin, M., Boirie, Y., Guillet, C., & Beaufrère, B. (2002). Influence of the protein digestion rate on protein turnover in young and elderly subjects. *The Journal of Nutrition*, 132(10), 3228-3233. <https://doi.org/10.1093/jn/131.10.3228S>
16. Dekkers, B. L., Kolodziejczyk, E., Acquistapace, S., Engmann, J., & Wooster, T. J. (2016). Impact of gastric pH profiles on the proteolytic digestion of mixed β lg-Xanthan biopolymer gels. *Food & Function*, 7(1), 58-68. <https://doi.org/10.1039/C5FO01085C>
17. Dias, C. B., Zhu, X., Thompson, A. K., Singh, H., & Garg, M. L. (2019). Effect of the food form and structure on lipid digestion and postprandial lipaemic response. *Food & Function*, 10(1), 112-124. <https://doi.org/10.1039/C8FO01698D>
18. Dickinson, E. (2012). Emulsion gels: The structuring of soft solids with protein-stabilized oil droplets. *Food Hydrocolloids*, 28(1), 224-241. <https://doi.org/10.1016/j.foodhyd.2011.12.017>
19. Dimitrova, T. D., & Leal-Calderon, F. (2001). Bulk elasticity of concentrated protein-stabilized emulsions. *Langmuir*, 17(11), 3235-3244. <https://doi.org/10.1021/la001805n>

20. Dougkas, A., Minihane, A. M., Givens, D. I., Reynolds, C. K., & Yaqoob, P. (2012). Differential effects of dairy snacks on appetite, but not overall energy intake. *British Journal of Nutrition*, *108*(12), 2274-2285. <https://doi.org/10.1017/S0007114512000323>
21. Euston, S. R., Finnigan, S. R., & Hirst, R. L. (2002). Kinetics of droplet aggregation in heated whey protein-stabilized emulsions: Effect of polysaccharides. *Food Hydrocolloids*, *16*(5), 499-505. [https://doi.org/10.1016/S0268-005X\(01\)00130-8](https://doi.org/10.1016/S0268-005X(01)00130-8)
22. Evans, D. F., & Wennerström, H. (1994). *The colloidal domain: where physics, chemistry, biology, and technology meet*. VCH Publishers.
23. Fardet, A., Dupont, D., Rioux, L. E., & Turgeon, S. L. (2019). Influence of food structure on dairy protein, lipid and calcium bioavailability: A narrative review of evidence. *Critical Reviews in Food Science and Nutrition*, *59*(ue 13), 1987-2010. <https://doi.org/10.1080/10408398.2018.1435503>
24. Foster, T. J., & Norton, I. T. (2009). Self-assembling structures in the gastrointestinal tract. In *Designing Functional Foods* (pp. 601-622). Woodhead Publishing. <https://doi.org/10.1533/9781845696603.3.601>
25. Goh, K. K., Sarkar, A., & Singh, H. (2009). Milk protein-. Milk proteins from expression to Food (p. 347; A. Thompson, M. Boland, & H. Singh, Eds.). Elsevier Inc. <https://doi.org/10.1016/B978-0-12-374039-7.00012-X>
26. Golding, M., Wooster, T. J., Day, L., Xu, M., Lundin, L., Keogh, J., & Cliftonx, P. (2011). Impact of gastric structuring on the lipolysis of emulsified lipids. *Soft Matter*, *7*(7), 3513-3523. <https://doi.org/10.1039/c0sm01227k>

27. Guo, Q. (2015). *Behaviour of Emulsion Gels in the Human Mouth and Simulated Gastrointestinal Tract*. Massey University. <https://mro.massey.ac.nz/handle/10179/7196>
28. Guo, Q., Ye, A., Bellissimo, N., Singh, H., & Rousseau, D. (2017). Modulating fat digestion through food structure design. In *Progress in Lipid Research* (Vol. 68, pp. 109–118). Elsevier Ltd. <https://doi.org/10.1016/j.plipres.2017.10.001>
29. Guo, Q., Ye, A., Lad, M., Dalgleish, D., & Singh, H. (2014a). Behaviour of whey protein emulsion gel during oral and gastric digestion: effect of droplet size. *Soft Matter*, *10*(23), 4173-4183. <https://doi.org/10.1039/c4sm00598h>
30. Guo, Q., Ye, A., Lad, M., Dalgleish, D., & Singh, H. (2014b). Effect of gel structure on the gastric digestion of whey protein emulsion gels. *Soft Matter*, *10*(8), 1214-1223. <https://doi.org/10.1039/c3sm52758a>
31. Hall, W. L., Millward, D. J., Long, S. J., & Morgan, L. M. (2003). Casein and whey exert different effects on plasma amino acid profiles, gastrointestinal hormone secretion and appetite. *British Journal of Nutrition*, *89*(2), 239-248. <https://doi.org/10.1079/BJN2002760>
32. Hoad, C. L., Rayment, P., Spiller, R. C., Marciani, L., Alonso, B. D. C., Traynor, C., & Gowland, P. A. (2004). In vivo imaging of intragastric gelation and its effect on satiety in humans. *The Journal of Nutrition*, *134*(9), 2293-2300. <https://doi.org/10.1093/jn/134.9.2293>
33. Hunt, J. A., & Dalgleish, D. G. (1994). Adsorption behaviour of whey protein isolate and caseinate in soya oil-in-water emulsions. *Topics in Catalysis*, *8*(2), 175-187. [https://doi.org/10.1016/S0268-005X\(09\)80042-8](https://doi.org/10.1016/S0268-005X(09)80042-8)

34. Hussain, R., Gaiani, C., Jeandel, C., Ghanbaja, J., & Scher, J. (2012). Combined effect of heat treatment and ionic strength on the functionality of whey proteins. *Journal of Dairy Science*, *95*(11), 6260-6273. <https://doi.org/10.3168/jds.2012-5416>
35. Ikeda, S., Foegeding, E. A., & Hagiwara, T. (1999). Rheological Study on the Fractal Nature of the Protein Gel Structure. *Langmuir*, *15*(25), 8584–8589. <https://doi.org/10.1021/la9817415>
36. Jalabert-Malbos, M.-L., Mishellany-Dutour, A., Woda, A., & Peyron, M.-A. (2007). Particle size distribution in the food bolus after mastication of natural foods. *Food Quality and Preference*, *18*(5), 803–812. <https://doi.org/10.1016/j.foodqual.2007.01.010>
37. Juvonen, K. R., Macierzanka, A., Lille, M. E., Laaksonen, D. E., Mykkänen, H. M., Niskanen, L. K., ... Karhunen, L. J. (2015). Cross-linking of sodium caseinate-structured emulsion with transglutaminase alters postprandial metabolic and appetite responses in healthy young individuals. *British Journal of Nutrition*, *114*(3), 418-429. <https://doi.org/10.1017/S0007114515001737>
38. Krog, N. J., & Vang Sparsø, F. (2003). Food emulsifiers: Their chemical and physical properties. *In Food. Emulsions: CRC Press*. <https://doi.org/10.1201/9780203913222.ch2>
39. Kulmyrzaev, A. A., & Schubert, H. (2004). Influence of KCl on the physicochemical properties of whey protein stabilized emulsions. *Food Hydrocolloids*, *18*(1), 13-19. [https://doi.org/10.1016/S0268-005X\(03\)00037-7](https://doi.org/10.1016/S0268-005X(03)00037-7)
40. Le, X. T., L.-E. Rioux and S. L. Turgeon (2017). "Formation and functional properties of protein–polysaccharide electrostatic hydrogels in comparison to

- protein or polysaccharide hydrogels." *Advances in colloid and interface science* 239: 127-135.
41. Le, X. T., Rioux, L.-E., & Turgeon, S. L. (2017). Formation and functional properties of protein–polysaccharide electrostatic hydrogels in comparison to protein or polysaccharide hydrogels. *Advances in Colloid and Interface Science*, 239, 127–135. <https://doi.org/10.1016/j.cis.2016.04.006>
42. Li, J., Ye, A., Lee, S. J., & Singh, H. (2012). Influence of gastric digestive reaction on subsequent *in vitro* intestinal digestion of sodium caseinate-stabilized emulsions. *Food & Function*, 3(3), 320-326. <https://doi.org/10.1039/c2fo10242k>
43. Liu, F., Ma, C., McClements, D. J., & Gao, Y. (2016). Development of polyphenol-protein-polysaccharide ternary complexes as emulsifiers for nutraceutical emulsions: Impact on formation, stability, and bioaccessibility of β -carotene emulsions. *Food Hydrocolloids*, 61, 578-588. <https://doi.org/10.1016/j.foodhyd.2016.05.031>
44. Lorenzen, P. C., & Schrader, K. (2006). A comparative study of the gelation properties of whey protein concentrate and whey protein isolate. *Le Lait*, 86(4), 259-271. <https://doi.org/10.1051/lait:2006008>
45. Lovegrove, A., Edwards, C. H., Noni, I., Patel, H., El, S. N., Grassby, T., ... Shewry, P. R. (2017). Role of polysaccharides in food, digestion, and health. *Critical Reviews in Food Science and Nutrition*, 57(2), 237-253. <https://doi.org/10.1080/10408398.2014.939263>
46. Luo, N. (2021). *Structured emulsion gel systems for delivery of bioactive compounds: a thesis presented in partial fulfilment of the requirements for the degree of Doctor of Philosophy in Food Technology at Massey University*,

Manawatū, New Zealand (Doctoral dissertation, Massey University).

<https://mro.massey.ac.nz/handle/10179/16548>

47. Luo, N., Ye, A., Wolber, F. M., & Singh, H. (2019). Structure of whey protein emulsion gels containing capsaicinoids: Impact on in-mouth breakdown behaviour and sensory perception. *Food Hydrocolloids*, *92*, 19-29. <https://doi.org/10.1016/j.foodhyd.2019.01.019>
48. Luo, Q., Boom, R. M., & Janssen, A. E. M. (2015). Digestion of protein and protein gels in simulated gastric environment. *LWT - Food Science and Technology*, *63(1)*, 161-168. <https://doi.org/10.1016/j.lwt.2015.03.087>
49. Luo, Q., Borst, J. W., Westphal, A. H., Boom, R. M., & Janssen, A. E. (2017). Pepsin diffusivity in whey protein gels and its effect on gastric digestion. *Food Hydrocolloids*, *66*, 318-325. <https://doi.org/10.1016/j.foodhyd.2016.11.046>
50. Macierzanka, A., Böttger, F., Lansonneur, L., Groizard, R., Jean, A. S., Rigby, N. M., ... MacKie, A. R. (2012). The effect of gel structure on the kinetics of simulated gastrointestinal digestion of bovine β -lactoglobulin. *Food Chemistry*, *134(4)*, 2156-2163. <https://doi.org/10.1016/j.foodchem.2012.04.018>
51. Macierzanka, A., Sancho, A. I., Mills, E. N. C., Rigby, N. M., & MacKie, A. R. (2009). Emulsification alters simulated gastrointestinal proteolysis of β -casein and β -lactoglobulin. *Soft Matter*, *5(3)*, 538-550. <https://doi.org/10.1039/B811233A>
52. Mackie, A. (2020). Insights and gaps on protein digestion. *Current Opinion in Food Science*, *31*, 96-101. <https://doi.org/10.1016/j.cofs.2020.03.006>
53. Mackie, A. R., Rafiee, H., Malcolm, P., Salt, L., & Aken, G. (2013). Specific food structures suppress appetite through reduced gastric emptying rate. *American*

- Journal of Physiology-Gastrointestinal and Liver Physiology*, 304(11), 1038-1043. <https://doi.org/10.1152/ajpgi.00060.2013>
54. Mao, L., & Miao, S. (2015). Structuring Food Emulsions to Improve Nutrient Delivery During Digestion. *Food Engineering Reviews*, 7(ue 4), 439-451. <https://doi.org/10.1007/s12393-015-9108-0>
55. Marciani, L., Gowland, P. A., Fillery-Travis, A., Manoj, P., Wright, J., Smith, A., & Spiller, R. C. (2001). Assessment of antral grinding of a model solid meal with echo-planar imaging. *American Journal of Physiology-Gastrointestinal and Liver Physiology*, 280(5), 844-849. <https://doi.org/10.1152/ajpgi.2001.280.5.G844>
56. Marciani, L., Hall, N., Pritchard, S. E., Cox, E. F., Totman, J. J., Lad, M., & Spiller, R. C. (2012). Preventing gastric sieving by blending a solid/water meal enhances satiation in healthy humans. *The Journal of Nutrition*, 142(7), 1253-1258. <https://doi.org/10.3945/jn.112.159830>
57. Marciani, L., Wickham, M., Singh, G., Bush, D., Pick, B., Cox, E., & Spiller, R. C. (2007). Enhancement of intragastric acid stability of a fat emulsion meal delays gastric emptying and increases cholecystokinin release and gallbladder contraction. *American Journal of Physiology-Gastrointestinal and Liver Physiology*. <https://doi.org/10.1152/ajpgi.00452.2006>
58. McClements, D. J. (2012). Nanoemulsions versus microemulsions: Terminology, differences, and similarities. *Soft Matter*, 8(6), 1719-1729. <https://doi.org/10.1039/C2SM06903B>
59. McClements, D. J. (2015). *Food emulsions: principles, practices, and techniques*: CRC press.

60. McClements, D. J., & Li, Y. (2010). Structured emulsion-based delivery systems: Controlling the digestion and release of lipophilic food components. *Advances in Colloid and Interface Science*, *159*(ue 2), 213-228. <https://doi.org/10.1016/j.cis.2010.06.010>
61. McClements, D. J., Decker, E. A., Park, Y., & Weiss, J. (2009). Structural design principles for delivery of bioactive components in nutraceuticals and functional foods. *Critical Reviews in Food Science and Nutrition*, *49*(6), 577-606. <https://doi.org/10.1080/10408390902841529>
62. Melton, L. D., & Smith, B. G. (2001). Determination of the uronic acid content of plant cell walls using a colorimetric assay. *Current Protocols in Food Analytical Chemistry*, *1*, 3-3 <https://doi.org/10.1002/0471142913.fae0303s00>
63. Minekus, M., Alming, M., Alvito, P., Ballance, S., Bohn, T., Bourlieu, C., ... Brodkorb, A. (2014). A standardised static *in vitro* digestion method suitable for food-an international consensus. *Food and Function*, *5*(6), 1113-1124. <https://doi.org/10.1039/C3FO60702J>
64. Mouécoucou, J., Frémont, S., Villaume, C., Sanchez, C., & Méjean, L. (2007). Polysaccharides reduce *in vitro* IgG/IgE-binding of β -lactoglobulin after hydrolysis. *Food Chemistry*, *104*(3), 1242-1249. <https://doi.org/10.1016/j.foodchem.2007.01.057>
65. Munialo, C. D., Linden, E., & Jongh, H. H. J. (2014). The ability to store energy in pea protein gels is set by network dimensions smaller than 50nm. *Food Research International*, *64*, 482-491. <https://doi.org/10.1016/j.foodres.2014.07.038>

66. Nacer S, A., Sanchez, C., Villaume, C., Mejean, L., & Mouecoucou, J. (2004). Interactions between β -Lactoglobulin and Pectins during *in vitro* Gastric Hydrolysis. *Journal of Agricultural and Food Chemistry*, 52(2), 355-360. <https://doi.org/10.1021/jf034584a>
67. Nayak, N., & Singh, H. (2019). Milk Protein–Polysaccharide Interactions in Food Systems. In L. Melton, F. Shahidi, & P. Varelis (Eds.), *Encyclopedia of Food Chemistry* (pp. 431–438). Academic Press. <https://doi.org/10.1016/B978-0-08-100596-5.21472-8>
68. Nicolai, T., Britten, M., & Schmitt, C. (2011). β -Lactoglobulin and WPI aggregates: Formation, structure and applications. *Food Hydrocolloids*, 25(8), 1945-1962. <https://doi.org/10.1016/j.foodhyd.2011.02.006>
69. Nik, A. M., Wright, A. J., & Corredig, M. (2010). Surface adsorption alters the susceptibility of whey proteins to pepsin-digestion. *Journal of Colloid and Interface Science*, 344(2), 372-381. <https://doi.org/10.1016/j.jcis.2010.01.006>
70. Parker, H. L., Liu, D., Curcic, J., Ebert, M. O., Schwizer, W., Fried, M., & Steingoetter, A. (2017). Gastric and postgastric processing of ^{13}C markers renders the ^{13}C breath test an inappropriate measurement method for the gastric emptying of lipid emulsions in healthy adults. *The Journal of Nutrition*, 147(7), 1258-1266. <https://doi.org/10.3945/jn.117.248765>
71. Peram, M. R., Loveday, S. M., Ye, A., & Singh, H. (2013). *In vitro* gastric digestion of heat-induced aggregates of β -lactoglobulin. *Journal of Dairy Science*, 96(1), 63-74. <https://doi.org/10.3168/jds.2012-5896>

72. Remondetto, G. E., Beyssac, E., & Subirade, M. (2004). Iron Availability from Whey Protein Hydrogels: An *in vitro* Study. *Journal of Agricultural and Food Chemistry*, *52*(26), 8137-8143. <https://doi.org/10.1021/jf040286h>
73. Rinaldi, L., Rioux, L. E., Britten, M., & Turgeon, S. L. (2015). *In vitro* bioaccessibility of peptides and amino acids from yogurt made with starch, pectin, or β -glucan. *International Dairy Journal*, *46*, 39-45. <https://doi.org/10.1016/j.idairyj.2014.09.005>
74. Sah, B. N. P., McAinch, A. J., & Vasiljevic, T. (2016). Modulation of bovine whey protein digestion in gastrointestinal tract: A comprehensive review. *International Dairy Journal*, *62*, 10-18. <https://doi.org/10.1016/j.idairyj.2016.07.003>
75. Sarkar, A., & Mackie, A. R. (2020). Engineering oral delivery of hydrophobic bioactives in real-world scenarios. *Current Opinion in Colloid & Interface Science*, *48*, 40-52. <https://doi.org/10.1016/j.cocis.2020.03.009>
76. Sarkar, A., Goh, K. K., Singh, R. P., & Singh, H. (2009). Behaviour of an oil-in-water emulsion stabilized by β -lactoglobulin in an *in vitro* gastric model. *Food Hydrocolloids*, *23*(6), 1563-1569. <https://doi.org/10.1016/j.foodhyd.2008.10.014>
77. Sarkar, A., Juan, J.-M., Kolodziejczyk, E., Acquistapace, S., Donato-Capel, L., & Wooster, T. J. (2015). Impact of Protein Gel Porosity on the Digestion of Lipid Emulsions. *Journal of Agricultural and Food Chemistry*, *63*(40), 8829-8837. <https://doi.org/10.1021/acs.jafc.5b03700>
78. Sarojini, S., & Manavalan, R. (2012). An overview on various approaches to gastroretentive dosage forms. *The International Journal of Drug Development and Research*, *4*(1), 1-13.

79. Semenova, M. G., Moiseenko, D. v., Grigorovich, N. v., Anokhina, M. S., Antipova, A. S., Belyakova, L. E., Tsapkina, E. N. (2014). Protein-Polysaccharide Interactions and Digestion of the Complex Particles. *In Food Structures, Digestion and Health* (pp. 169-192). <https://doi.org/10.1016/B978-0-12-404610-8.00006-2>
80. Singh, H., & Sarkar, A. (2011). Behaviour of protein-stabilised emulsions under various physiological conditions. *Advances in colloid and interface science*, *165(1)*, 47-57. <https://doi.org/10.1016/j.cis.2011.02.001>
81. Singh, H., Ye, A., & Horne, D. (2009). Structuring food emulsions in the gastrointestinal tract to modify lipid digestion. *Progress in Lipid Research*, *48(2)*, 92-100. <https://doi.org/10.1016/j.plipres.2008.12.001>
82. Singh, Harjinder, Ye, A., & Horne, D. (2009). Structuring food emulsions in the gastrointestinal tract to modify lipid digestion. *Progress in Lipid Research*, *48(2)*, 92-100. <https://doi.org/10.1016/j.plipres.2008.12.001>
83. Singh, Harjinder, Ye, A., & Horne, D. (2020). Structural changes to milk protein products during gastrointestinal digestion. *In Milk Proteins* (671-700). <https://doi.org/10.1016/B978-0-12-815251-5.00019-0>
84. Singh, T. K., Øiseth, S. K., Lundin, L., & Day, L. (2014). Influence of heat and shear induced protein aggregation on the *in vitro* digestion rate of whey proteins. *Food & Function*, *5(11)*, 2686-2698. <https://doi.org/10.1039/C4FO00454J>
85. Steingoetter, A., Radovic, T., Buetikofer, S., Curcic, J., Menne, D., Fried, M., & Wooster, T. J. (2015). Imaging gastric structuring of lipid emulsions and its effect on gastrointestinal function: a randomized trial in healthy subjects. *The American*

- Journal of Clinical Nutrition*, 101(4), 714-724.
<https://doi.org/10.3945/ajcn.114.100263>
86. Tadros, T. F. (2013). *Emulsion Formation and Stability*.
<https://doi.org/10.1002/9783527647941>
87. Tromp, R. H., Kruif, C. G., Eijk, M., & Rolin, C. (2004). On the mechanism of stabilisation of acidified milk drinks by pectin. *Food Hydrocolloids*, 18(4), 565-572. <https://doi.org/10.1016/j.foodhyd.2003.09.005>
88. Truong, V. and C. Daubert (2000). "Comparative study of large strain methods for assessing failure characteristics of selected food gels." *Journal of Texture Studies*, 31(3), 335–353. <https://doi.org/10.1111/j.1745-4603.2000.tb00294.x>
89. Tuinier, R., Rolin, C., & Kruif, C. G. (2002). Electrosorption of pectin onto casein micelles. *Biomacromolecules*, 3(3), 632-638. <https://doi.org/10.1021/bm025530x>
90. Turgeon, S. L., Beaulieu, M., Schmitt, C., & Sanchez, C. (2003). Protein-polysaccharide interactions: phase-ordering kinetics, thermodynamic and structural aspects. *Current Opinion in Colloid & Interface Science*, 8(4-5), 401-414. [https://doi.org/10.1016/S1359-0294\(03\)00093-1](https://doi.org/10.1016/S1359-0294(03)00093-1)
91. Vassallo, M. J., Camilleri, M., Prather, C. M., Hanson, R. B., & Thomforde, G. M. (1992). Measurement of axial forces during emptying from the human stomach. *American Journal of Physiology-Gastrointestinal and Liver Physiology*, 263(2), 230-239. <https://doi.org/10.1152/ajpgi.1992.263.2.G230>
92. Wackerbarth, H., Schön, P., & Bindrich, U. (2009). Preparation and characterization of multilayer coated microdroplets: Droplet deformation simultaneously probed by atomic force spectroscopy and optical detection. *Langmuir*, 25(5), 2636-2640. <https://doi.org/10.1021/la802898k>

93. Walstra, P. (2002). *Physical chemistry of foods*. CRC Press.<https://doi.org/10.1201/9780203910436>
94. Wang, X., Lin, Q., Ye, A., Han, J., & Singh, H. (2019). Flocculation of oil-in-water emulsions stabilised by milk protein ingredients under gastric conditions: Impact on *in vitro* intestinal lipid digestion. *Food Hydrocolloids*, *88*, 272-282. <https://doi.org/10.1016/j.foodhyd.2018.10.001>
95. Wang, X., Ye, A., Dave, A., & Singh, H. (2021). In vitro digestion of soymilk using a human gastric simulator: Impact of structural changes on kinetics of release of proteins and lipids. *Food Hydrocolloids*, *111*, 106235. <https://doi.org/10.1016/j.foodhyd.2020.106235>
96. Wang, X., Ye, A., Lin, Q., Han, J., & Singh, H. (2018). Gastric digestion of milk protein ingredients: Study using an *in vitro* dynamic model. *Journal of Dairy Science*, *101*(8), 6842-6852. <https://doi.org/10.3168/jds.2017-14284>
97. Wee, M. S. M., Yusoff, R., Chiang, J. H., & Xu, Y. (2017). In vitro and In vivo studies on intragastric soya protein-polysaccharide gels in a beverage matrix. *International Journal of Food Science & Technology*, *52*(6), 1358-1366. <https://doi.org/10.1111/ijfs.13415>
98. Wijaya, W., Patel, A. R., Setiowati, A. D., & Meeren, P. (2017). Functional colloids from proteins and polysaccharides for food applications. *Trends in Food Science and Technology*, *68*, 56-69. <https://doi.org/10.1016/j.tifs.2017.08.003>
99. Ye, A. (2008). Complexation between milk proteins and polysaccharides via electrostatic interaction: principles and applications - a review. *International Journal of Food Science & Technology*, *43*(3), 406-415. <https://doi.org/10.1111/j.1365-2621.2006.01454.x>

100. Ye, A., Cui, J., & Singh, H. (2010). Effect of the fat globule membrane on *in vitro* digestion of milk fat globules with pancreatic lipase. *International Dairy Journal*, *20*(12), 822-829. <https://doi.org/10.1016/j.idairyj.2010.06.007>
101. Ye, A., Wang, X., Lin, Q., Han, J., & Singh, H. (2020). Dynamic gastric stability and *in vitro* lipid digestion of whey-protein-stabilised emulsions: *Effect of heat treatment*. *Food Chemistry*, *318*, 126463. <https://doi.org/10.1016/j.foodchem.2020.126463>
102. Zhang, S., Zhang, Z., & Vardhanabhuti, B. (2014). Effect of charge density of polysaccharides on self-assembled intragastric gelation of whey protein/polysaccharide under simulated gastric conditions. *Food & function*, *5*(8), 1829-1838. <https://doi.org/10.1039/C4FO00019F>
103. Zhang, Z., Zhang, R., & McClements, D. J. (2017). Control of protein digestion under simulated gastrointestinal conditions using biopolymer microgels. *Food Research International*, *100*, 86-94. <https://doi.org/10.1016/j.foodres.2017.08.037>